TEXAS
The University of Texas at Austin

WHAT STARTS HERE CHANGES THE WORLD

MECHANICS OF 2D MATERIALS AND INTERFACES

A tutorial (virtual) at the 2021 MRS Fall Meeting

Rui Huang

Department of Aerospace Engineering & Engineering Mechanics

University of Texas at Austin

11/29/2021

Outline

- Part I: Mechanics and mechanical properties of 2D materials
  - Elastic and thermoelastic properties
  - Inelastic properties: strength and toughness

- Part II: Interfacial properties of 2D materials (adhesion and friction)
  - 2D-3D interactions
  - 2D-2D interactions

Extreme Mechanics Letters 13 (2017) 42–72
Contents lists available at ScienceDirect
Extreme Mechanics Letters
journal homepage: www.elsevier.com/locate/eml

A review on mechanics and mechanical properties of 2D materials—Graphene and beyond

Deji Akinwande [a], Christopher J. Brennan [a], J. Scott Bunch [b], Philip Egberts [c], Jonathan R. Felts [d], Huajian Gao [e], Rui Huang [f,*], Joon-Seok Kim [a], Teng Li [g], Yao Li [h], Kenneth M. Liechti [f,*], Nanshu Lu [f], Harold S. Park [b], Evan J. Reed [i], Peng Wang [f], Boris I. Yakobson [j,k,l], Teng Zhang [m], Yong-Wei Zhang [n], Yao Zhou [i], Yong Zhu [o]

Part I:

- Mechanical properties: elastic and inelastic
- Electromechanical coupling
- Interfacial properties: adhesion and friction
- Applications (synthesis, origami/kirigami, devices)

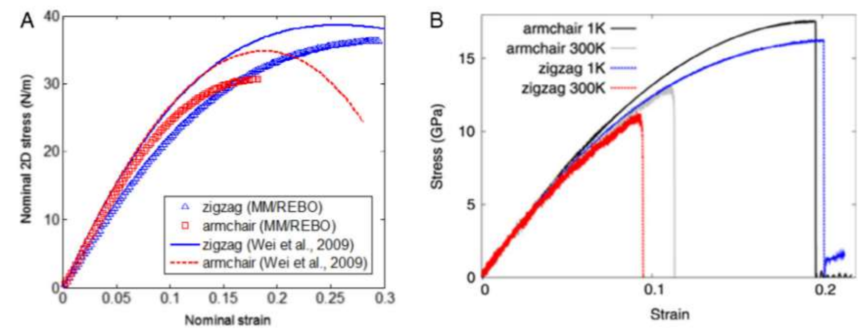

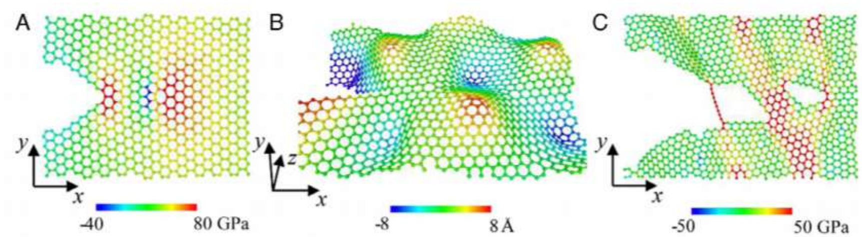

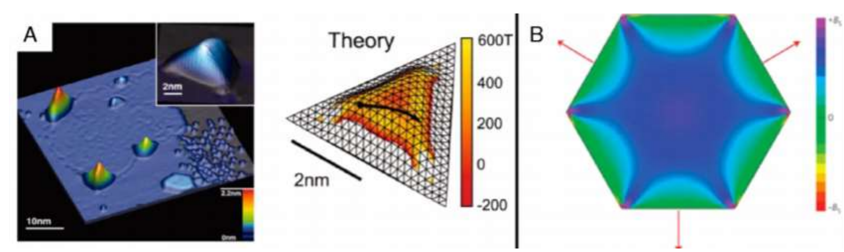

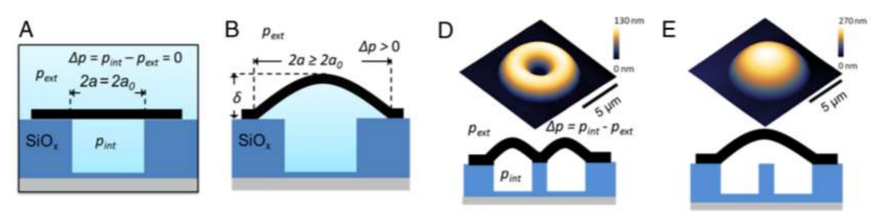

Elastic properties of monolayer 2D materials

- Young's modulus (N/m)
- Poisson's ratio
- Bending modulus (eV or J)
- Gaussian modulus (eV or J)

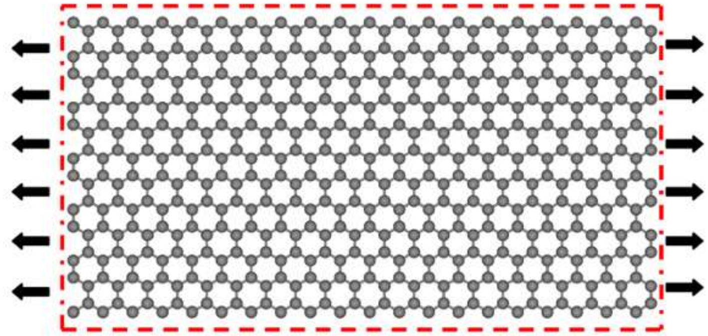

Uniaxial tension

$$\sigma_{2D} \equiv \frac{F}{b} = E_{2D}\varepsilon_x$$

$$\varepsilon_y = -\nu\varepsilon_x$$

Table 2
Linearly elastic properties of 2D materials predicted by first principles or empirical potential based calculations.

2D materials	Y_{2D} (N/m)	Poisson's ratio	D_m (eV)
Graphene [46]	345	0.149	1.49
h-BN [46]	271	0.211	1.34
MoS_2 [5,75]	118–141	~0.3	~11.7
Phosphorene [69,76]	23.0–92.3[a]	0.064–0.703[a]	–
Silicene [66,67]	~60	~0.4	–

[a] Highly anisotropic.

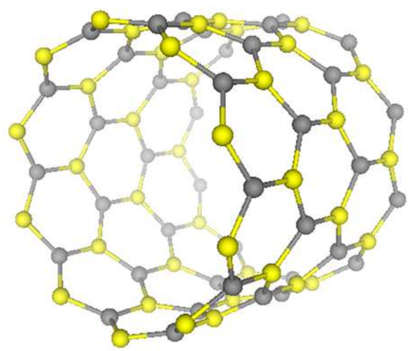

Pure bending: $M = D_m\kappa$

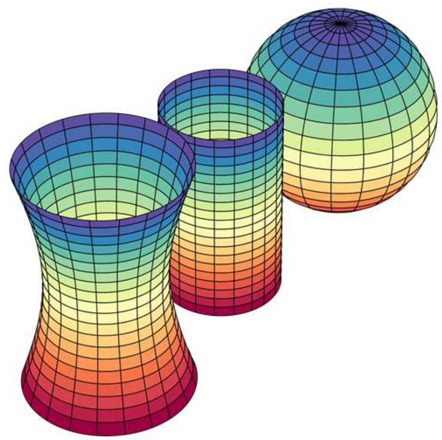

Gaussian curvatures

A linear elastic sheet model

Elastic strain energy density (per unit area)

$$U = U_s(\boldsymbol{\varepsilon}) + U_b(\boldsymbol{\kappa})$$

$$U_s(\boldsymbol{\varepsilon}) = \frac{E_{2D}}{2(1+\nu)}\left(\varepsilon_{ij}\varepsilon_{ij} + \frac{\nu}{1-\nu}\varepsilon_{jj}^2\right)$$

$$U_b(\boldsymbol{\kappa}) = \frac{1}{2}D_m\kappa_{jj}^2 + \frac{1}{2}D_G\left(\kappa_{ij}\kappa_{ij} - \kappa_{jj}^2\right)$$

2D stresses and moments:

$$\sigma_{ij} = \frac{\partial U}{\partial \varepsilon_{ij}} = \frac{E_{2D}}{1+\nu}\left(\varepsilon_{ij} + \frac{\nu}{1-\nu}\varepsilon_{kk}\delta_{ij}\right)$$

$$M_{ij} = \frac{\partial U}{\partial \kappa_{ij}} = D_m\kappa_{kk}\delta_{ij} + D_G\left(\kappa_{ij} - \kappa_{kk}\delta_{ij}\right)$$

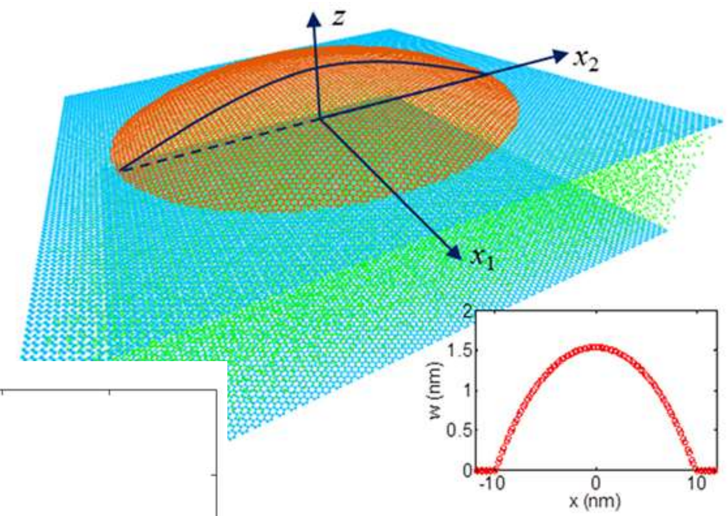

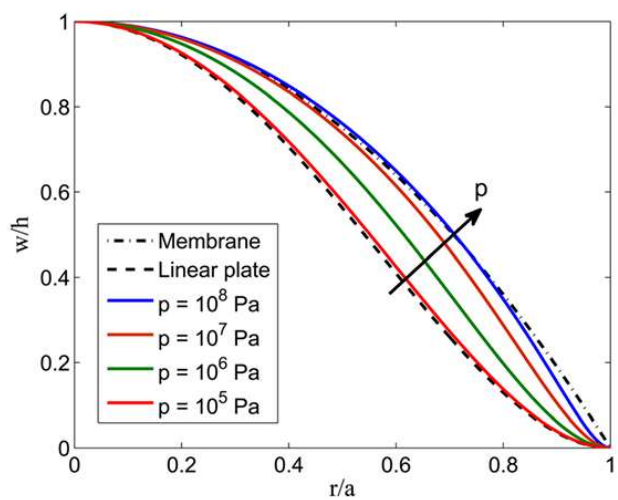

Transition from plate-like to membrane-like behavior

Wang, et al., J. Applied Mechanics 80, 040905 (2013).

Nonlinear elasticity at large strain

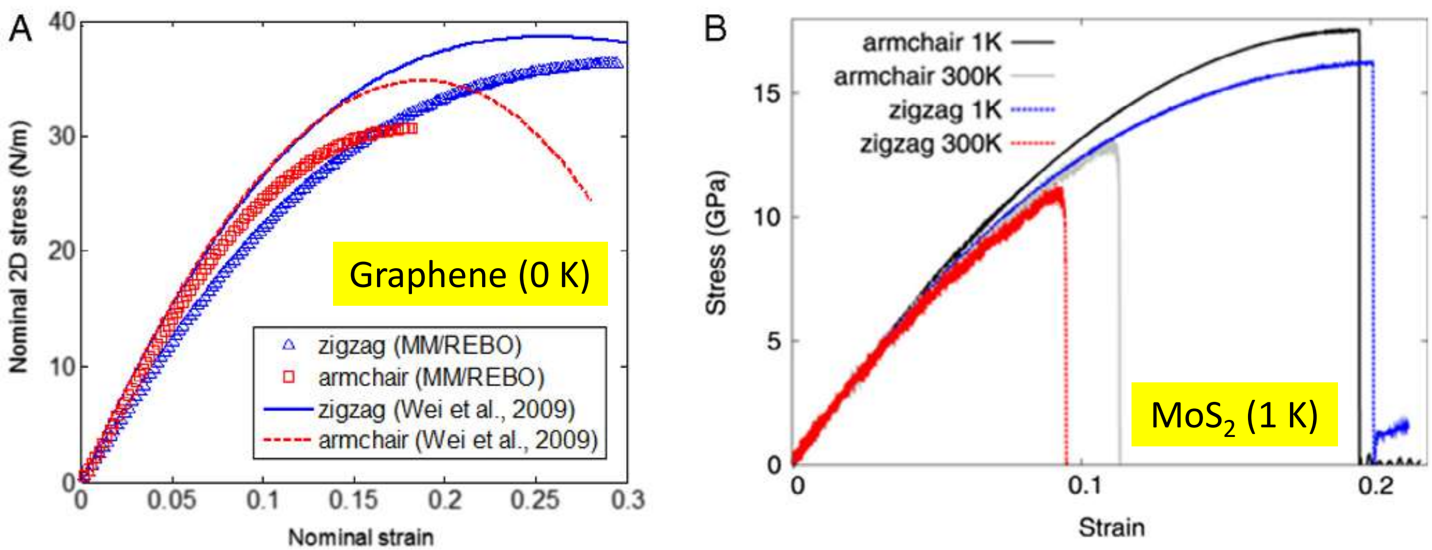

- Linear elasticity is typically acceptable for small strains (< 5%).
- At large strains, additional material properties are needed to describe the nonlinear and anisotropic elastic behavior of 2D materials.

AFM indentation experiment

Lee et al., Science 321, 385-388 (2008)

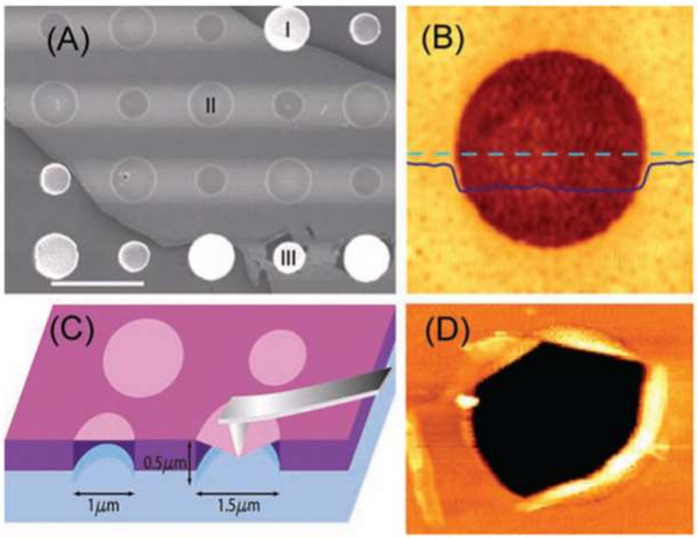

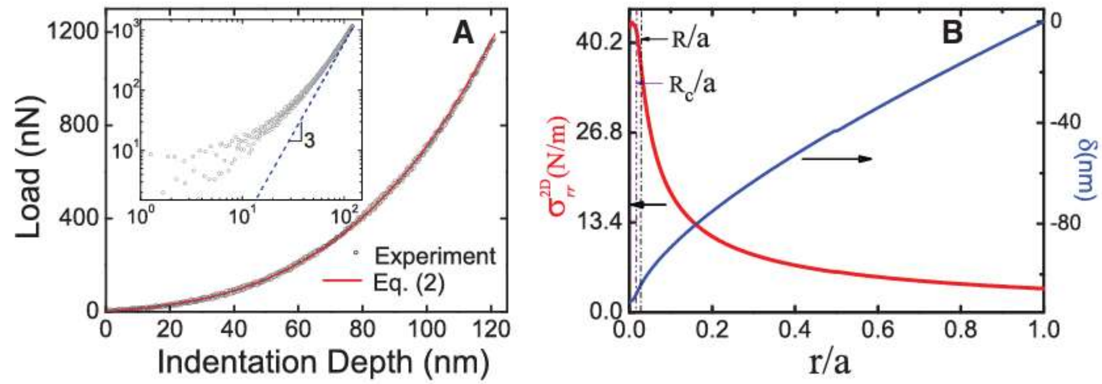

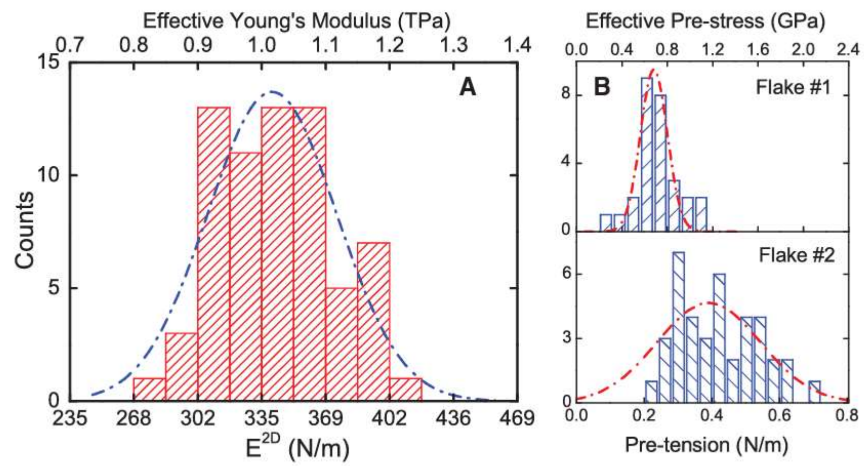

- A nonlinear elastic membrane model, with a pre-stress and negligible bending rigidity

$$\sigma_{2D} = E_{2D}\varepsilon + D_{2D}\varepsilon^2$$

$$F = \sigma_0^{2D}(\pi a)\left(\frac{\delta}{a}\right) + E^{2D}(q^3 a)\left(\frac{\delta}{a}\right)^3$$

$$\nu = 0.165$$

$$q(\nu) = 1.02$$

"Intrinsic" Strength of Graphene

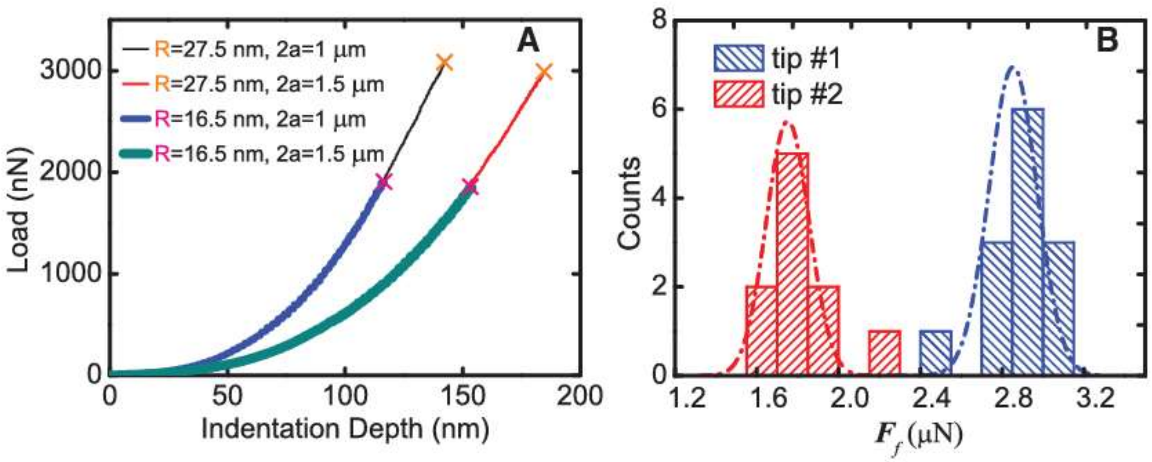

$$\sigma_m^{2D} = \left(\frac{FE^{2D}}{4\pi R}\right)^{\frac{1}{2}}$$

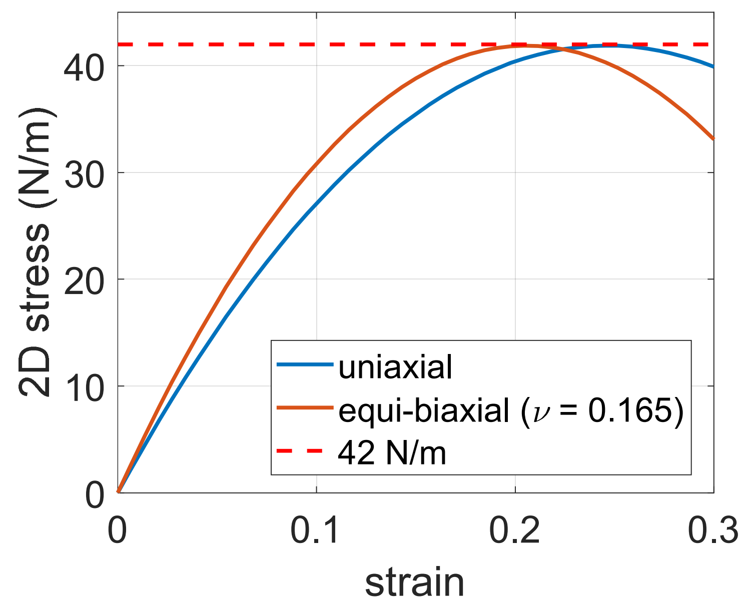

$$\sigma_{2D} = E_{2D}\varepsilon + D_{2D}\varepsilon^2$$

- A linear elasticity model overestimates the strength (~55 N/m).
- Numerical simulations with nonlinear elasticity ($D_{2D} = -690$ N/m and $E_{2D} = 340$ N/m) yields an intrinsic strength of 42 N/m.

➢ The corresponding stress-strain curves have a peak stress, defining the intrinsic strength as a result of elastic instability.

Lee et al., Science 321, 385-388 (2008)

Membrane-like vs Plate-like behaviors

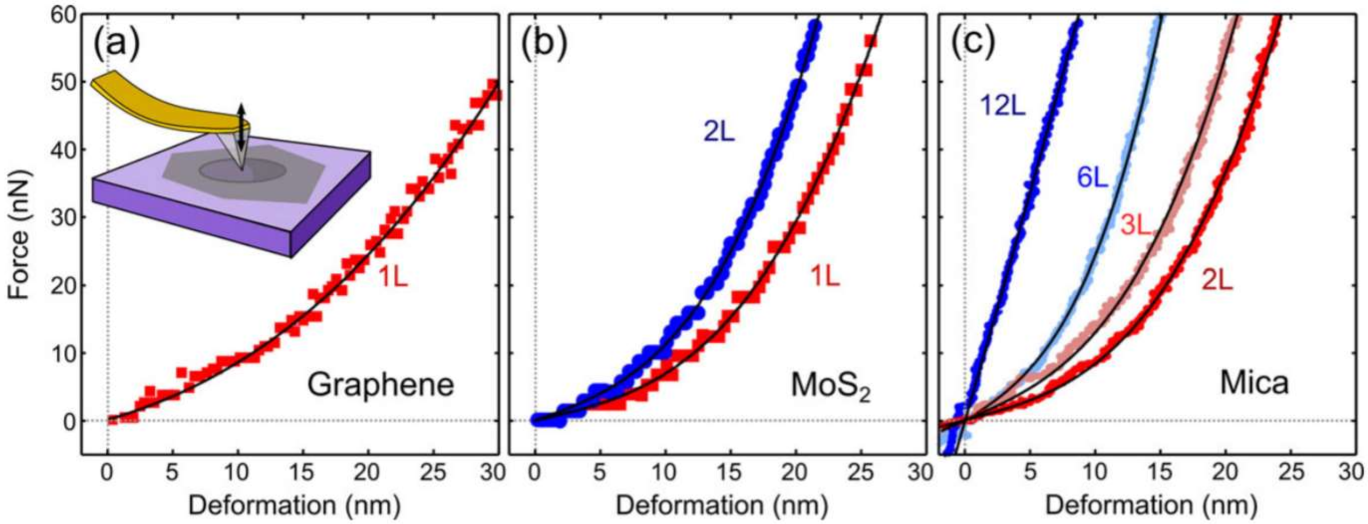

$$F = q^3 a E_{2D}\left(\frac{\delta}{a}\right)^3 + \pi a\left(\sigma_0^{2D} + \frac{16}{a^2}D\right)\frac{\delta}{a}$$

Membrane-like: $$F = q^3 a E_{2D}\left(\frac{\delta}{a}\right)^3 + \pi a(\sigma_0^{2D})\frac{\delta}{a}$$ $$\sigma_0^{2D} \gg \frac{16}{a^2}D$$

Plate-like: $$F = \pi a\left(\frac{16}{a^2}D\right)\frac{\delta}{a}$$ $$\sigma_0^{2D} \ll \frac{16}{a^2}D \qquad E_{2D}\left(\frac{\delta}{a}\right)^2 \ll \left(\frac{16}{a^2}D\right)$$

Castellanos-Gomez, et al., Ann. Phys. (Berlin), 1–18 (2014)

Pressurized blister experiment

Koenig et al., Nature Nanotech. 6, 543–546 (2011)

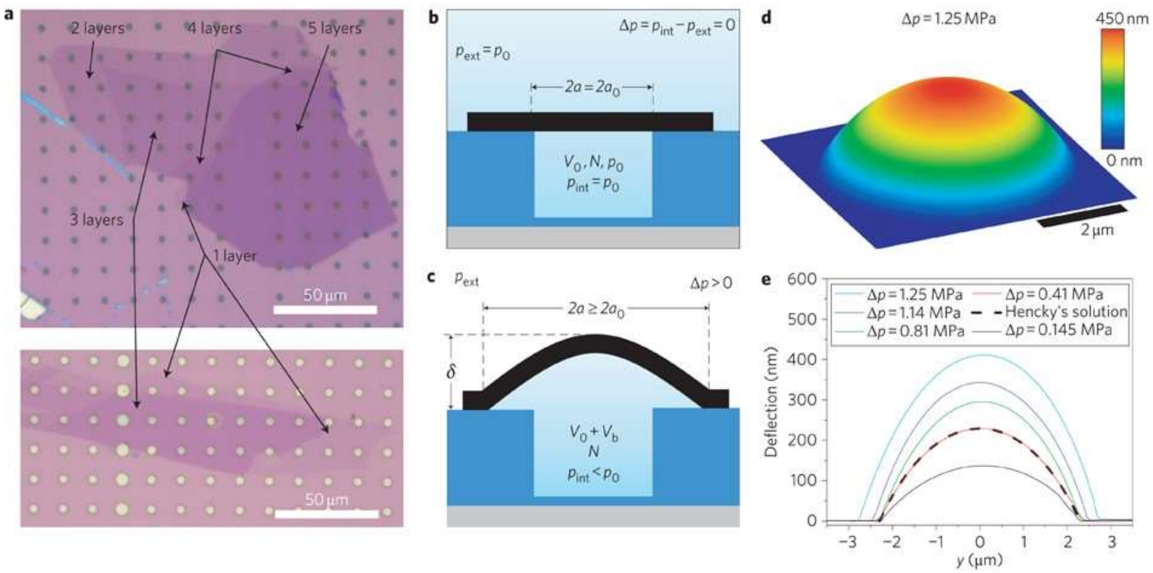

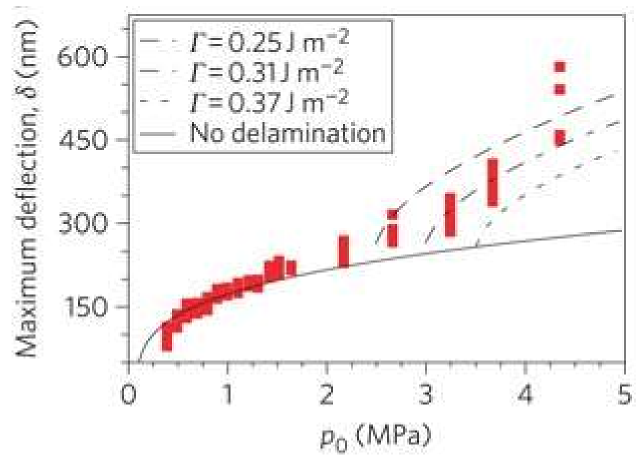

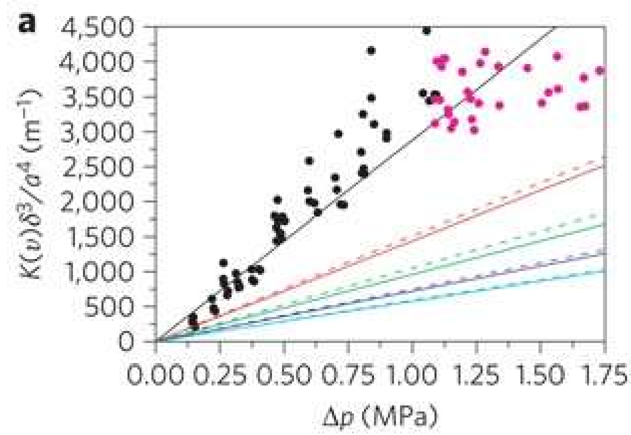

Geometrically nonlinear response of a linearly elastic membrane

$$\Delta p = K(\nu)\frac{E_{2D}}{a}\left(\frac{\delta}{a}\right)^3 \qquad K(\nu = 0.16) \approx 3.09 \qquad \Rightarrow \qquad E_{2D} = 347 \text{ N/m}$$

Multilayer graphene: elastic modulus and adhesion

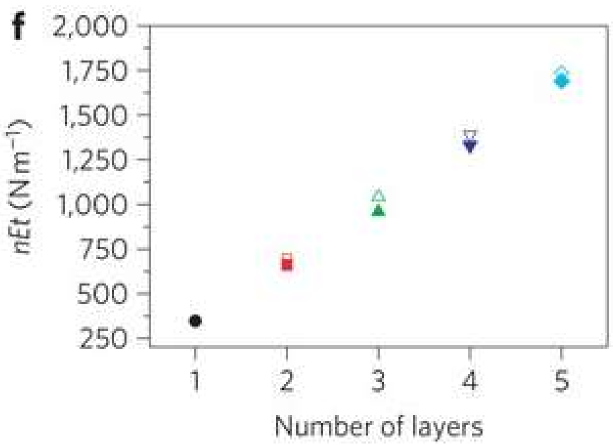

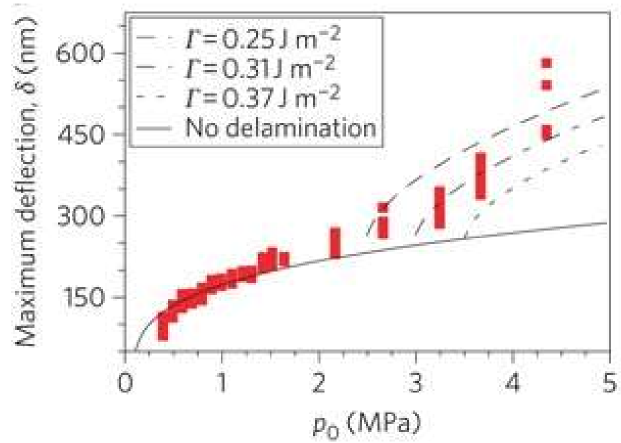

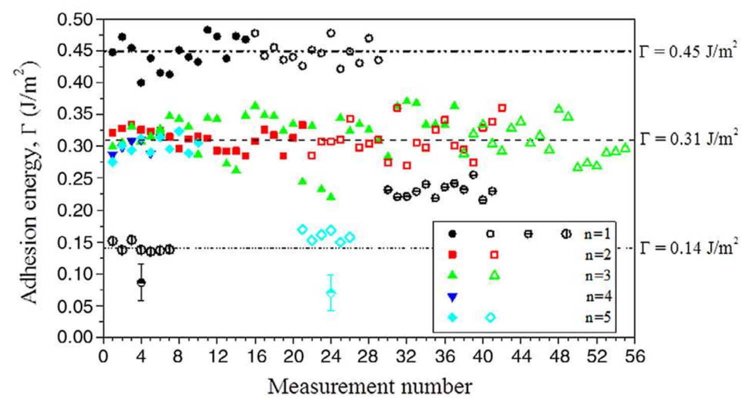

Elastic response before delamination: the in-plane stiffness (Et) is proportional to the number of layers

$$Et = nE_{2D}$$

$$\Delta p = K(\nu)\frac{Et}{a}\left(\frac{\delta}{a}\right)^3$$

Pressure induced delamination:

$$\Gamma = \phi(\nu)\, Et \left(\frac{\delta}{a}\right)^4$$

- Pressurized blisters or bubbles can be used to measure elastic and interfacial properties of 2D materials (monolayer and multilayer)

Koenig et al., Nature Nanotech. 6, 543–546 (2011)

Bending moduli of multilayer 2D materials

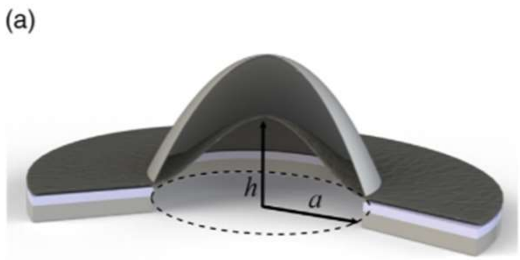

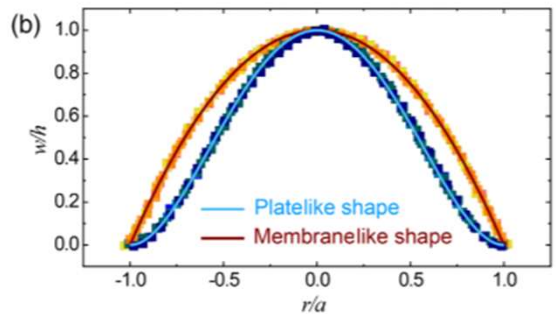

A nonlinear plate model:

$$\frac{\Delta p a^4}{h^3 t} = A(\nu)E + \frac{64D}{t^3}\left(\frac{t}{h}\right)^2$$

$$D = \frac{Et^3}{12(1-\nu^2)} f(N)$$

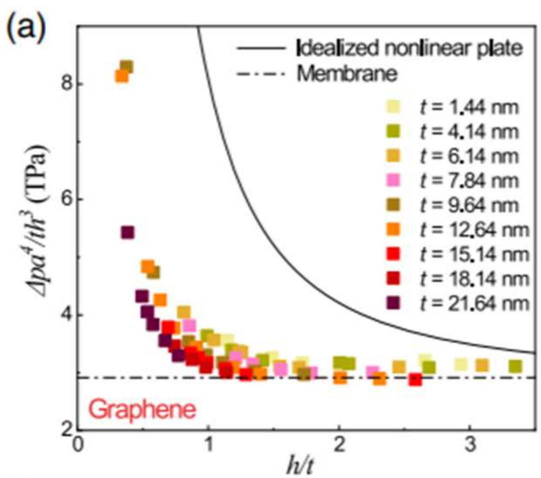

$$Et = NE_{2D}$$

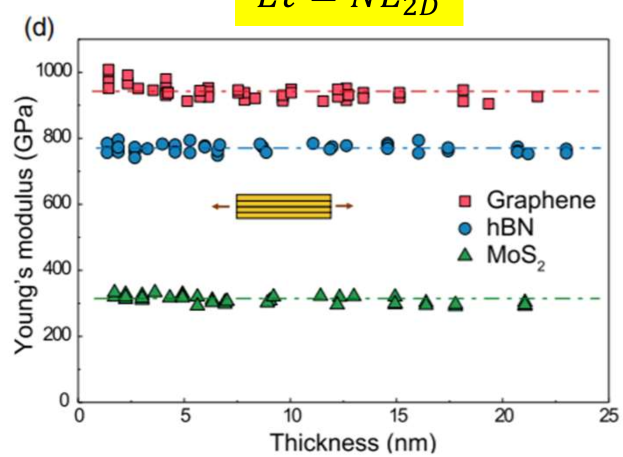

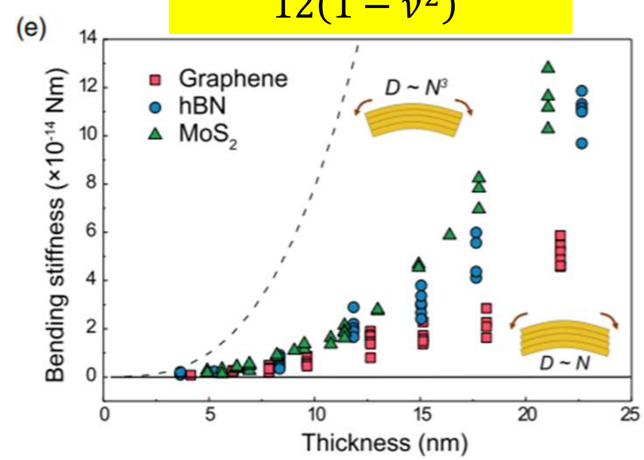

$$t = Nt_1$$

Wang et al., PRL 123, 116101 (2019).

Bending with interlayer slip

$$D = \frac{Et^3}{12(1-\nu^2)} f(N)$$

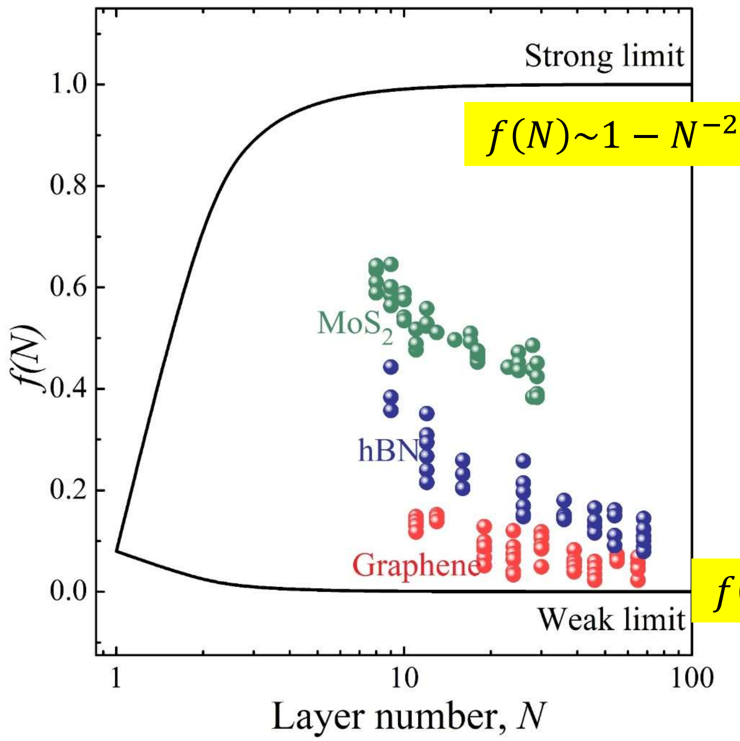

$f(N) \sim 1 - N^{-2}$

$f(N) \sim N^{-2}$

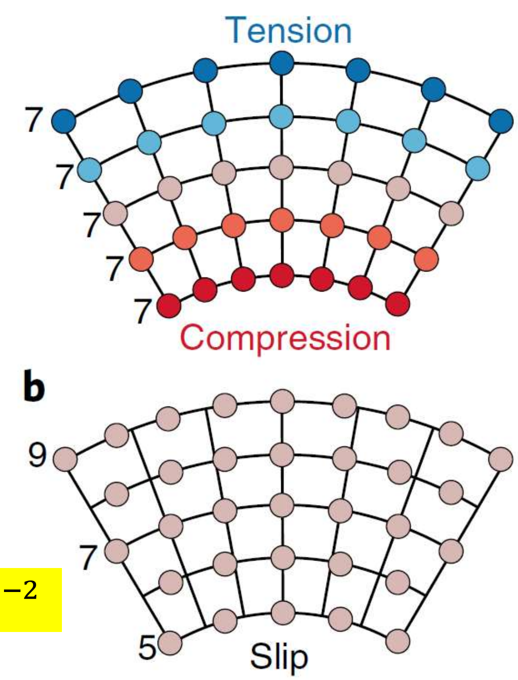

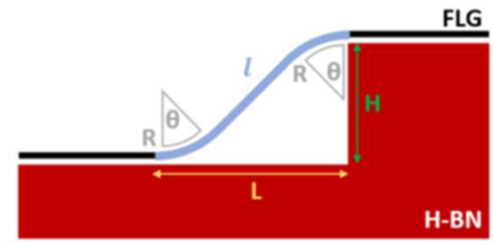

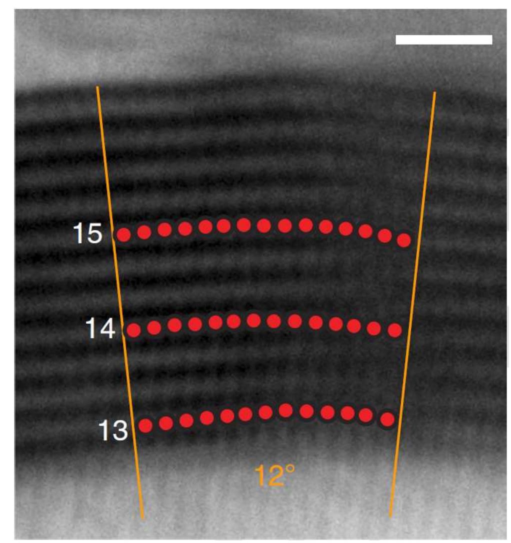

Wang et al., PRL 123, 116101 (2019).

Han et al., Nature Materials 19, 305–309 (2020).

Thermoelastic properties of graphene

- Thermal rippling
- Thermal expansion/contraction
- Thermal stress
- Temperature/size-dependent mechanical properties

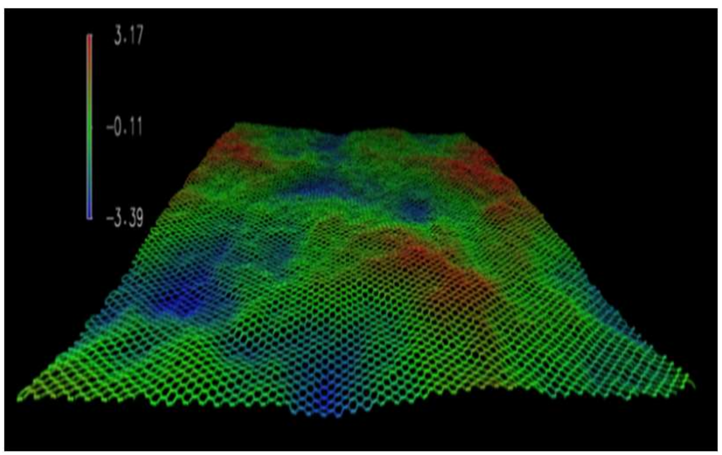

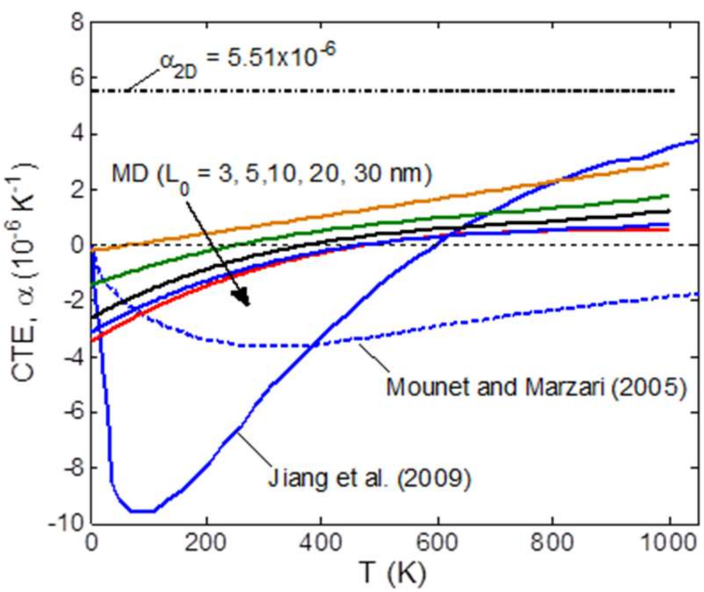

Thermal rippling of freestanding graphene

A statistical mechanics analysis under harmonic approximation:

$$w(\mathbf{r}) = \sum_k \hat{w}(\mathbf{q}_k) e^{i\mathbf{q}_k \cdot \mathbf{r}}$$

Boltzmann distribution:

$$P = \frac{1}{Z} \exp\left[-\frac{U_b + U_s}{k_B T} \right]$$

Rippling amplitude with no pretension:

$$\langle h^2 \rangle = \sum_k \langle |\hat{w}(\boldsymbol{q}_k)|^2 \rangle \sim \left(\frac{k_B T}{D} \right) L_0^2$$

Rippling amplitude with pre-strain:

$$\langle h^2 \rangle \sim \left(\frac{k_B T}{E^* \varepsilon_0} \right) \ln \left(1 + \frac{E^* \varepsilon_0 L_0^2}{4\pi^2 D} \right)$$

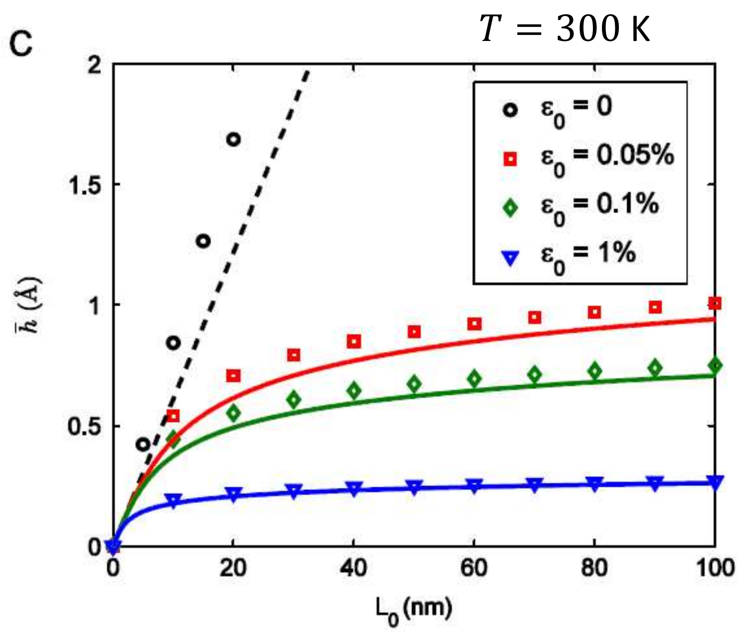

Gao and Huang, JMPS 66, 42-58 (2014).

Anharmonic Effects (MD simulations)

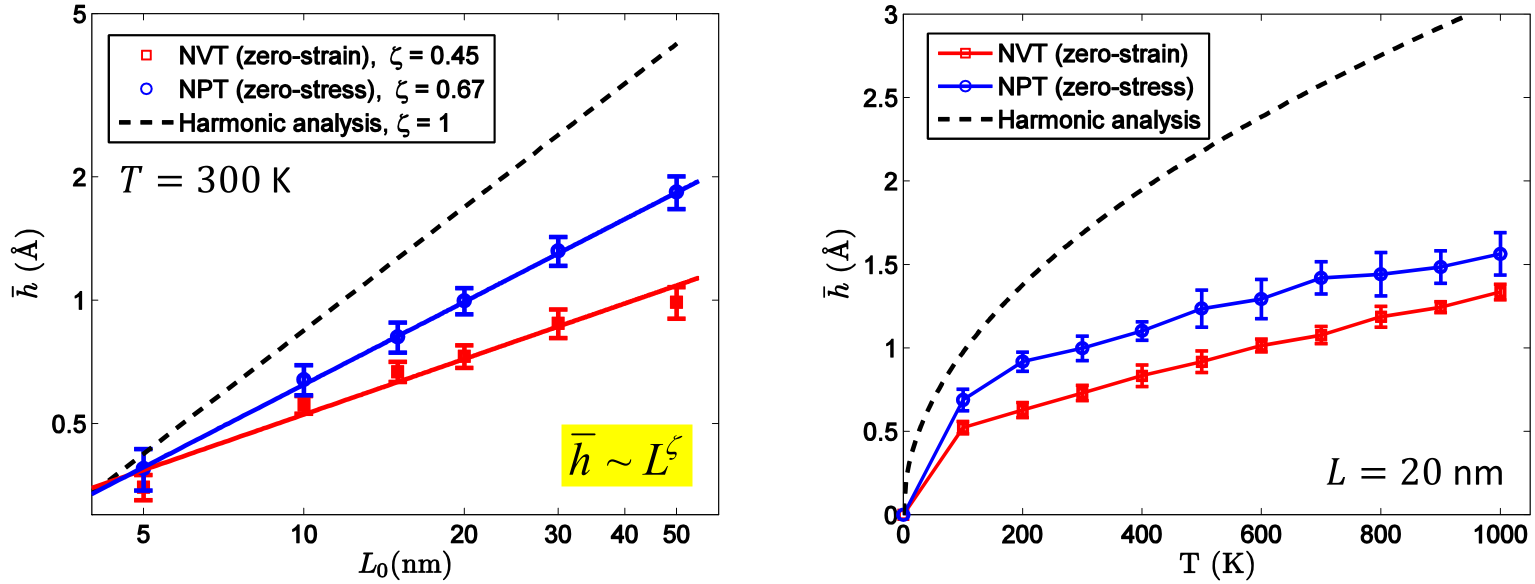

Harmonic approximation: $\bar{h} = \sqrt{\langle h^2 \rangle} = L\sqrt{\frac{\gamma_n k_B T}{16\pi^4 D}}$

- $\zeta < 1$: Significant anharmonic effects due to coupling between bending and stretching (similar to biomembranes).

Gao and Huang, JMPS 66, 42-58 (2014).

A nonlinear (anharmonic) analysis of thermal rippling

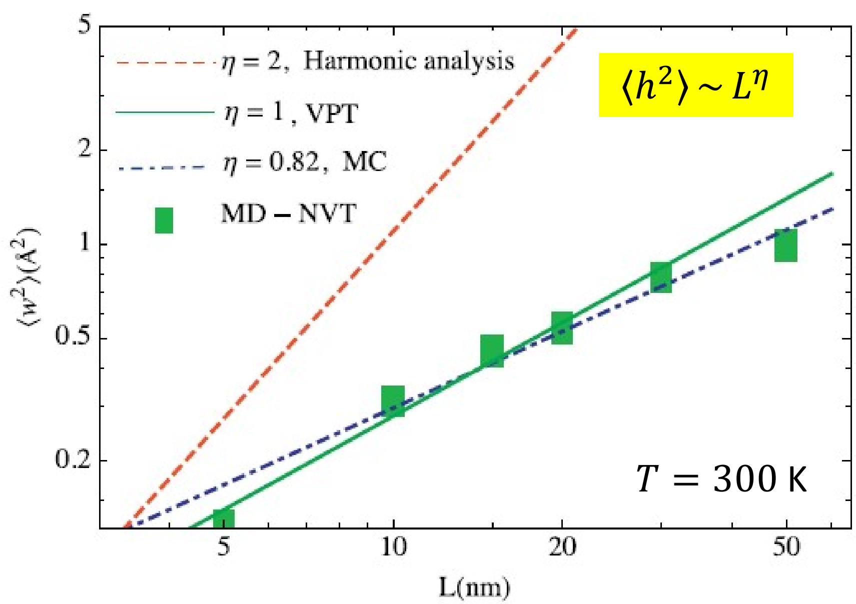

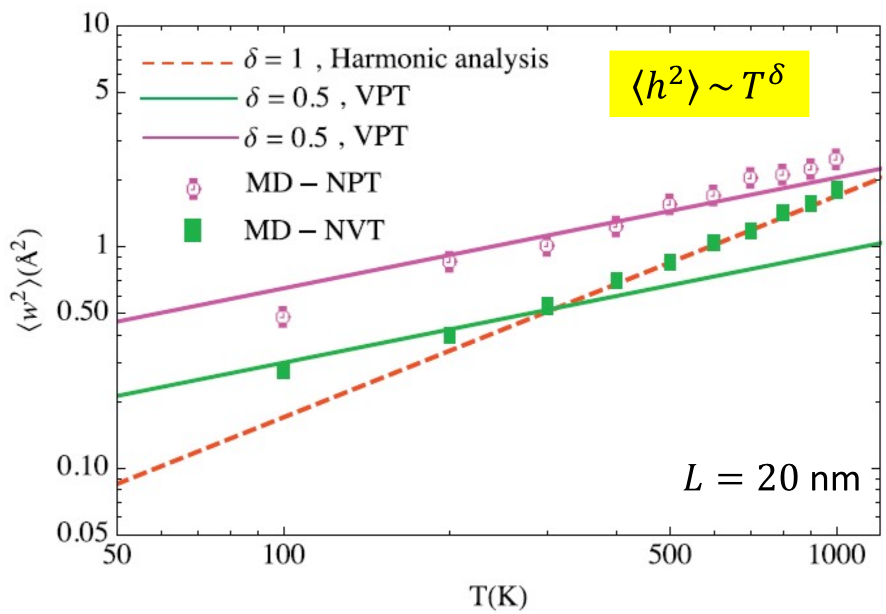

Variational perturbation theory (VPT): $\langle h^2 \rangle \sim L \sqrt{\dfrac{k_B T}{E_{2D}}}$

- Thermal rippling amplitude depends on the membrane size and temperature nonlinearly.
- Thermal rippling also depends on the boundary constraints (pre-strain, NVT vs NPT).

Ahmadpoor et al., JMPS 107, 294-310 (2017)

Free energy, Stress and Entropy

Boltzmann statistics: $P = \frac{1}{Z}\exp\left[-\frac{U}{k_B T}\right]$ $\quad Z = \int \exp\left[-\frac{U}{k_B T}\right]$

Helmholtz free energy: $A(\varepsilon, T, L_0) = -k_B T \ln Z$

Stress and Entropy: $\sigma = \frac{1}{L_0^2}\left(\frac{\partial A}{\partial \varepsilon}\right)_{T, L_0}$ $\quad S = -\left(\frac{\partial A}{\partial T}\right)_{\varepsilon, L_0}$

$$\sigma = E^* \varepsilon_0 - E^* \alpha_{2D} T + \tilde{\sigma}(\varepsilon_0, T, L_0)$$

Define rippling stress: $\tilde{\sigma} \approx \sigma - E^*(\varepsilon_0 - \alpha_{2D} T)$

Biaxially strained graphene (T = 300 K)

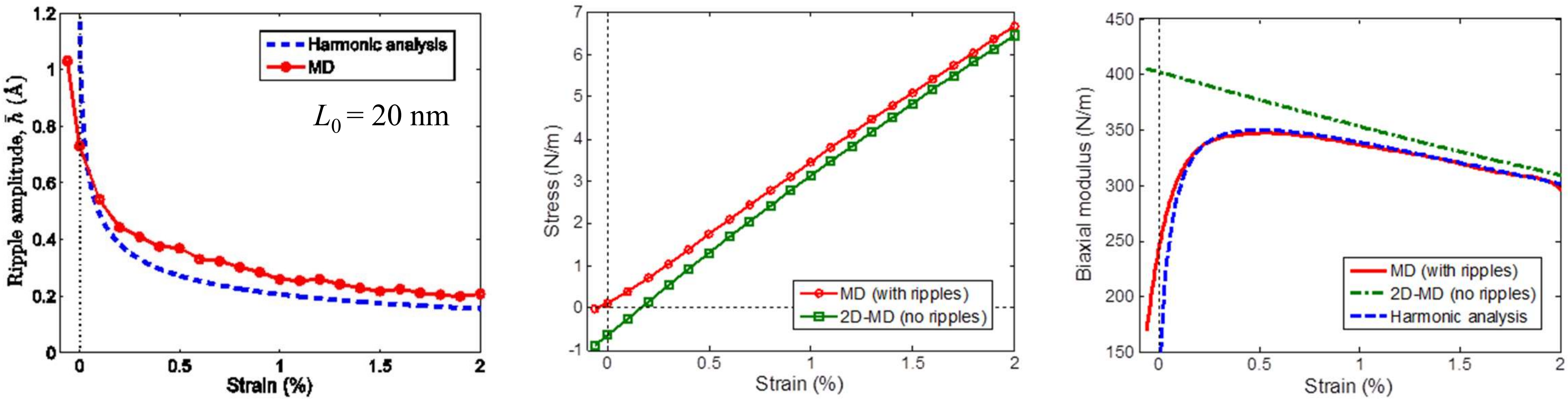

Nonlinear elasticity due to two effects:

(1) Strain *stiffening*, due to thermal rippling (small strain behavior)

(2) Strain *softening*, intrinsic large strain behavior (> 0.5%)

Gao and Huang, JMPS 66, 42-58, 2014.

Nonlinear Thermoelasticity:

Thermal Expansion and Thermal Stress

$$\boxed{\sigma(\varepsilon_0, T, L_0) = E^*(\varepsilon_0 - \alpha_{2D}T) + \tilde{\sigma}(\varepsilon_0, T, L_0)}$$

Stress-free thermal expansion (NPT):

$$\sigma = 0 \quad \Longrightarrow \quad \varepsilon = f(T, L_0) \approx \alpha_{2D}T \boxed{-\tilde{\varepsilon}(T, L_0)}$$

Rippling induced contraction

Thermal stress at zero strain (NVT):

$$\varepsilon_0 = 0 \quad \Longrightarrow \quad \sigma_T = -E^*\alpha_{2D}T \boxed{+\tilde{\sigma}(0, T, L_0)}$$

Rippling induced tension

NPT: Thermal Expansion/Contraction

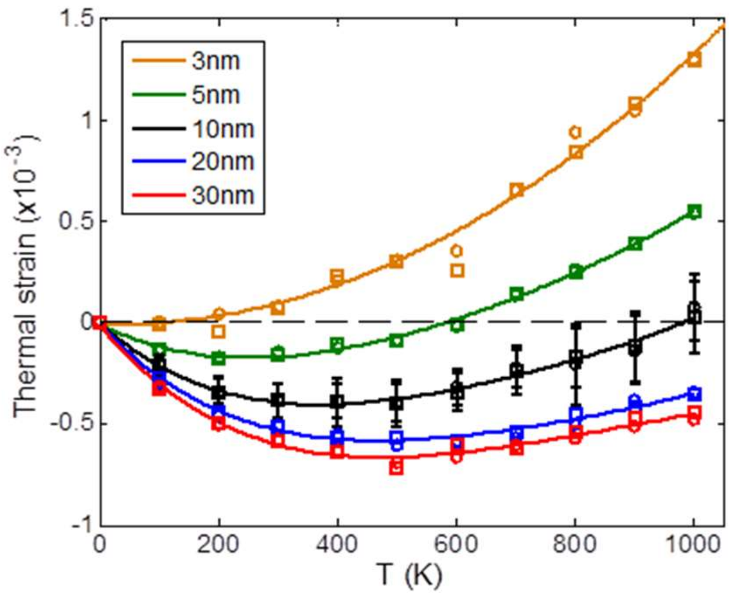

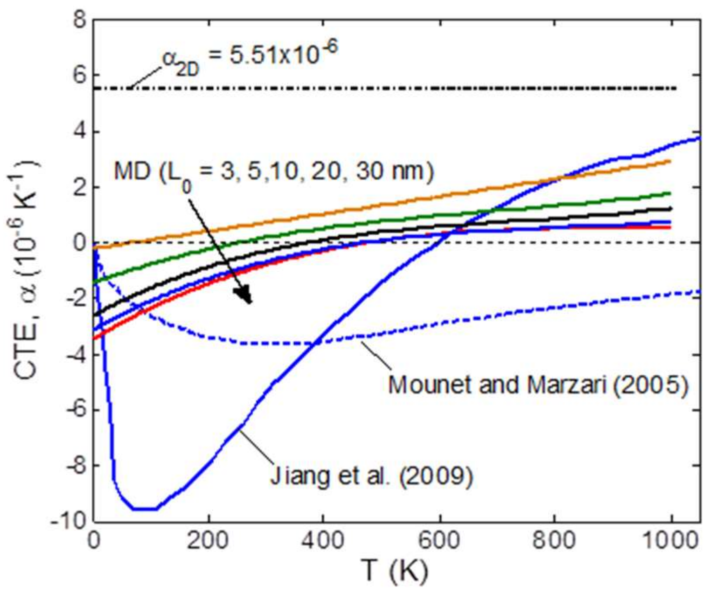

- Negative thermal expansion at low T, and positive at high T.
- Thermal expansion/contraction is size dependent!
- By suppressing out-of-plane fluctuations, 2D simulations predict a constant positive CTE (size-independent).

Gao and Huang, JMPS 66, 42-58, 2014.

NVT: Thermal Stress at Zero Strain

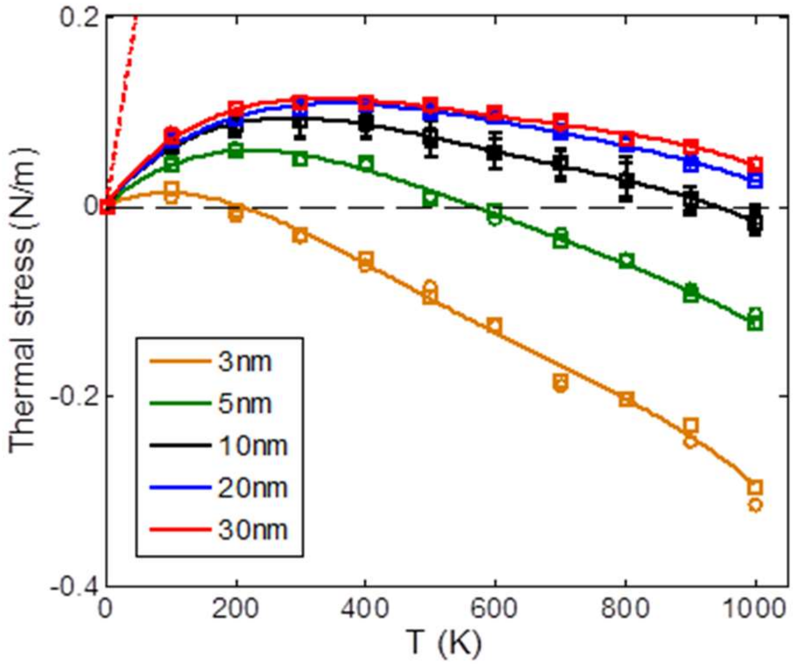

$$\sigma_T = -E^* \alpha_{2D} T + \tilde{\sigma}(0, T, L_0)$$

- Thermal rippling leads to a tensile stress that depends on size, which may be interpreted (qualitatively) as a result of negative thermal expansion.

Gao and Huang, JMPS 66, 42-58, 2014.

Effective Elastic Properties

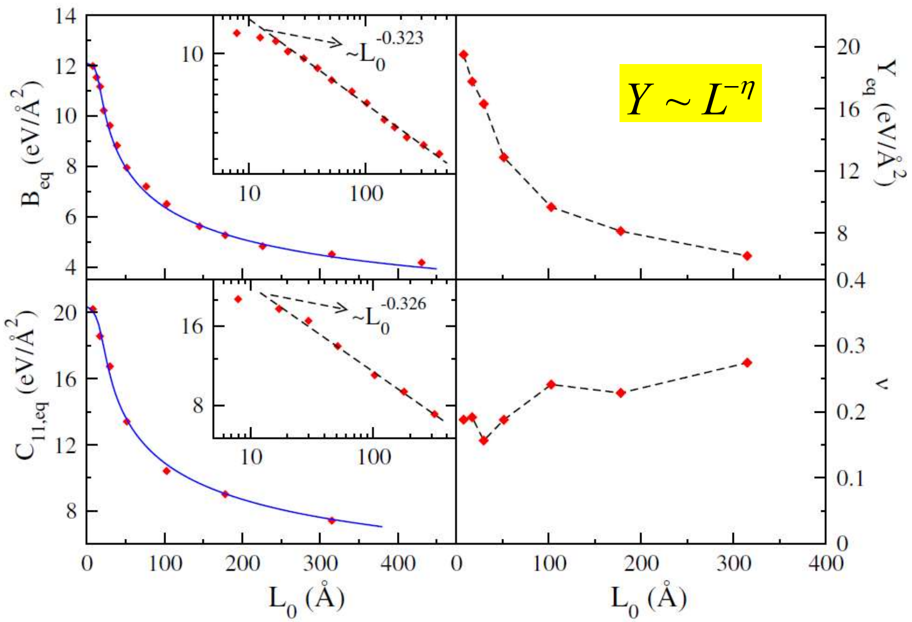

FIG. 3. Left panels: equilibrium bulk modulus B_{eq} and uniaxial modulus $C_{11,eq}$ as a function of L_0. The insets in log-log scale demonstrate the power law behavior. The solid lines are fits according to the expressions in Table I. Right panels: Young modulus Y_{eq} and Poisson ratio ν as a function of L_0. The dashed lines are guides to the eye.

- Both the statistical membrane theory and atomistic MC simulations predicted a power-law dependence of the in-plane elastic moduli of graphene on the size at a finite temperature.
- However, experimental data is lacking on the size and temperature dependence of the elastic properties for graphene and other 2D materials.

(Los et al, PRL 2016)

Effective Bending Moduli

Variational perturbation theory (VPT):

$$\langle h^2 \rangle \sim L\sqrt{\frac{k_B T}{E}} \sim L^2\left(\frac{k_B T}{D_{eff}}\right)$$

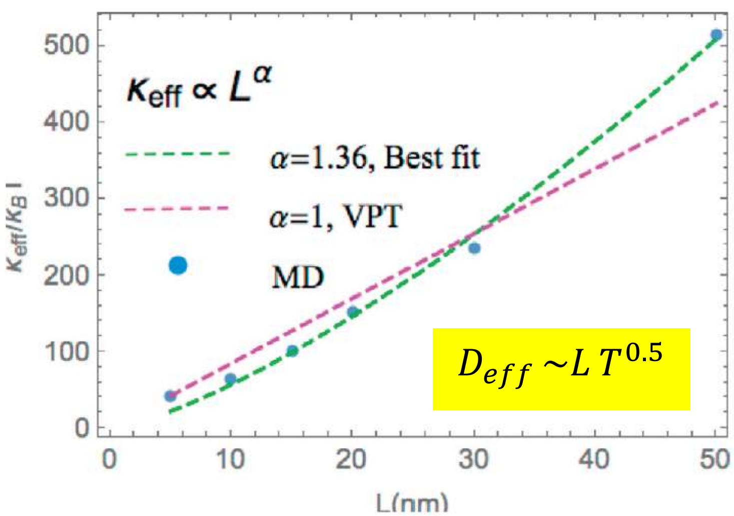

Ahmadpoor et al., JMPS 107, 294-310 (2017)

- A surprisingly high bending modulus for monolayer graphene was obtained by Blees et al. (2015), which was attributed to the effect of thermal rippling (Košmrlj and Nelson, 2016).

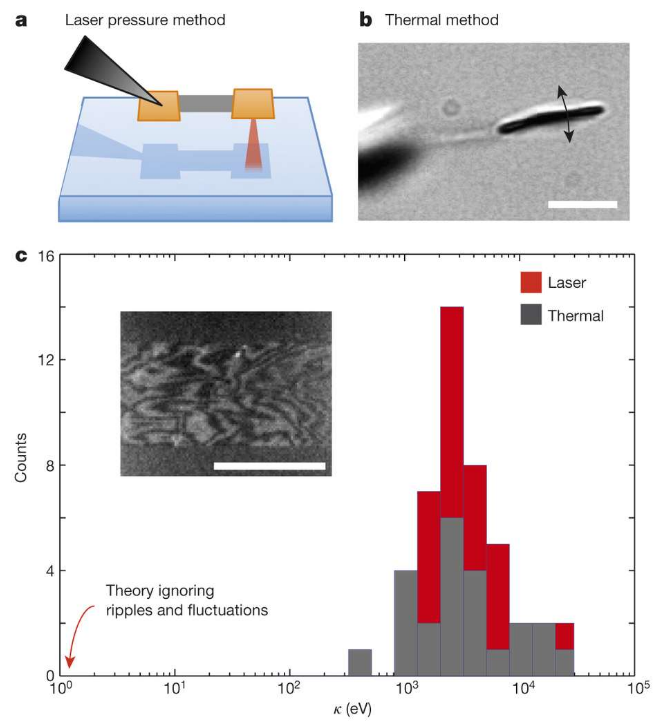

$$D_{eff}(L) \sim D_0\left(\frac{L}{l_{th}}\right)^{\eta}$$

$$\eta \sim 0.82 \quad l_{th} \sim 2nm$$

Beyond Linear Elasticity

- High-order elastic moduli for nonlinear elasticity
- Tensile strength, anisotropic (zigzag vs armchair)
- Fracture toughness (energy), brittle or ductile
- Effects of defects, grain boundaries, etc.

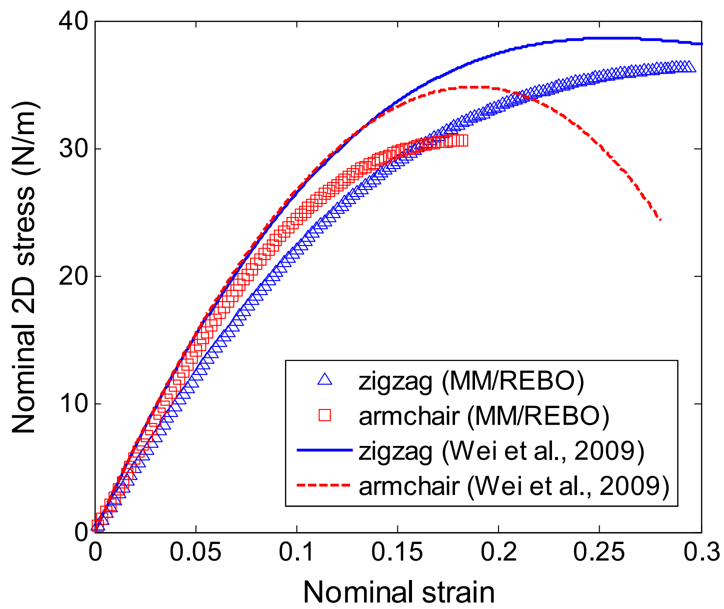

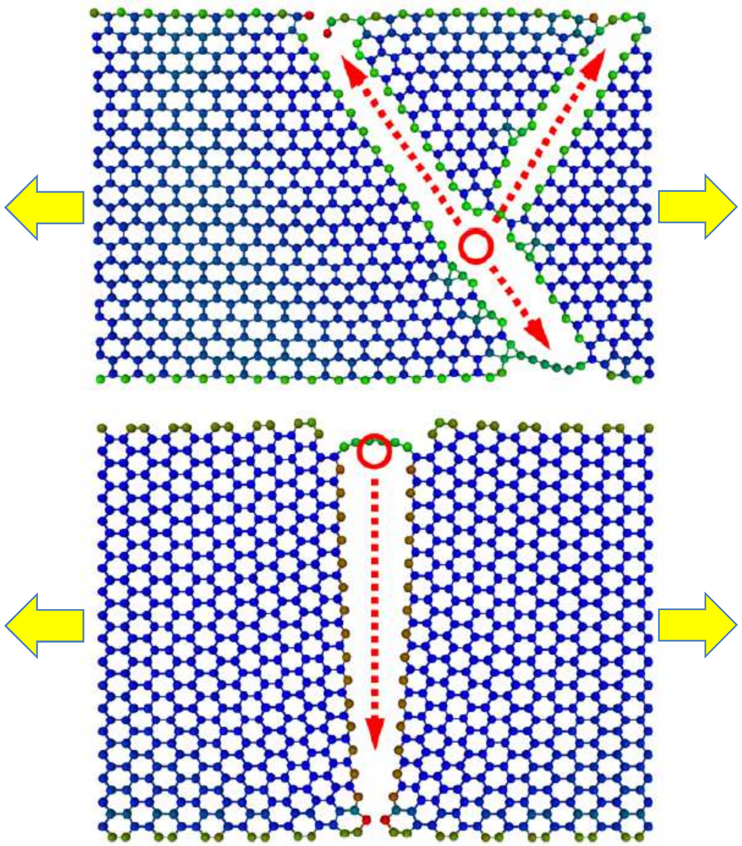

Lu et al., Modelling and Simulation in Materials Science and Engineering 19, 054006 (2011).

Graphene nanoribbons under uniaxial tension

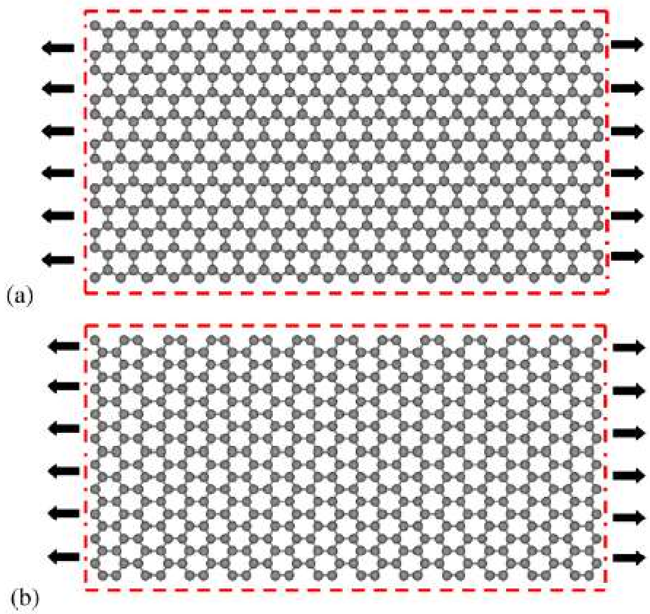

GNRs with unpassivated zigzag and armchair edges

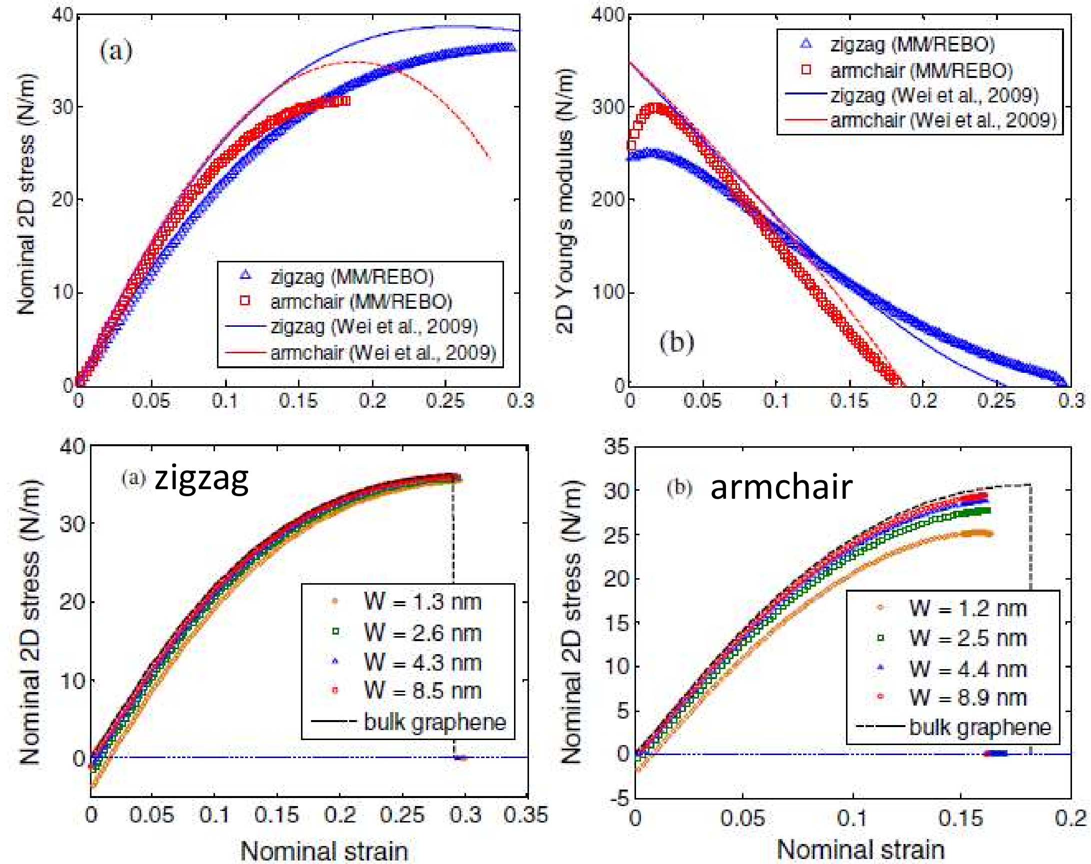

Lu et al., MSMSE19, 054006 (2011).

Size-dependent modulus and strength

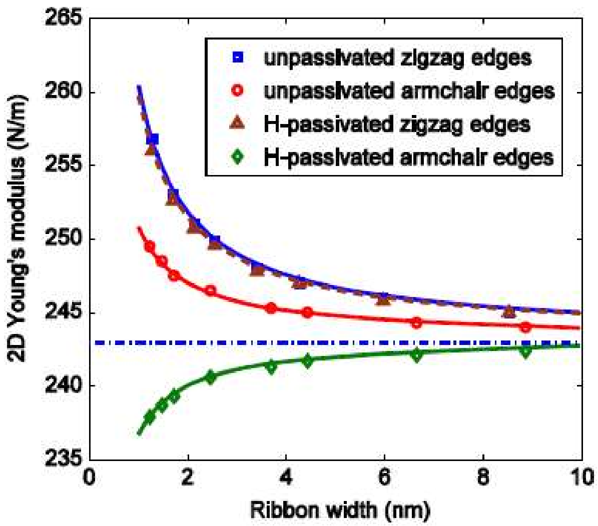

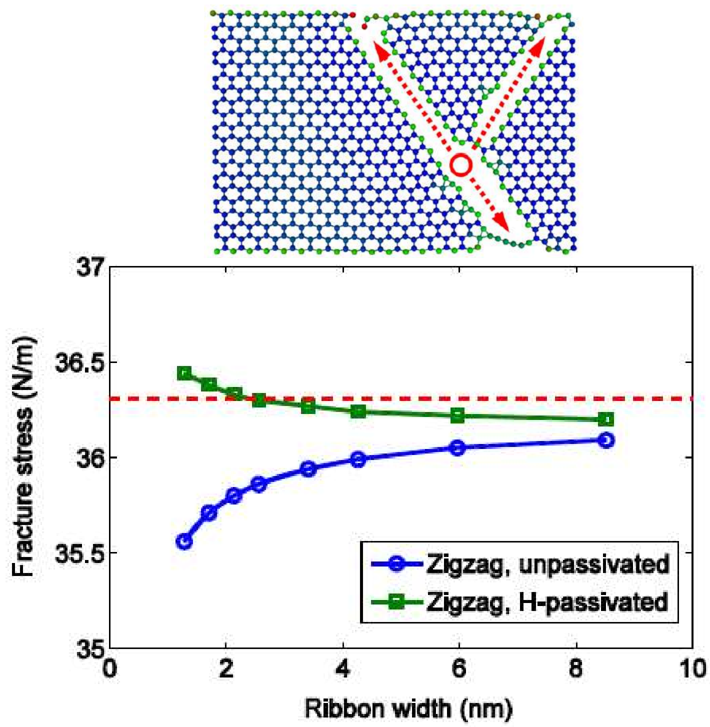

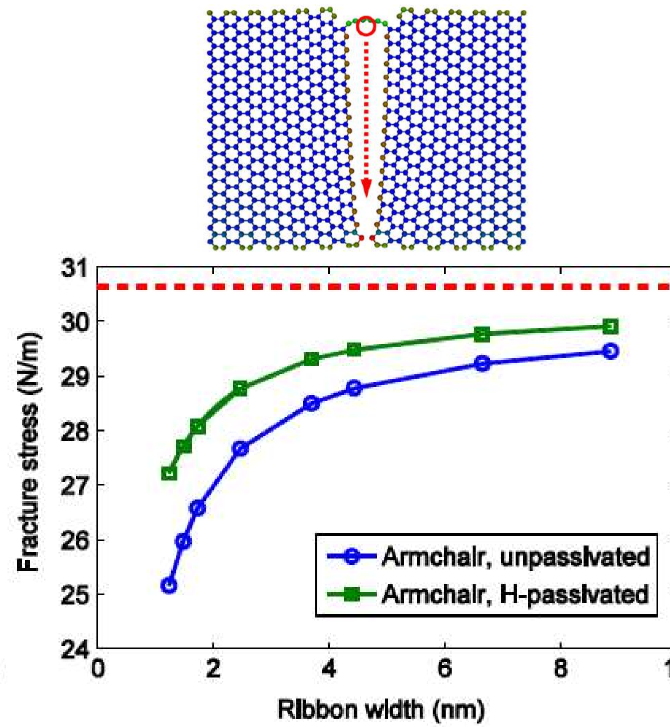

- ➢ The edge effects (e.g., passivation and reconstruction) lead to size-dependent elastic modulus and tensile strength of GNRs.

Lu et al., MSMSE19, 054006 (2011).

Fracture toughness measurements

Zhang et al, Nature Comm. 5:3782 (2014).

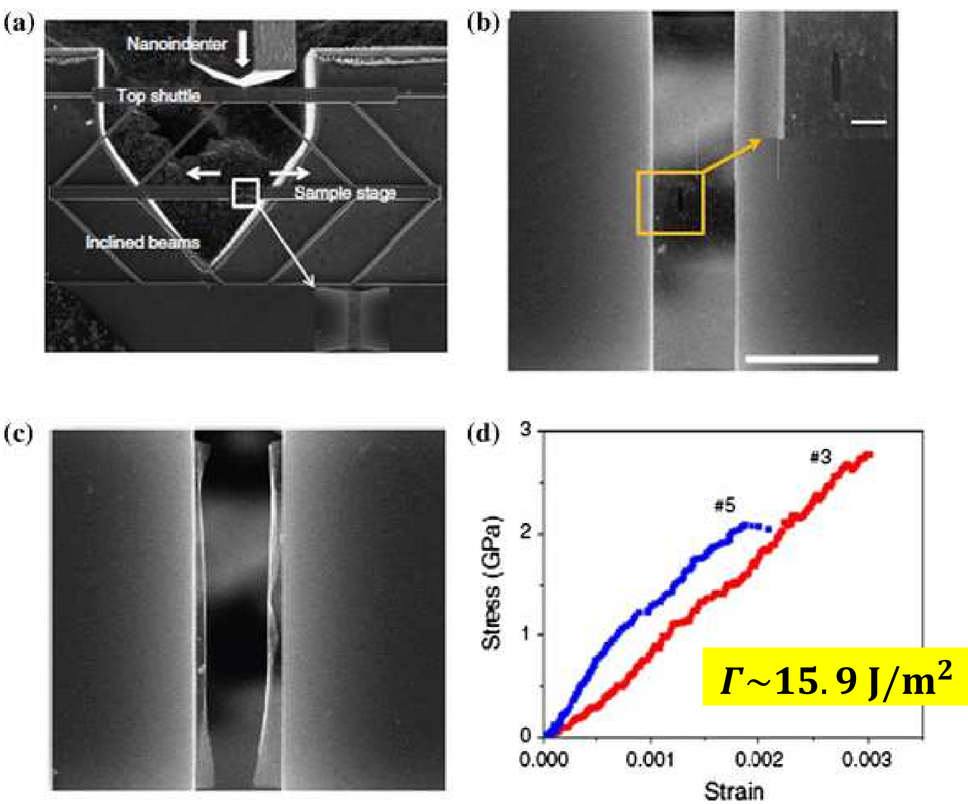

Na et al, ACS Nano 10, 9616-9625 (2016).

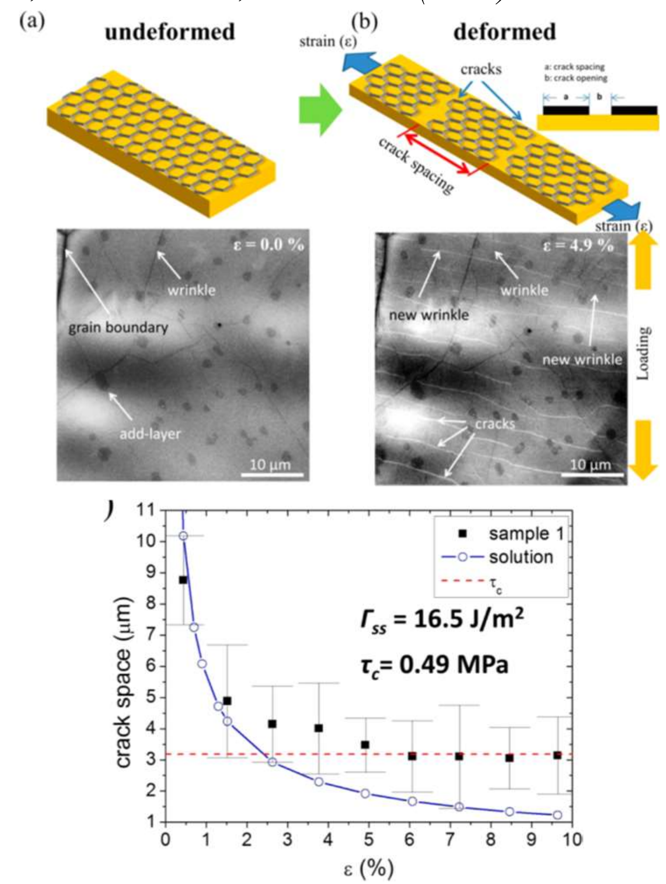

Mechanics of brittle fracture

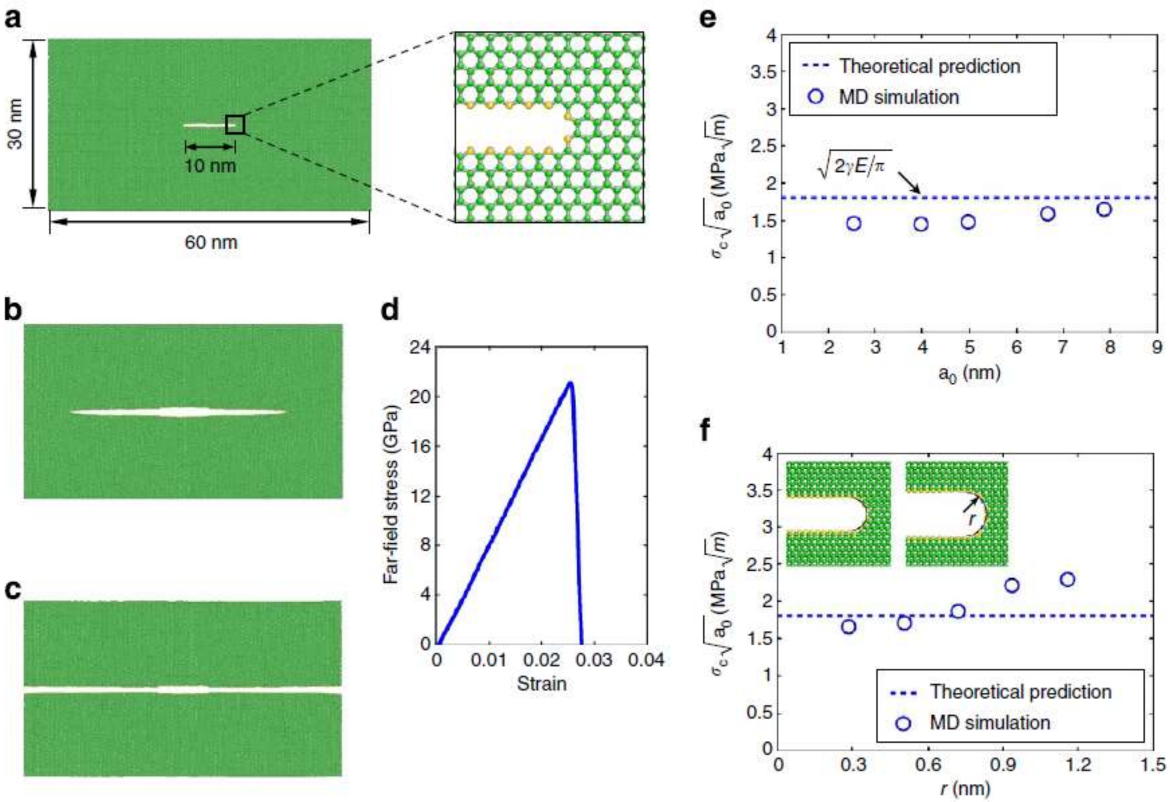

Zhang et al, Nature Comm. 5:3782 (2014).

Fracture stress by Griffith criterion

$$\sigma_c = \sqrt{\frac{E\Gamma}{\pi a_0}}$$

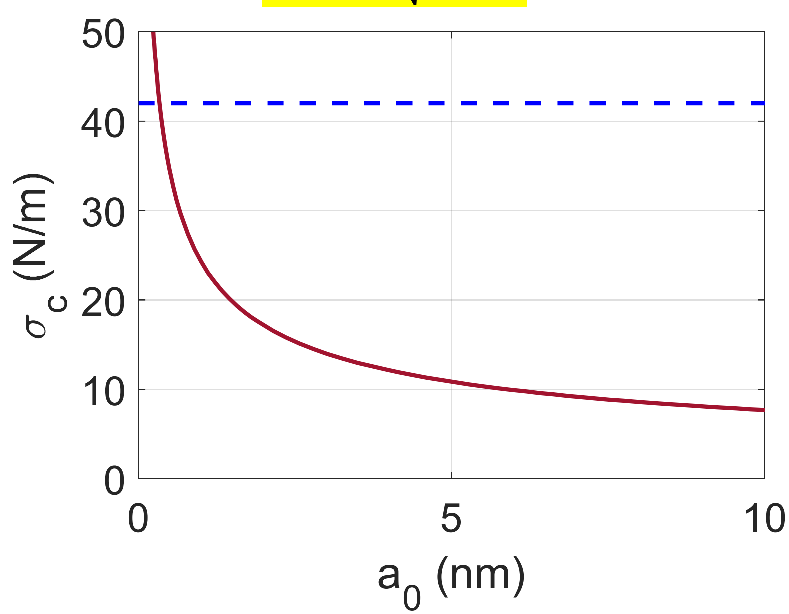

Toughening Mechanisms

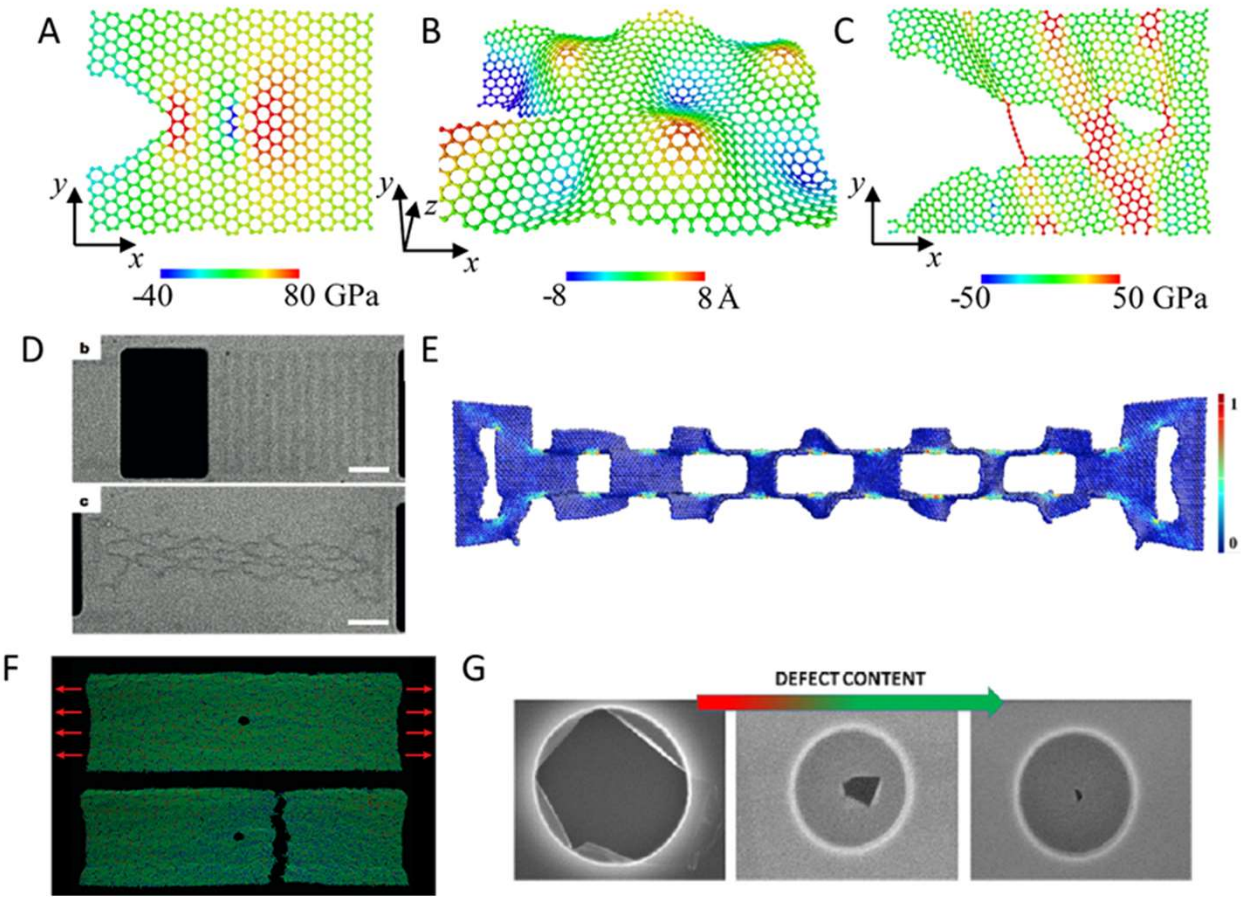

- 2D materials are typically brittle
- Various defect engineering approaches may enhance the toughness of 2D materials
- Polycrystalline graphene could be tougher than pristine graphene (depending on the grain size).
- The strength of nanocrystalline graphene could become insensitive to the pre-existing flaw.
- Some concentration of defects can change the catastrophic failure of a pristine graphene to a localized failure mode under a nanoindenter.

Current Opinion in Solid State & Materials Science 24 (2020) 100837

Contents lists available at ScienceDirect

Current Opinion in Solid State & Materials Science

journal homepage: www.elsevier.com/locate/cossms

Mechanics at the interfaces of 2D materials: Challenges and opportunities

Zhaohe Dai, Nanshu Lu, Kenneth M. Liechti, Rui Huang*

Department of Aerospace Engineering and Engineering Mechanics, University of Texas, Austin, TX 78712, United States

Part II: Mechanical interactions between 2D materials

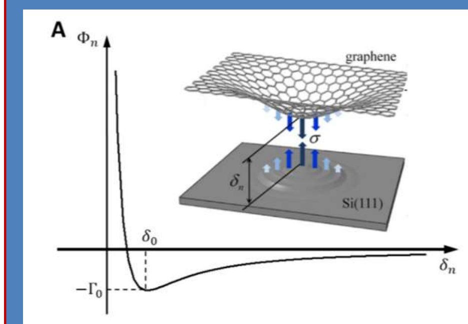

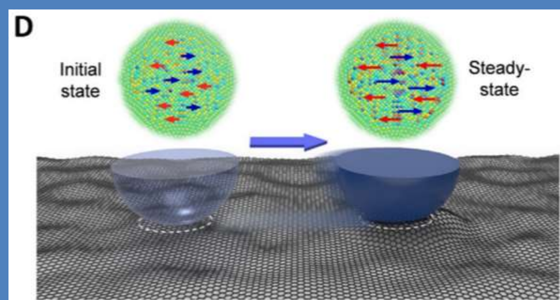

2D-3D interactions
- **Adhesion**
- **Friction and shear**
- **Mixed mode interactions**

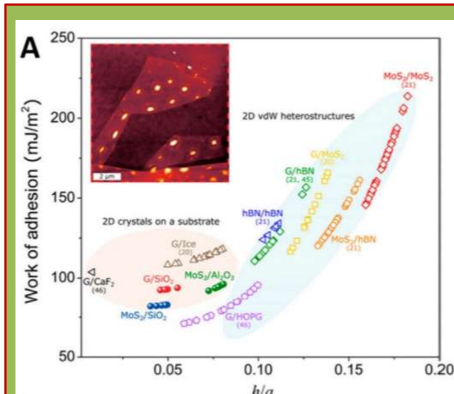

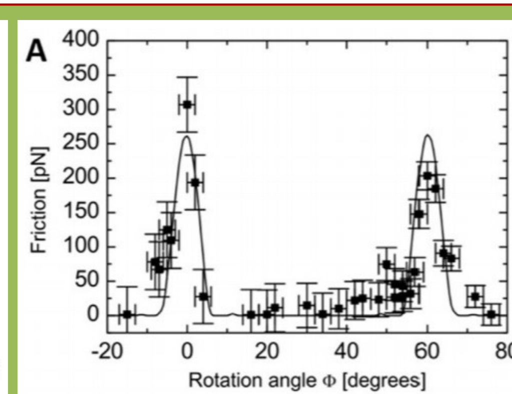

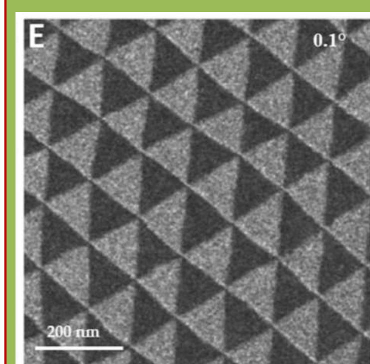

2D-2D (interlayer) interactions
- **Adhesion/compression**
- **Friction (superlubricity) and shear**
- **Interlayer phenomena (moiré)**

Adhesion experiments

Koenig et al., Nature Nanotech. 6, 543–546 (2011)

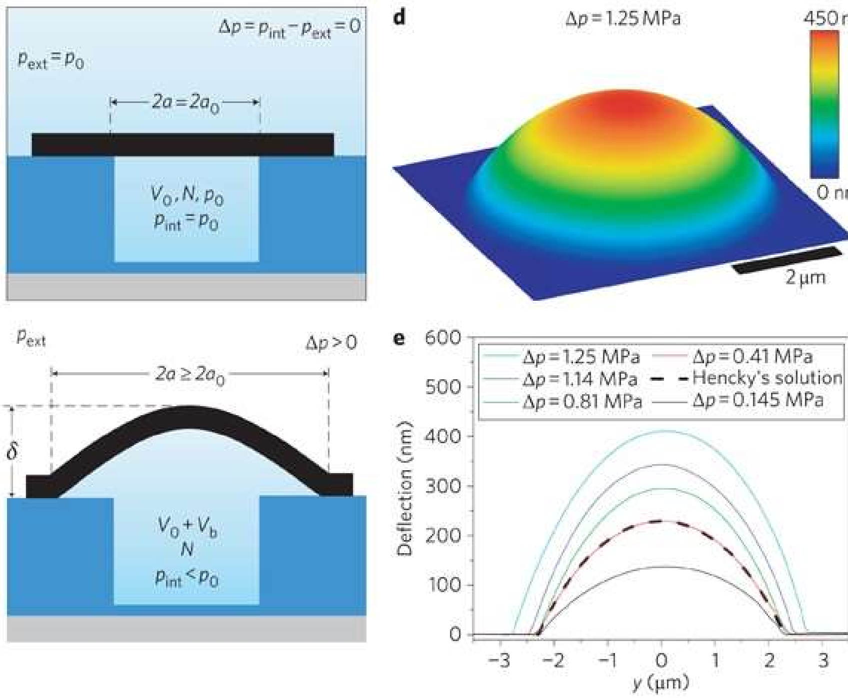

Jiang and Zhu, Nanoscale 7 (2015) 10760–10766.

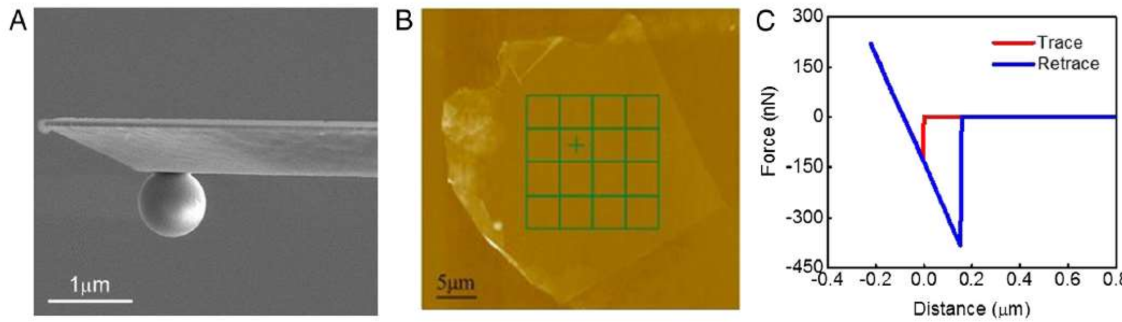

- Bubbles/blisters
- Nanoindentation
- DCB

Na, et al., ACS Nano 8 (2014) 11234–11242.

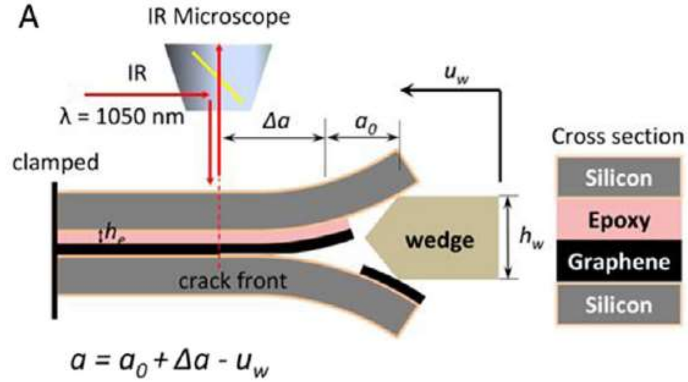

➢ In addition to adhesion energy, the adhesive interactions can be described by a traction-separation relation (with hysteresis).

Friction experiments

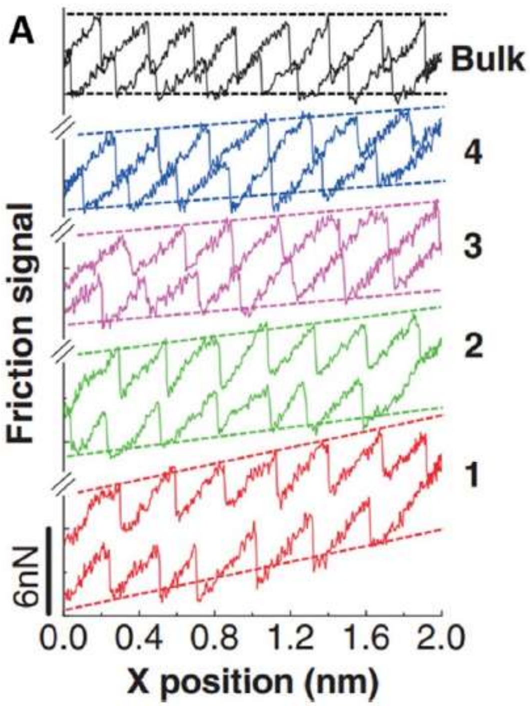

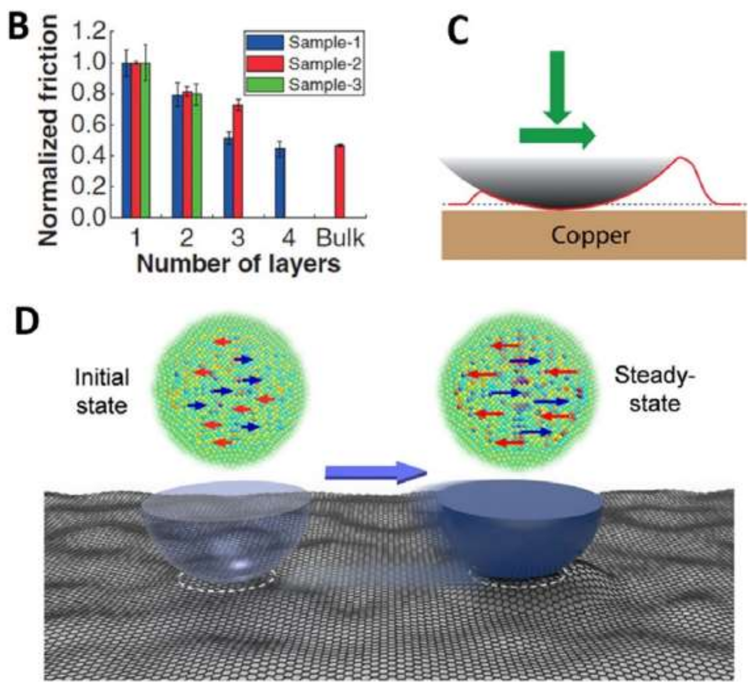

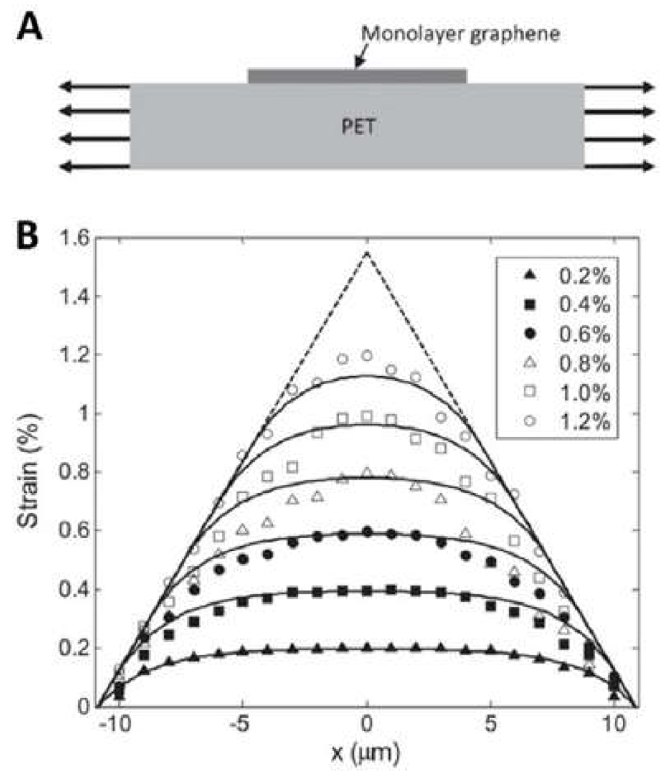

- ➢ Friction force microscopy (FFM): friction signal/force, friction coefficients (?)
- ➢ Sliding of 2D materials on substrates: shear strength, traction-separation relation (?)

Coupling adhesion and friction: mixed-mode interactions

Egberts, et al. ACS Nano 8: 5010-5021 (2014).

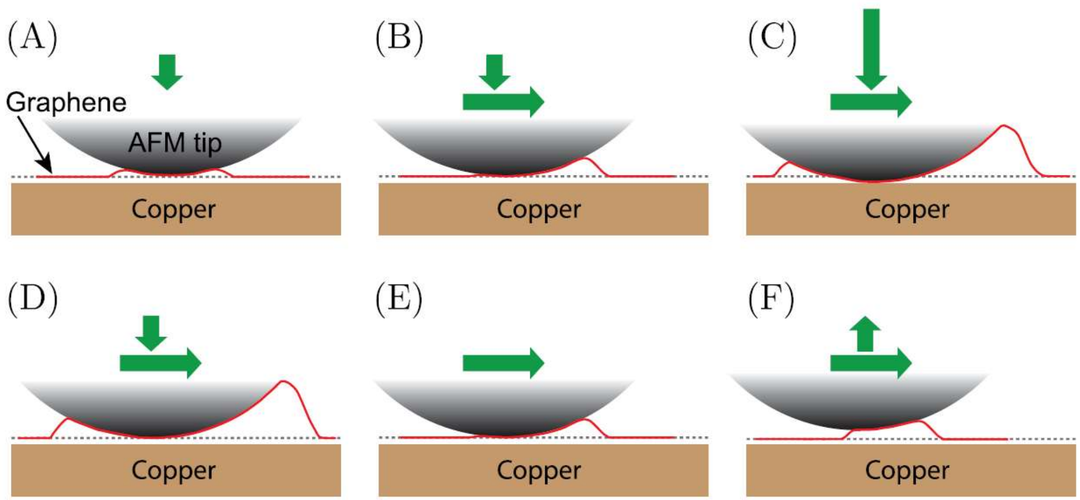

- FFM experiment: indentation-sliding-retraction
- Pressurized bubble/blister: inherently mixed-mode

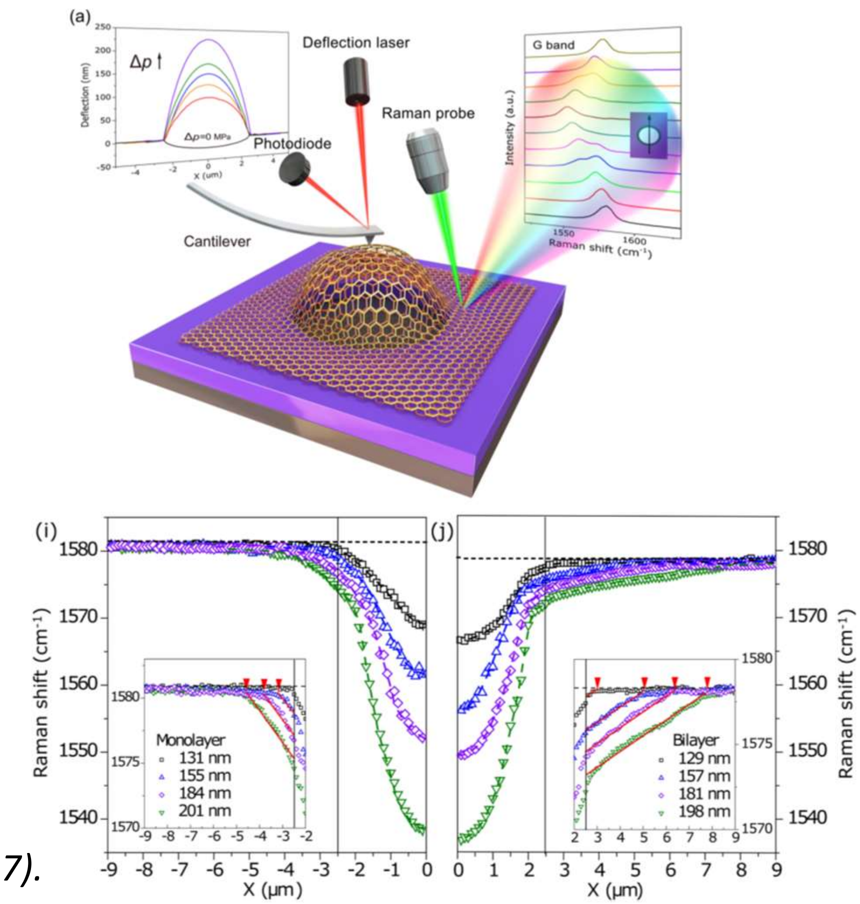

Wang et al., PRL 119, 036101 (2017).

2D-2D interlayer adhesion: normal interactions

- Primarily van der Waals interactions
- Binding energy from DFT: 20 to 120 meV/atom
- Adhesion energy: ~ 100 mJ/m^2
- Interlayer separation: 3-7 Å

- How to measure the adhesion energy?
- How to characterize the normal interactions?

Traction-separation relation:

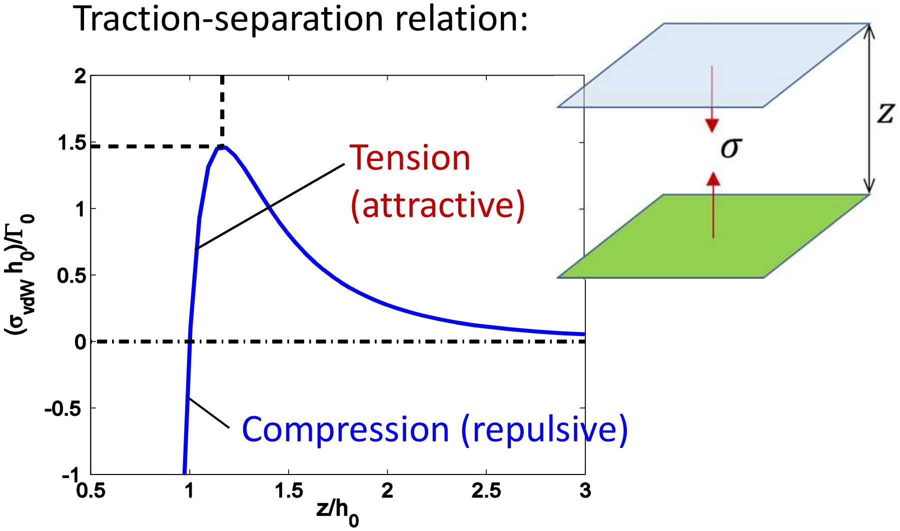

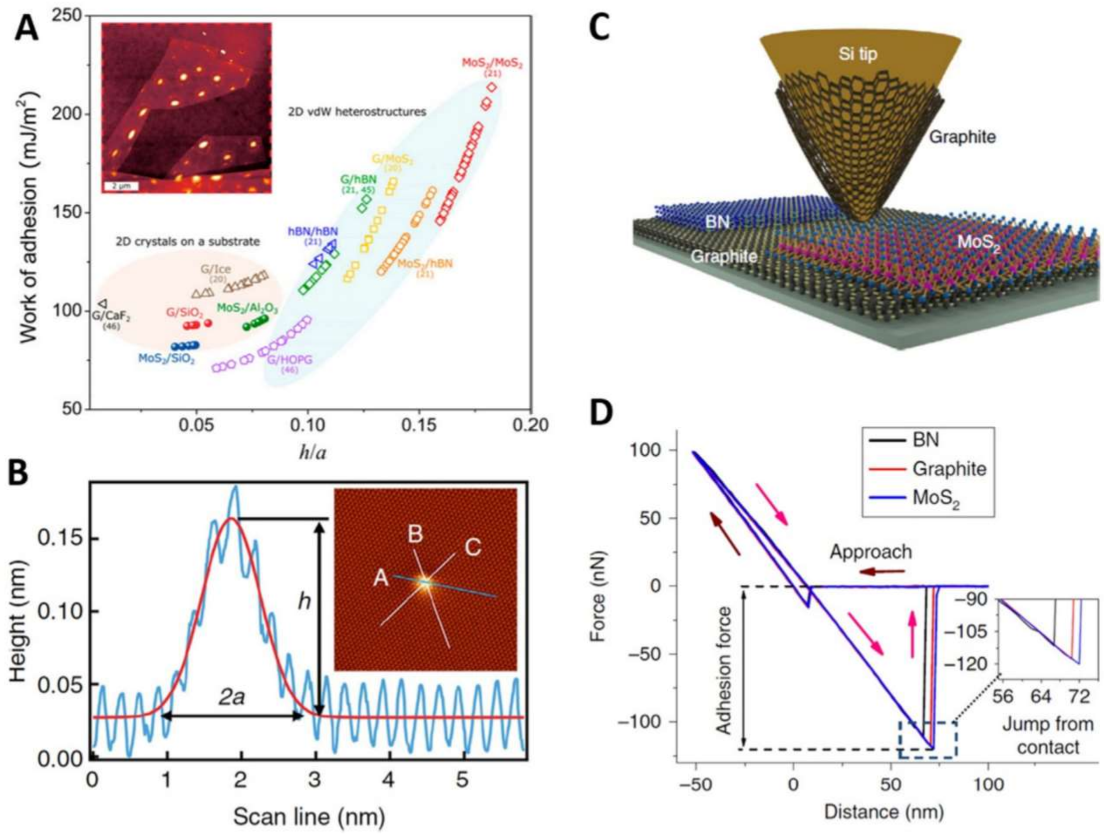

Interlayer friction: shear interactions

- Generally low friction (friction coefficient < 0.01)
- Superlubricity
- Commensurate/incommensurate stacking

- Interlayer shear strength (~0.04 MPa for G/G)

- Friction is more than just shear interactions, depending on adhesion and deformation of the 2D layers.

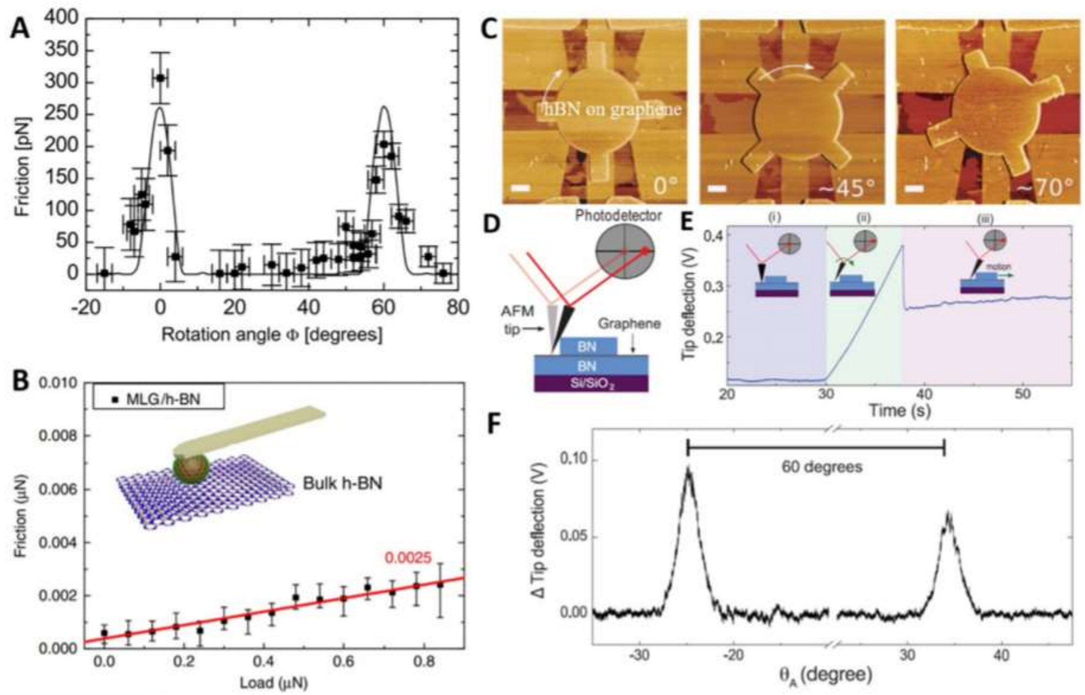

Shear traction-separation relations

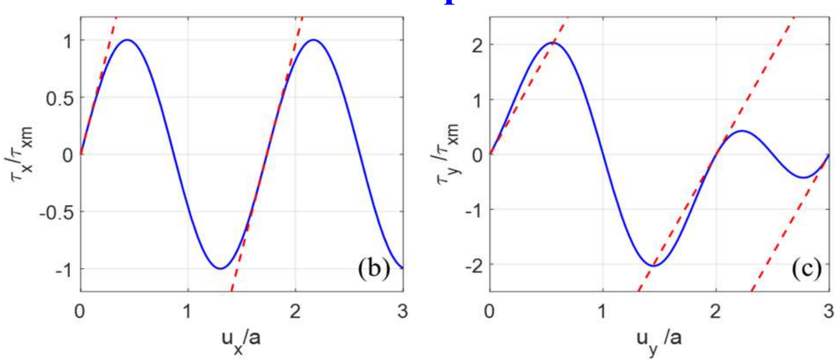

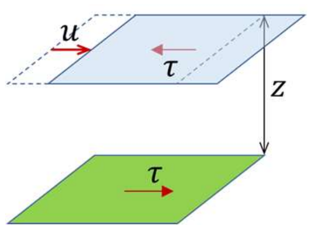

Dienwiebel, et al., Phys. Rev. Lett. 92 (2004) 126101.
Ribeiro-Palau, et al., Science 361 (2018) 690–693.
Liu, et al., Nat. Commun. 8 (2017) 14029.

Micro/nano-bubbles of 2D materials

Bunch et al, 2011-2013

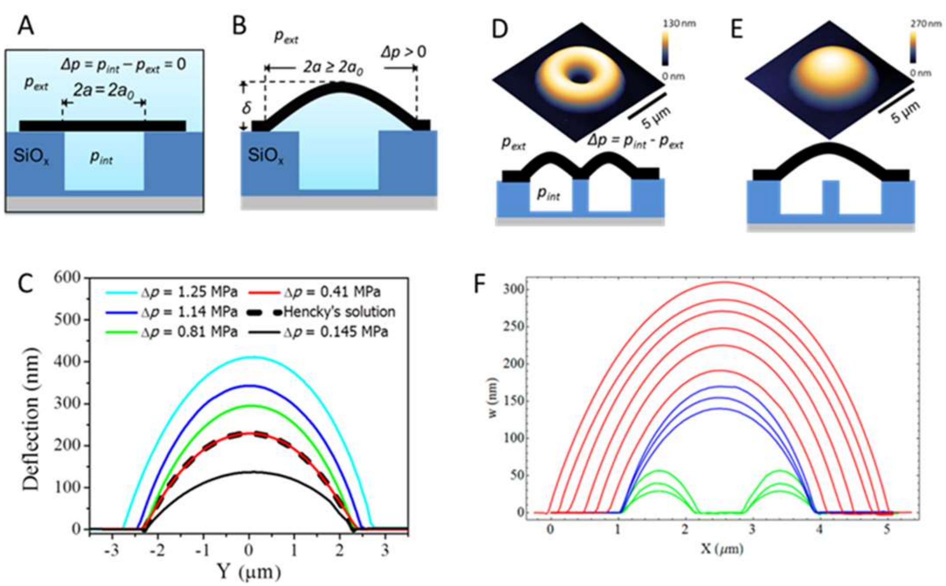

Levy et al, 2010

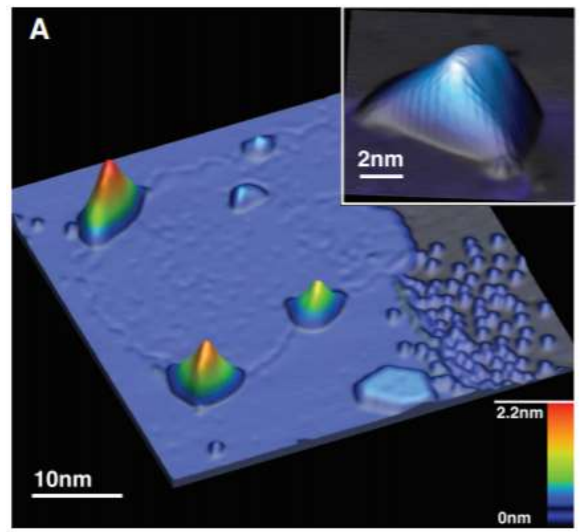

Darlington et al, 2020

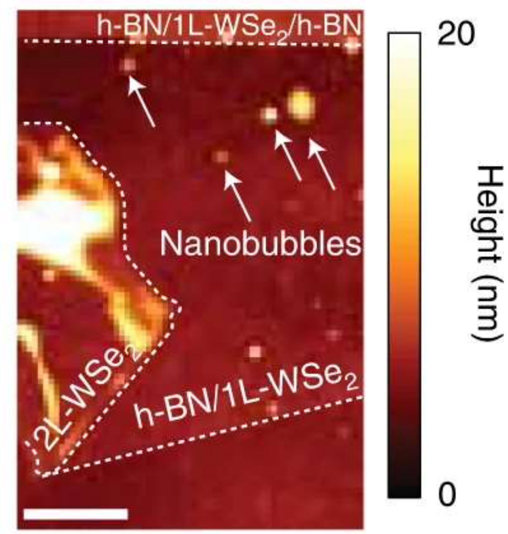

- Measuring interfacial/interlayer adhesion
- Measuring interfacial/interlayer shear strength
- Measuring elastic and bending moduli of multilayers
- Strain engineering (e.g., pseudo-magnetic fields, quantum emitters)

Adhesion of 2D materials from spontaneously formed bubbles

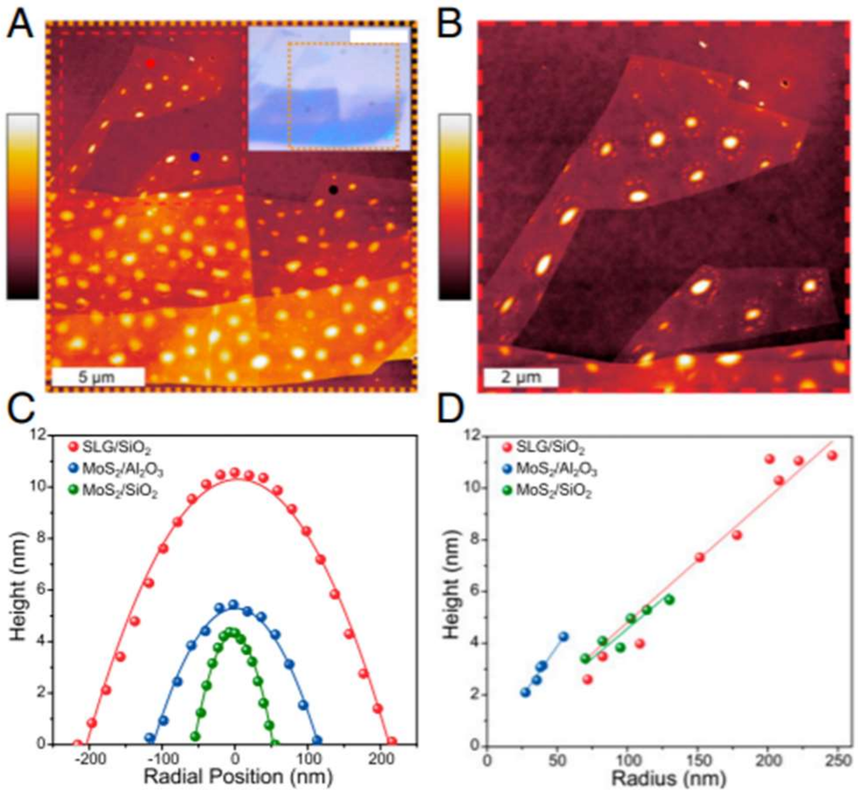

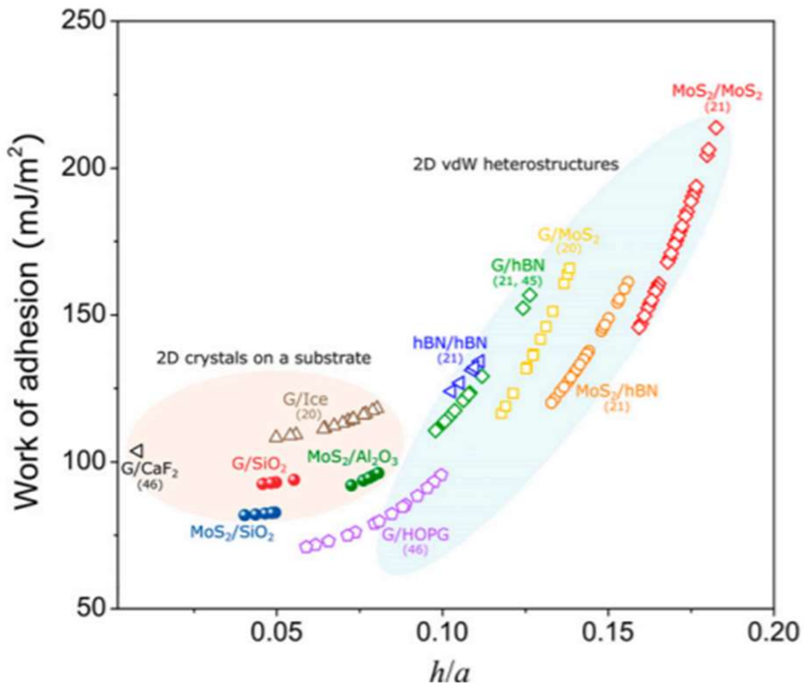

Elastocapillary: $$\Gamma = \frac{E_{2D} h^4}{\phi a^4} + \gamma_w (\cos\theta_m + \cos\theta_s)$$

Sanchez et al., PNAS 115, 7884-7889 (2018)

Water-filled graphene bubbles

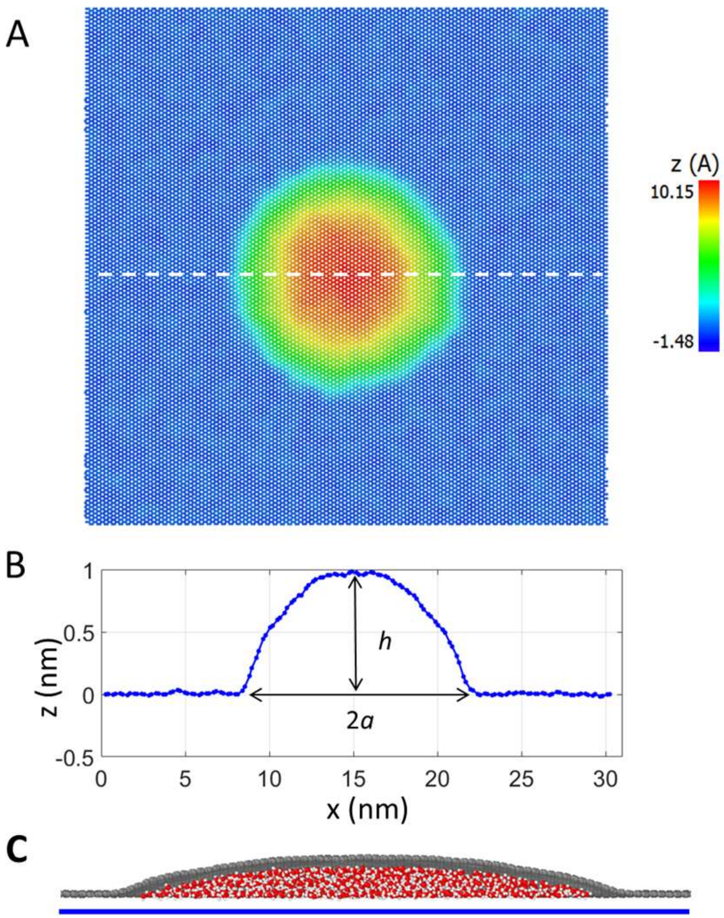

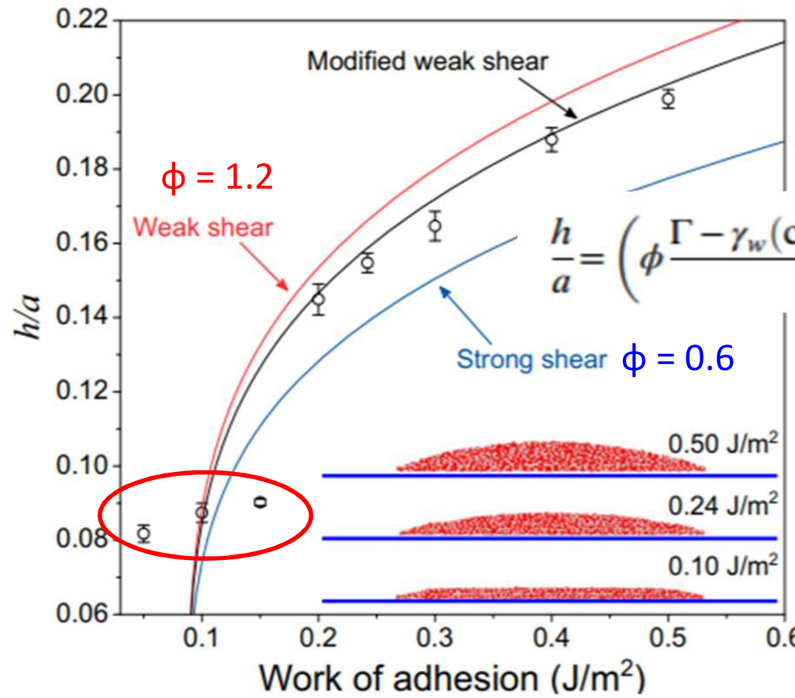

$$\frac{h}{a} = \left(\phi \frac{\Gamma - \gamma_w(\cos\theta_m + \cos\theta_s)}{E_{2D}}\right)^{1/4}$$

A continuum model predicts the aspect ratio as a function of the adhesion energy, independent of the number of water molecules.

Sanchez et al., PNAS 115, 7884-7889 (2018)

However, the continuum model breaks down when the adhesion is too weak or the number of water molecules is too small.

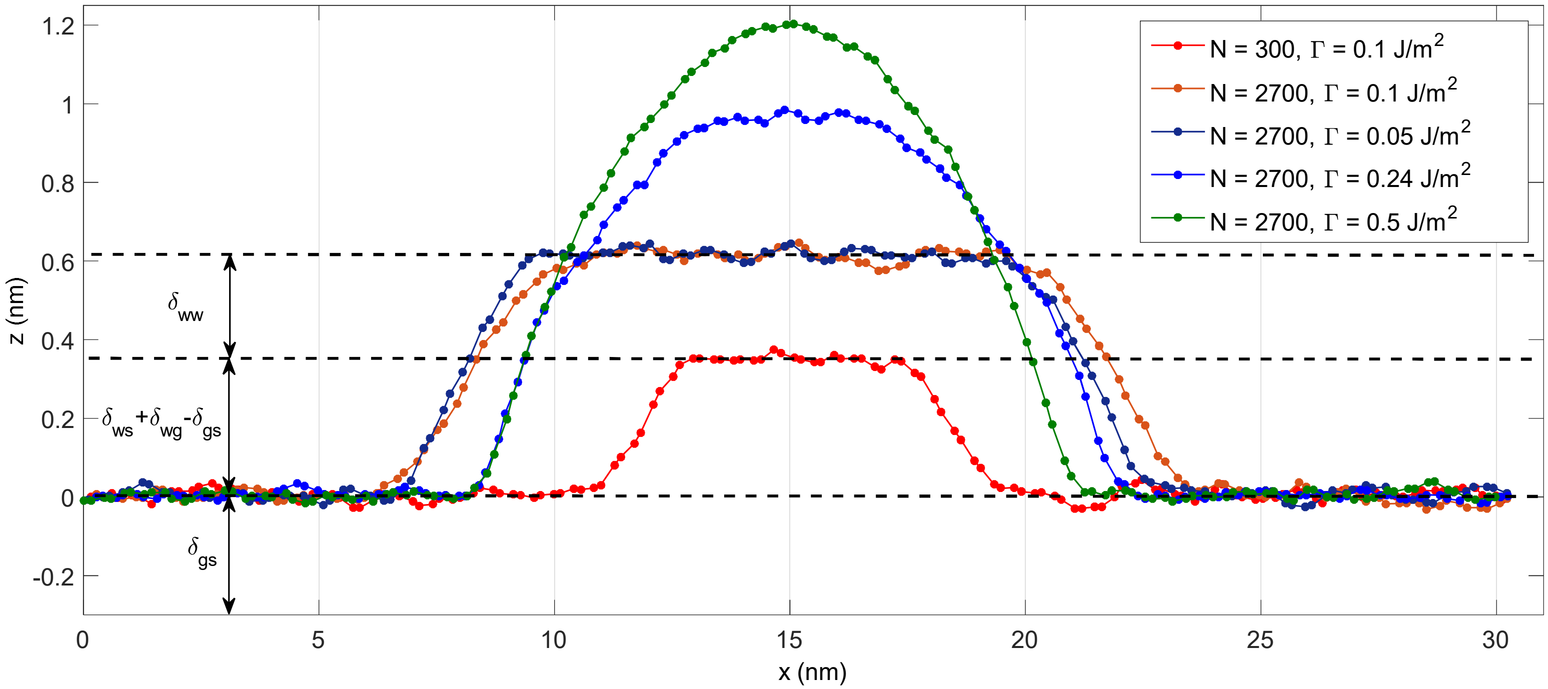

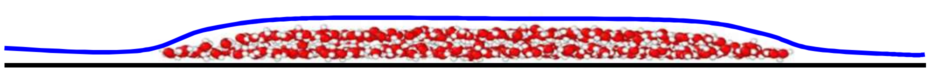

Sanchez et al., PNAS 115, 7884-7889 (2018)

Interlayer shear in bilayer graphene

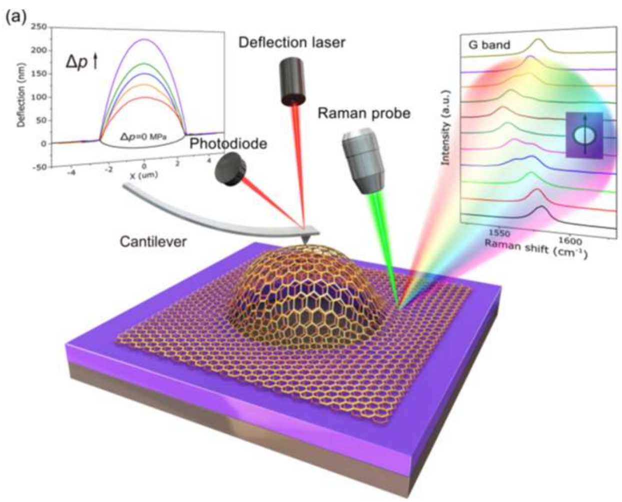

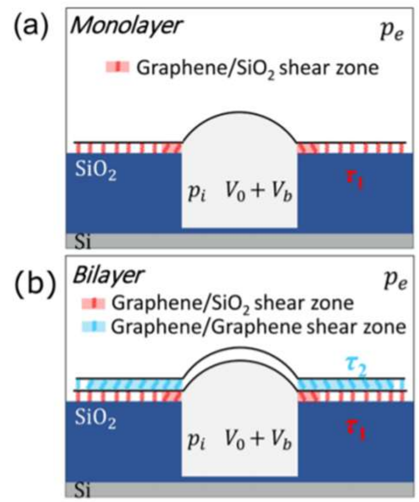

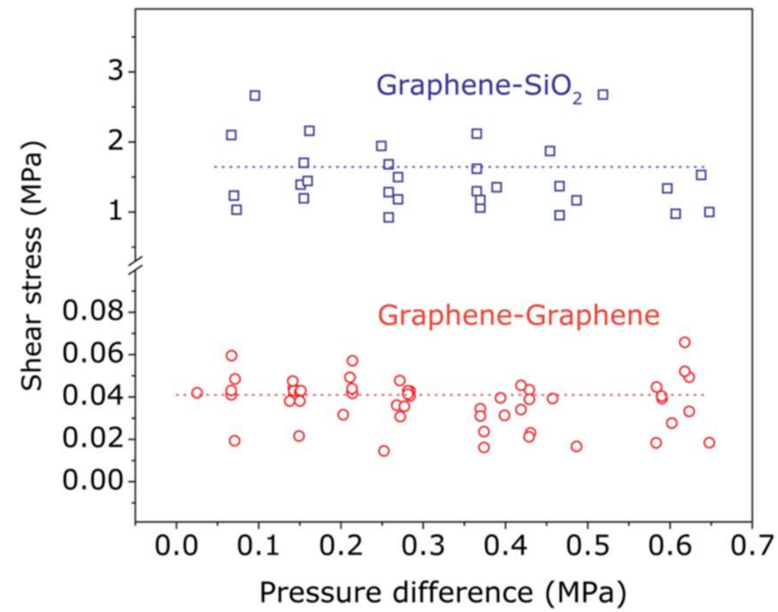

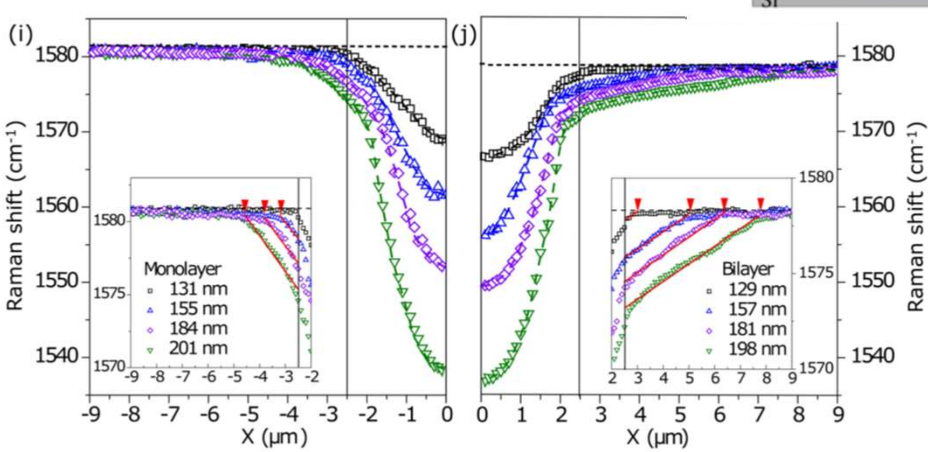

- ➢ More sliding of bilayer graphene due to weaker interlayer shear strength.

Wang et al., PRL 119, 036101 (2017).

Strain distributions and wrinkles

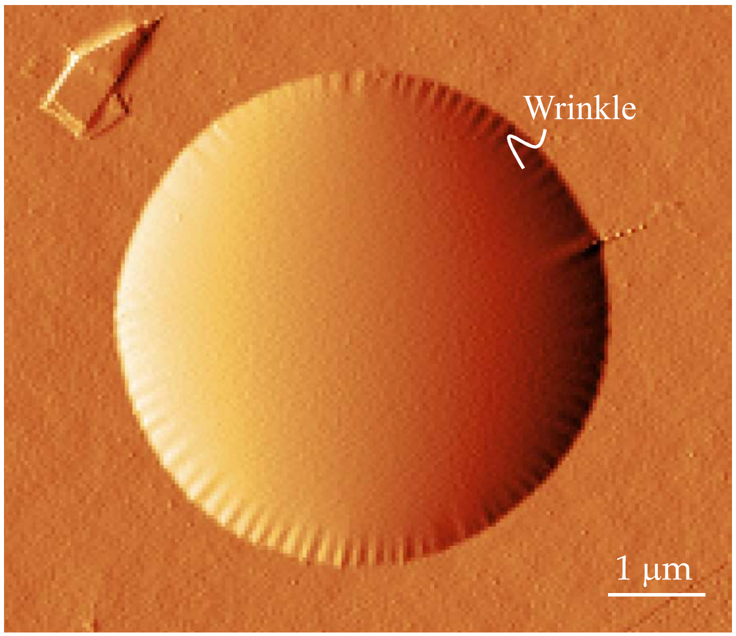

AFM image of a bilayer graphene bubble (Dai and Lu, JMPS 2021)

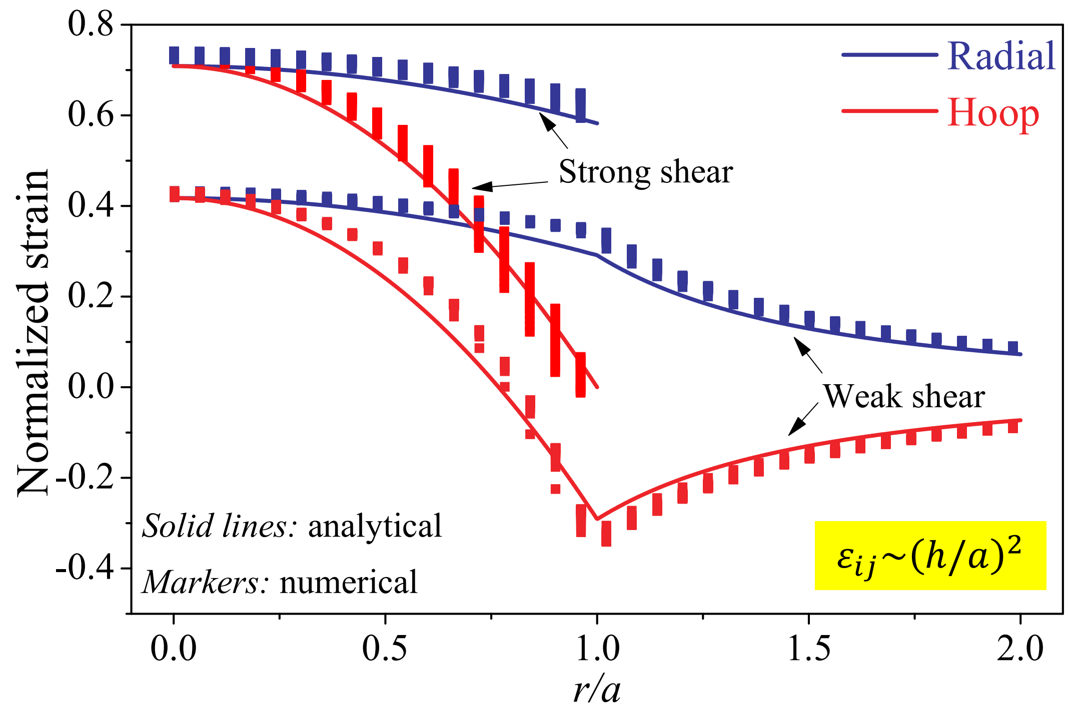

The interfacial sliding and wrinkling could considerably affect the strain distributions in bubbles of 2D materials.

Peeling and sliding of graphene nanoribbons

SCIENCE 351 (6276), 957-961, 2016.

Superlubricity of graphene nanoribbons on gold surfaces

Shigeki Kawai,[1,2*†] Andrea Benassi,[3,4*†] Enrico Gnecco,[5,6] Hajo Söde,[3] Rémy Pawlak,[1] Xinliang Feng,[7] Klaus Müllen,[8] Daniele Passerone,[3] Carlo A. Pignedoli,[3] Pascal Ruffieux,[3] Roman Fasel,[3,9] Ernst Meyer[1]

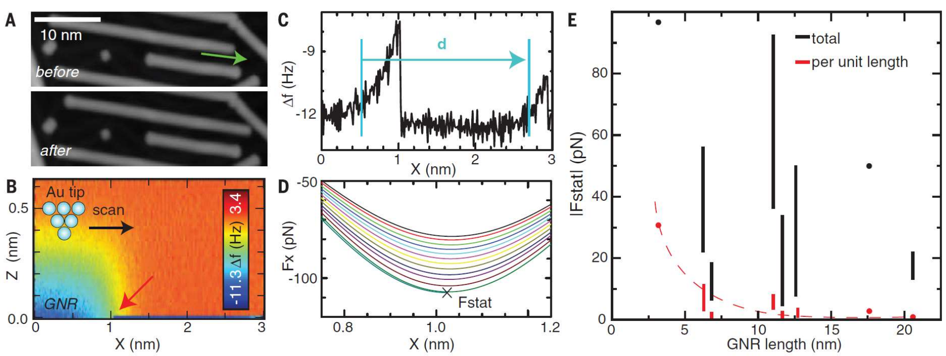

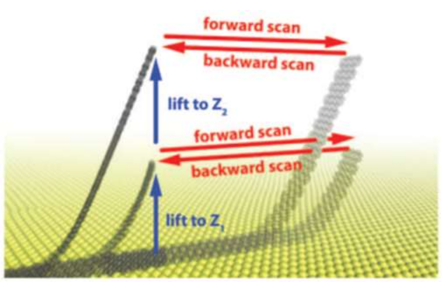

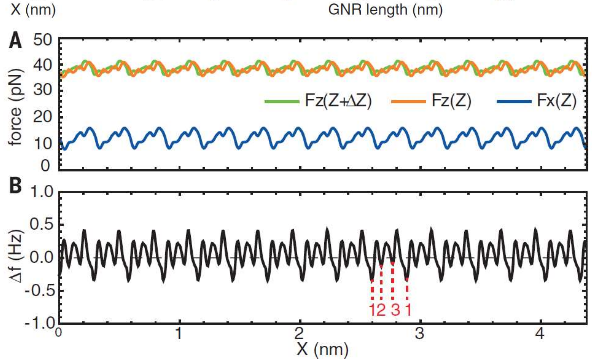

Nanoscale

PAPER
View Article Online
View Journal | View Issue

Check for updates

Cite this: *Nanoscale*, 2018, **10**, 2073

Lifted graphene nanoribbons on gold: from smooth sliding to multiple stick-slip regimes†

L. Gigli,[a] N. Manini,[b] E. Tosatti,[a,c,d] R. Guerra[b,e] and A. Vanossi[d,a]

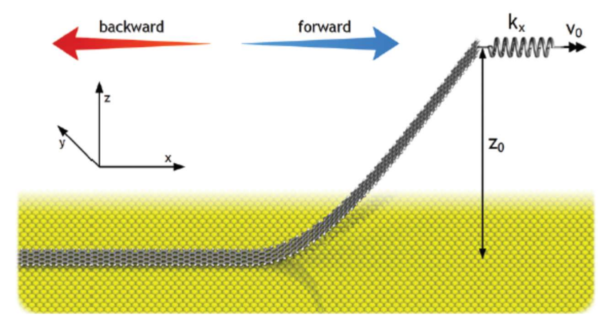

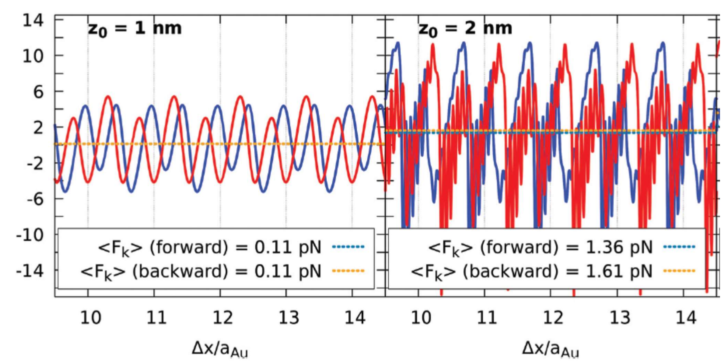

Peeling and sliding of GNRs

ACS NANO Cite This: ACS Nano 2019, 13, 689–697 www.acsnano.org

Detachment Dynamics of Graphene Nanoribbons on Gold

Lorenzo Gigli,[*,†] Shigeki Kawai,[*,‡] Roberto Guerra,[§,∥] Nicola Manini,[§] Rémy Pawlak,[⊥] Xinliang Feng,[#] Klaus Müllen,[⊗] Pascal Ruffieux,[∇] Roman Fasel,[∇] Erio Tosatti,[†,Δ,%] Ernst Meyer,[⊥] and Andrea Vanossi[*,†,Δ]

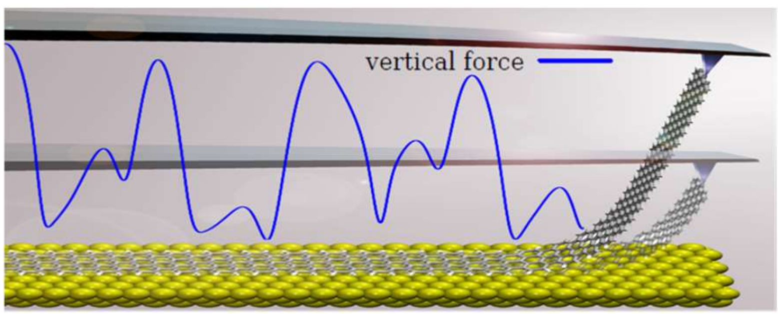

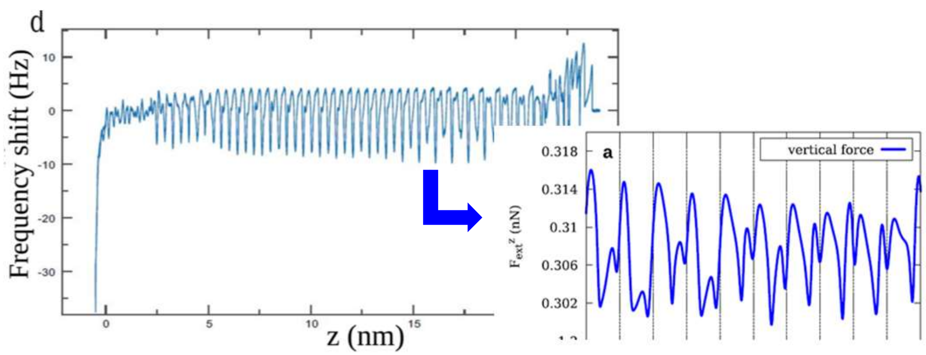

NANO LETTERS Letter Cite This: Nano Lett. 2018, 18, 6009–6016 pubs.acs.org/NanoLett

Nanoserpents: Graphene Nanoribbon Motion on Two-Dimensional Hexagonal Materials

Wengen Ouyang, Davide Mandelli, Michael Urbakh,[*] and Oded Hod

School of Chemistry and The Sackler Center for Computational Molecular and Materials Science, Tel Aviv University, Tel Aviv 6997801, Israel

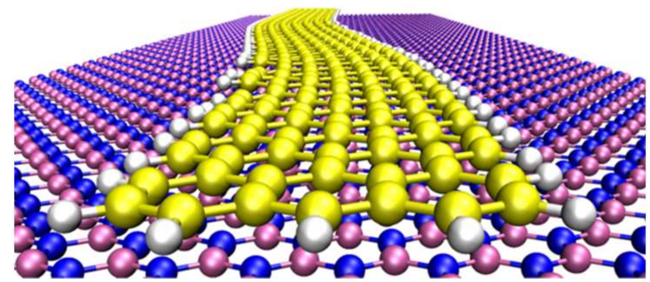

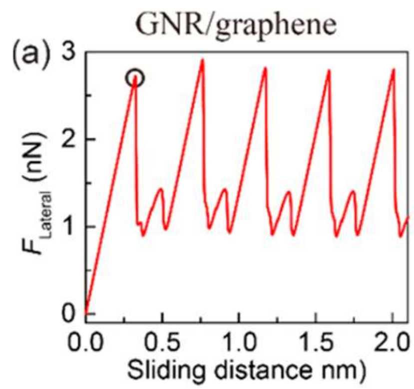

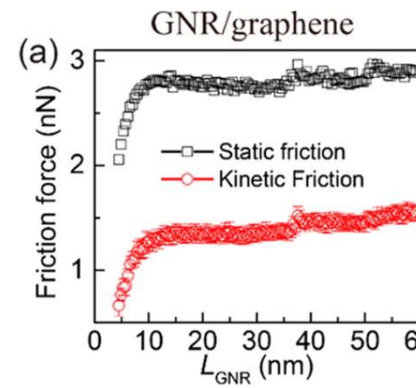

A continuum model for peeling and sliding of GNRs

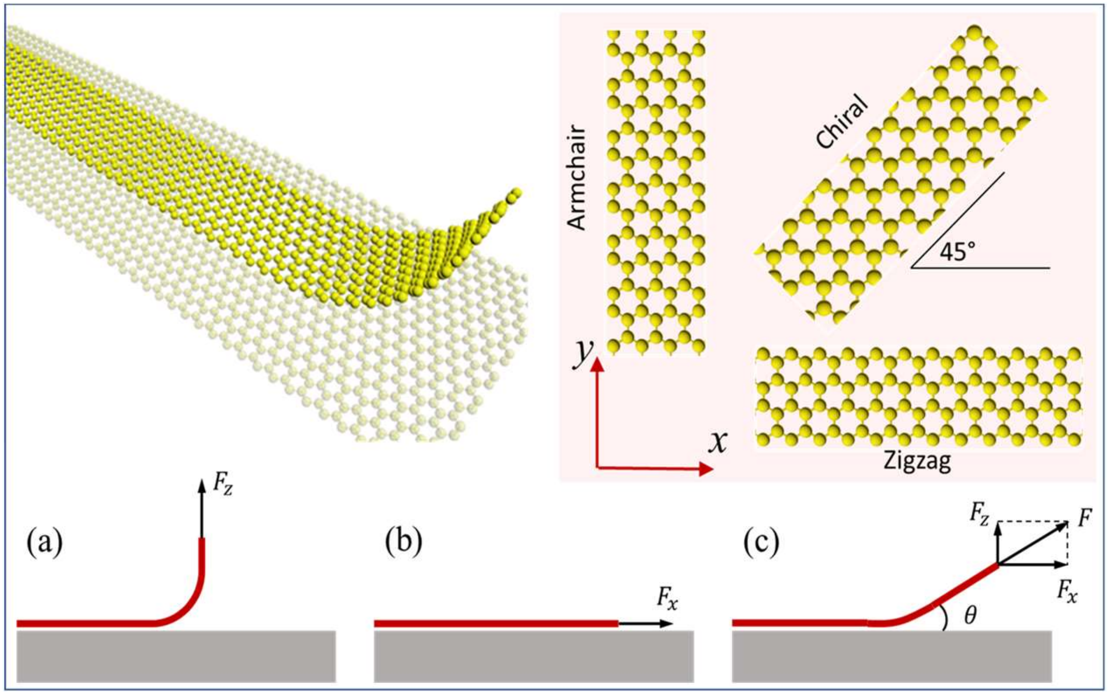

(a) Peeling -> adhesion
(b) Pulling -> sliding friction
(c) Coupled peeling and pulling

$\Gamma_0 = 0.25\ \mathrm{J/m^2}$
$z_0 = 0.335\ \mathrm{nm}$
$\varepsilon_1 = 1.33 \times 10^{-4}\ \mathrm{eV}$
$\beta = 28.7$

Xue et al., J. Mech. Phys. Solids 158, 104698 (2022).

Periodic interlayer potential

$$U(u_x, u_y, u_z) = U_0(u_z) + U_1(u_z) f(u_x, u_y)$$

$$U_0(u_z) = \Gamma_0 \left[-\frac{5}{3}\left(\frac{z_0}{z_0 + u_z}\right)^4 + \frac{2}{3}\left(\frac{z_0}{z_0 + u_z}\right)^{10} \right]$$

$$U_1(u_z) = \frac{\varepsilon_1}{A_0}\left[-\left(\frac{z_0}{z_0 + u_z}\right)^4 + \beta\left(\frac{z_0}{z_0 + u_z}\right)^{10} \right]$$

$$f(u_x, u_y) = \frac{3}{2} + \cos\left(G_1(u_y - a)\right) + 2\cos\left(\frac{G_1(u_y - a)}{2}\right)\cos\left(\frac{\sqrt{3}G_1 u_x}{2}\right)$$

Interlayer normal/shear tractions

$$\sigma = \frac{\partial U}{\partial u_z}, \tau_x = \frac{\partial U}{\partial u_x}, \tau_y = \frac{\partial U}{\partial u_y}$$

implemented as a user subroutine (UINTER) in ABAQUS

Interlayer potential and traction-separation relations

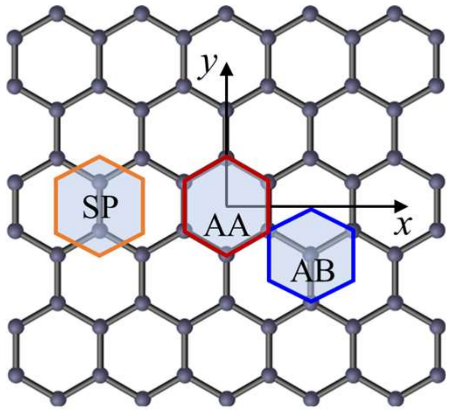

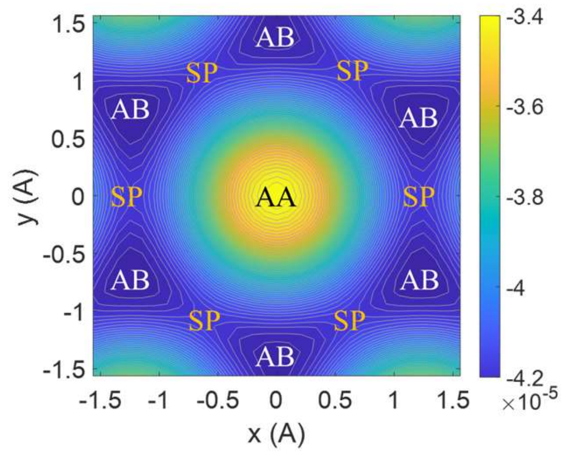

Different stacking orders in a periodic landscape of the interlayer potential energy

Normal traction (AB)

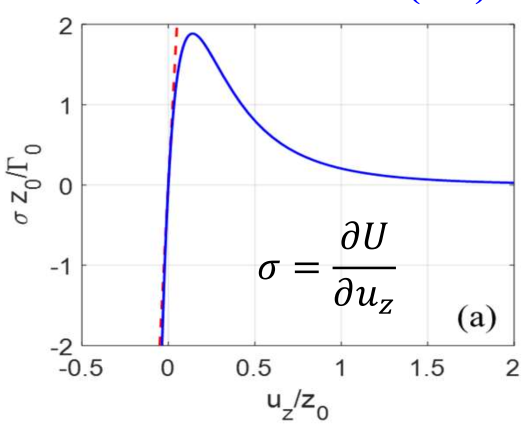

Shear traction (zigzag)

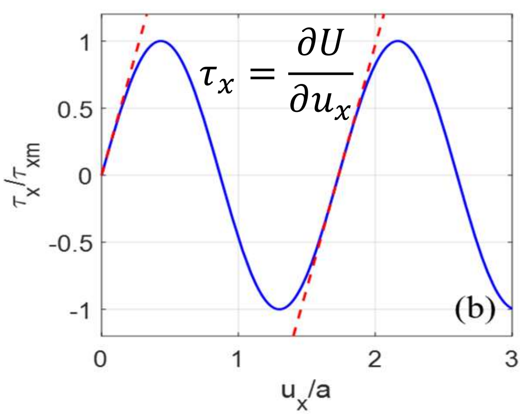

Shear traction (armchair)

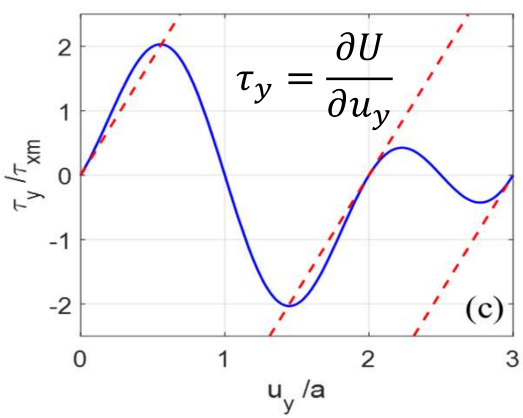

$$\tau_{xm} = (\beta - 1)\frac{8\pi\varepsilon_1}{9a^3}$$

The shear interaction is isotropic in the linear regime but anisotropic in general.

Simple peeling vs Fixed-end peeling

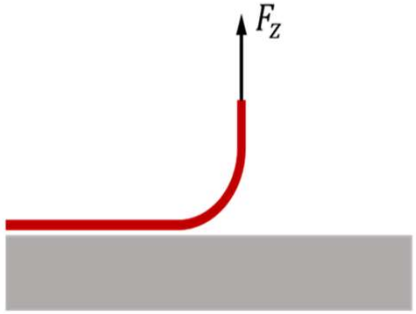

Simple peeling

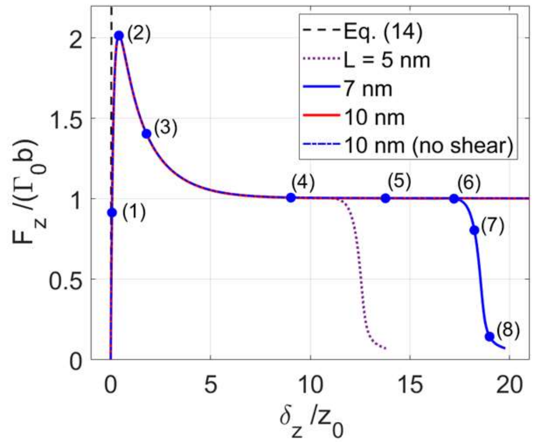

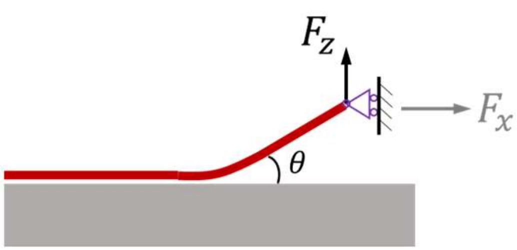

Peeling with fixed end

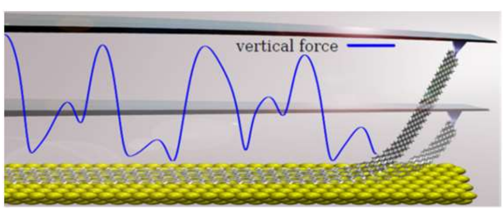

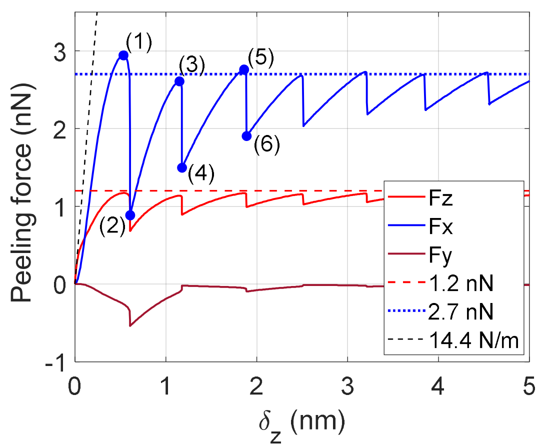

- Initial peeling stiffness:

$$K_z = \frac{\sqrt{2}}{2} b D^{1/4} \left(\frac{40\Gamma_0}{z_0^2}\right)^{3/4}$$

- Peak force:

$$F_z^{peak} \approx 2\Gamma_0 b$$

- Steady-state peeling force (no stick-slip):

$$F_z^{SS} = \Gamma_0 b$$

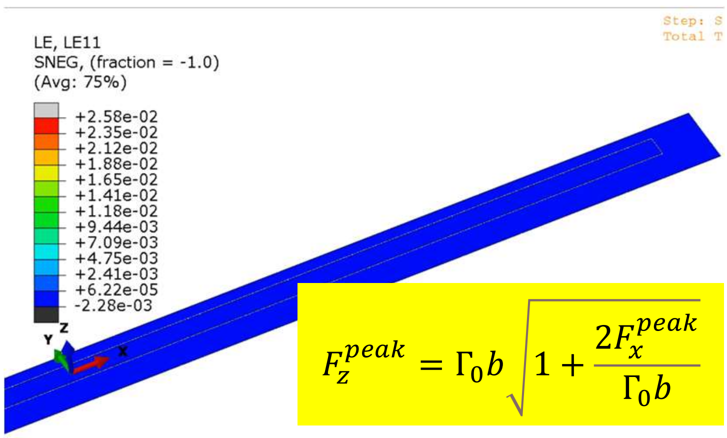

$$F_z^{peak} = \Gamma_0 b \sqrt{1 + \frac{2F_x^{peak}}{\Gamma_0 b}}$$

Peeling with sliding — zigzag vs armchair

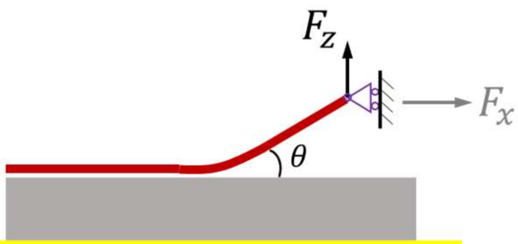

$$F_z^{peak} = \Gamma_0 b \sqrt{1 + \frac{2F_x^{peak}}{\Gamma_0 b}}$$

$$\cos\theta_p = \left(1 + \frac{\Gamma_0 b}{F_x^{peak}}\right)^{-1}$$

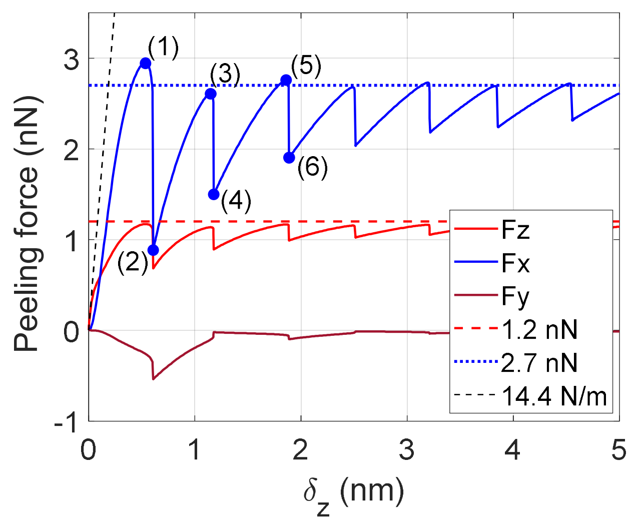

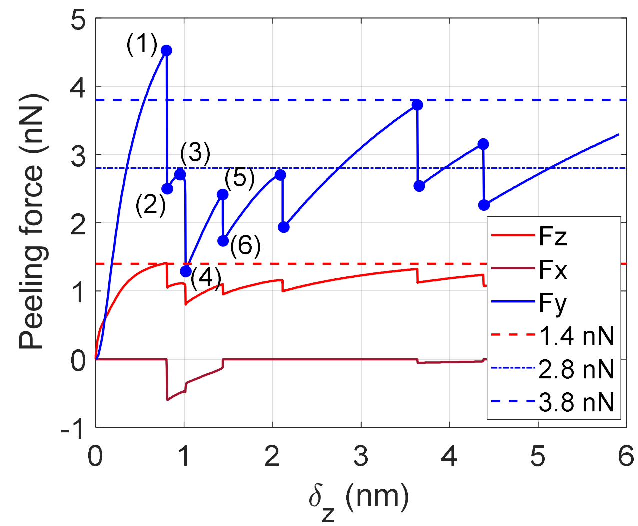

- ❑ Unlike simple peeling, the fixed-end peeling depends on the GNR orientation due to coupling with stick-slip sliding;
- ❑ Different types of strain solitons lead to different peak pulling forces, and correspondingly different peak peeling forces.
- ❑ Compared to the zigzag GNR, the peak peeling force is slightly higher for the armchair GNR.

Xue et al., J. Mech. Phys. Solids 158, 104698 (2022).

Constrained 1D sliding in the zigzag direction

$$Et\frac{d^2u_x}{dx^2} = \tau_{xm}\sin\left(\frac{\sqrt{3}}{2}G_1u_x\right)$$

Sine-Gordon equation
(1D Frenkel-Kontorova model)

Linear solution:

$$\tau_x \approx \frac{\sqrt{3}}{2}\tau_{xm}G_1u_x = k_xu_x$$

Sliding stiffness:

$$K_x = \frac{F_x}{\delta_x} = \frac{Etb}{\lambda_x}\tanh\left(\frac{L}{\lambda_x}\right)$$

Characteristic length:

$$\lambda_x = \sqrt{\frac{Et}{k_x}} \quad (\sim 4.85 \text{ nm})$$

Inhomogeneous, nonlinear solution for a long GNR:

$$\varepsilon_x = \sqrt{\frac{4\tau_{xm}}{\sqrt{3}G_1Et}\left[1-\cos\left(\frac{\sqrt{3}}{2}G_1u_x\right)\right]}$$

$$\tau_{xm} = (\beta-1)\frac{8\pi\varepsilon_1}{9a^3}$$

$$F_x = b\sqrt{\frac{4\tau_{xm}Et}{\sqrt{3}G_1}\left[1-\cos\left(\frac{\sqrt{3}}{2}G_1\delta_x\right)\right]}$$

Maximum strain and force:

$$\varepsilon_{xm} = \sqrt{\frac{8\tau_{xm}}{\sqrt{3}G_1Et}}$$

$$F_x^{max} = \frac{4b}{3^{3/4}a}\sqrt{(\beta-1)Et\varepsilon_1}$$

Xue et al., J. Mech. Phys. Solids 158, 104698 (2022).

Constrained sliding in the zigzag direction

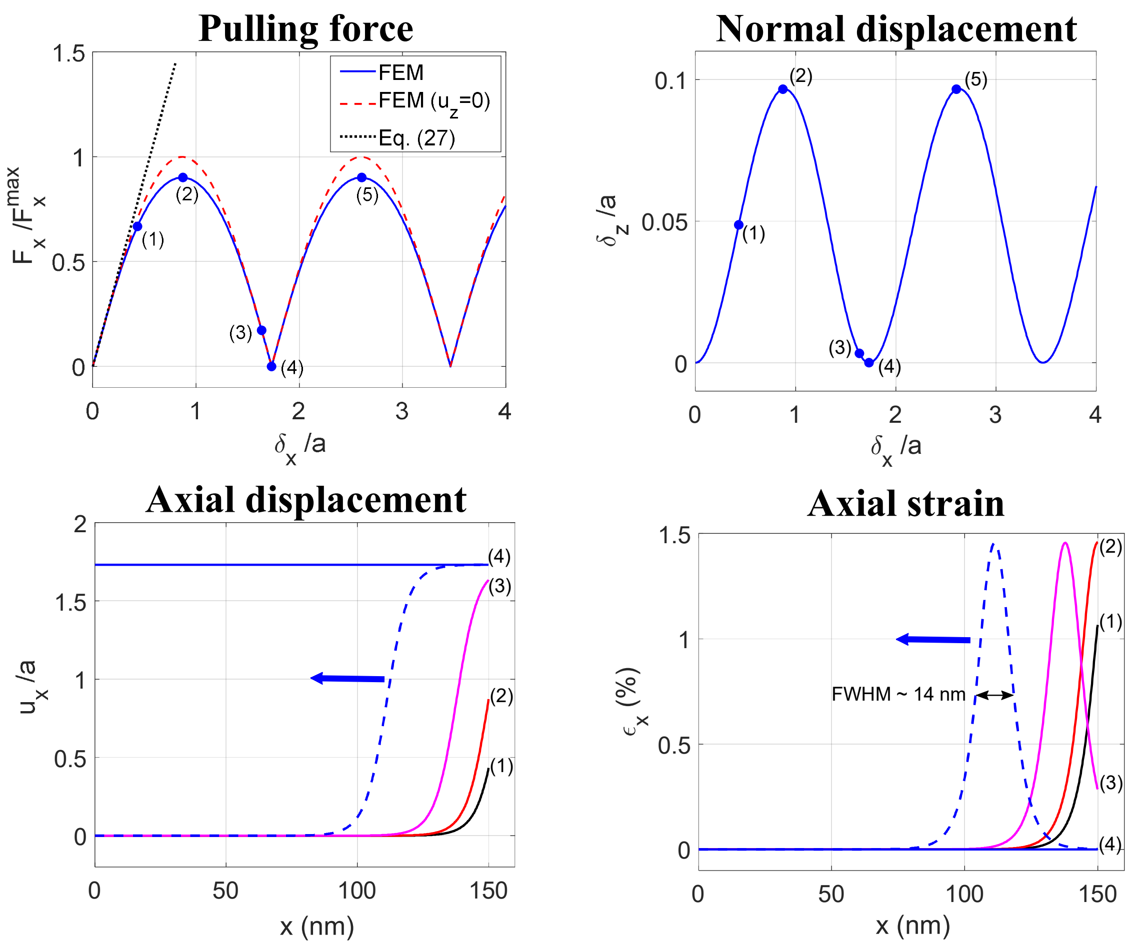

Effect of elastic deformation in GNR

- Reduces the friction remarkably (as opposed to uniform sliding of a rigid flake);
- Strain solitons form and glide to facilitate the stick-slip sliding;
- The peak pulling force is reduced by ~10% due to the normal displacement.

Xue et al., J. Mech. Phys. Solids 158, 104698 (2022).

Unconstrained sliding in the zigzag direction

Pulling force

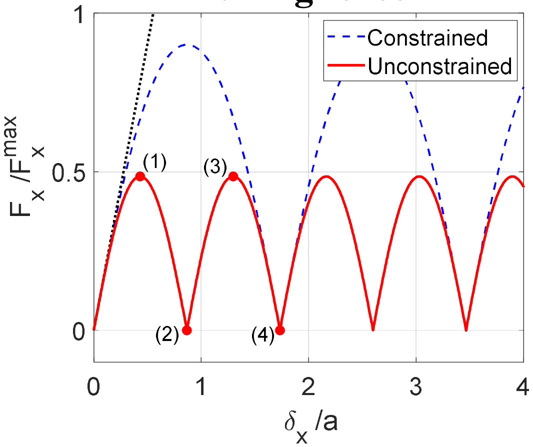

Lateral displacement

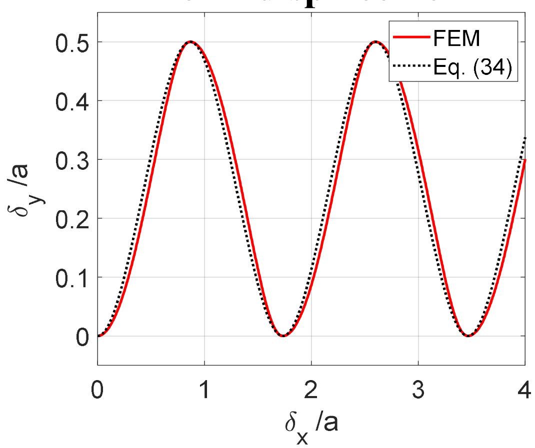

Axial displacement

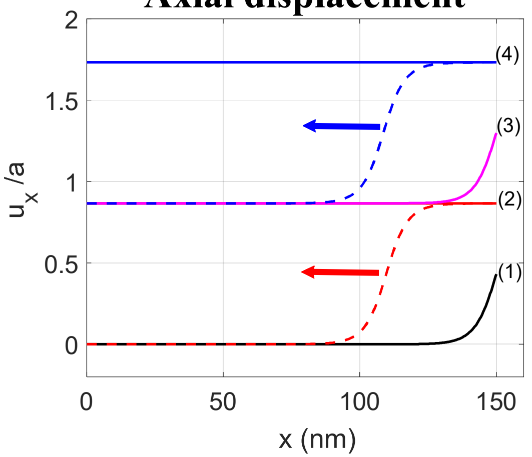

Axial strain

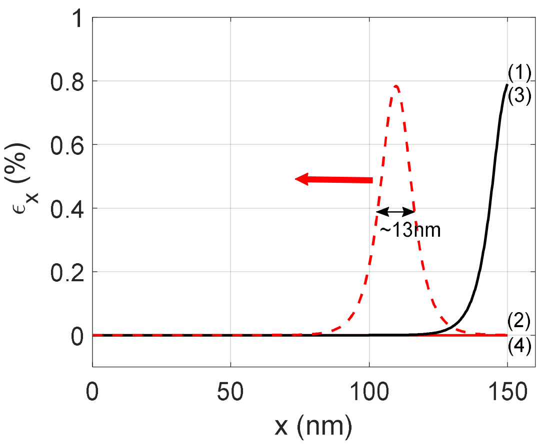

Compared to the constrained sliding: reduced peak force, half period, lateral displacement

For a narrow GNR, $\tau_y \approx 0$ and thus

$$2\cos\left(\frac{G_1(u_y - a)}{2}\right) + \cos\left(\frac{\sqrt{3}}{2}G_1 u_x\right) = 0$$

$$\tau_x = \frac{1}{2}\tau_{xm}\sin\left(\sqrt{3}G_1 u_x\right)$$

$$F_x = b\sqrt{\frac{\tau_{xm}Et}{\sqrt{3}G_1}\left[1 - \cos\left(\sqrt{3}G_1\delta_x\right)\right]}$$

Xue et al., J. Mech. Phys. Solids 158, 104698 (2022).

Unconstrained sliding in the zigzag direction

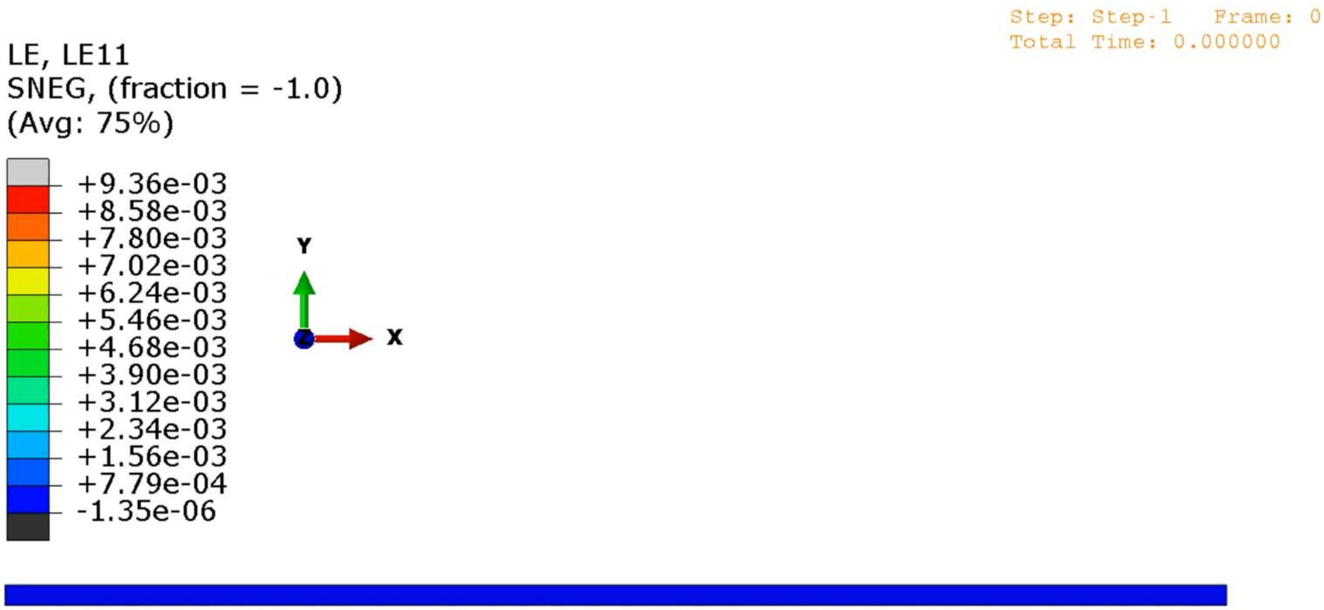

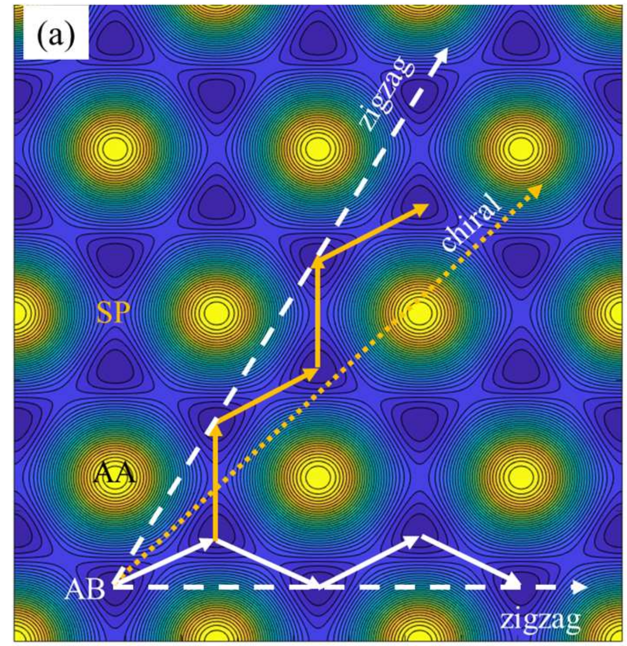

- Following the lateral displacement of the pulling end, the entire GNR oscillates laterally between 0 and $a/2$, similar to snake-like sliding in fully atomistic simulations (Ouyang et al., 2018);
- Once the pulling end slides laterally by $a/2$, a strain soliton forms and glides through the GNR;
- For a narrow GNR (b ~ 1 nm), the strain soliton is primarily tensile with a small kink due to lateral bending.

Unconstrained sliding in the armchair direction

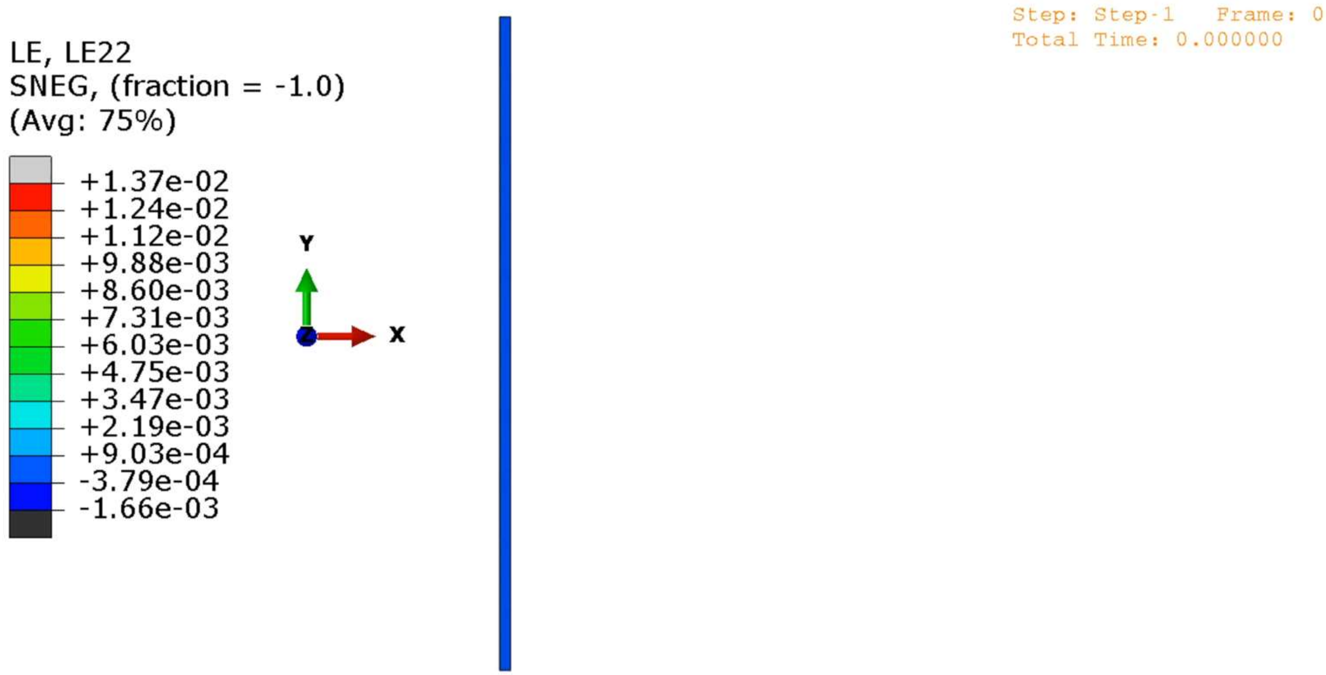

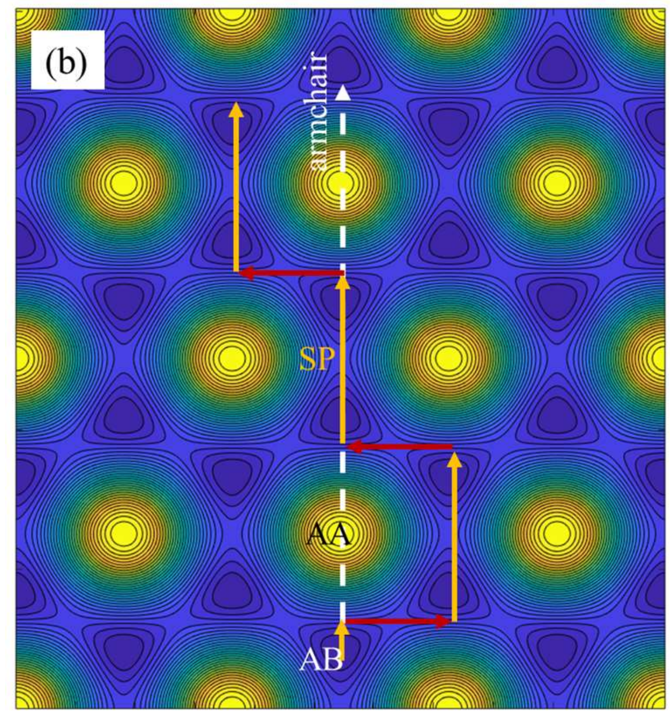

Stair-like sliding trajectories over the interlayer energy landscape

Xue et al., J. Mech. Phys. Solids 158, 104698 (2022).

Unconstrained sliding in the armchair direction: strain solitons

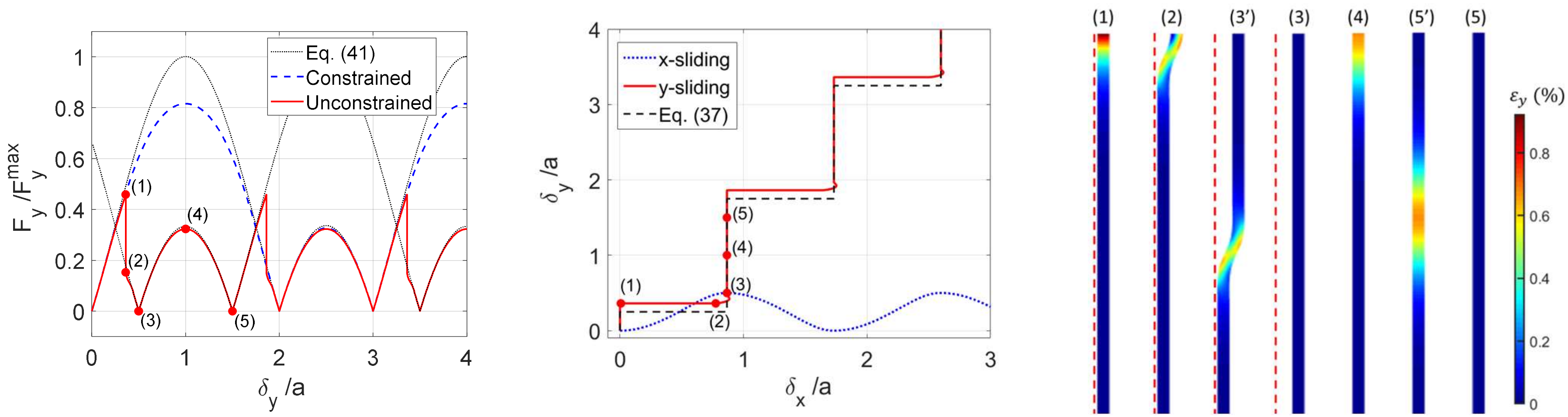

- Two branches are predicted analytically for unconstrained sliding in the armchair direction;
- The lateral jump (point 1 to 2) precedes the formation of the first soliton (point 3) and leads to a kink near the pulling end;
- The first strain soliton glides simultaneously with the kink at point 3 ($\delta_y = 0.5a$);
- Another strain soliton forms and glides at point 5, with no kink;
- Two kinds of strain solitons alternate to form, and both are are primarily tensile strain solitons for a narrow GNR.

Effects of ribbon length and width on sliding

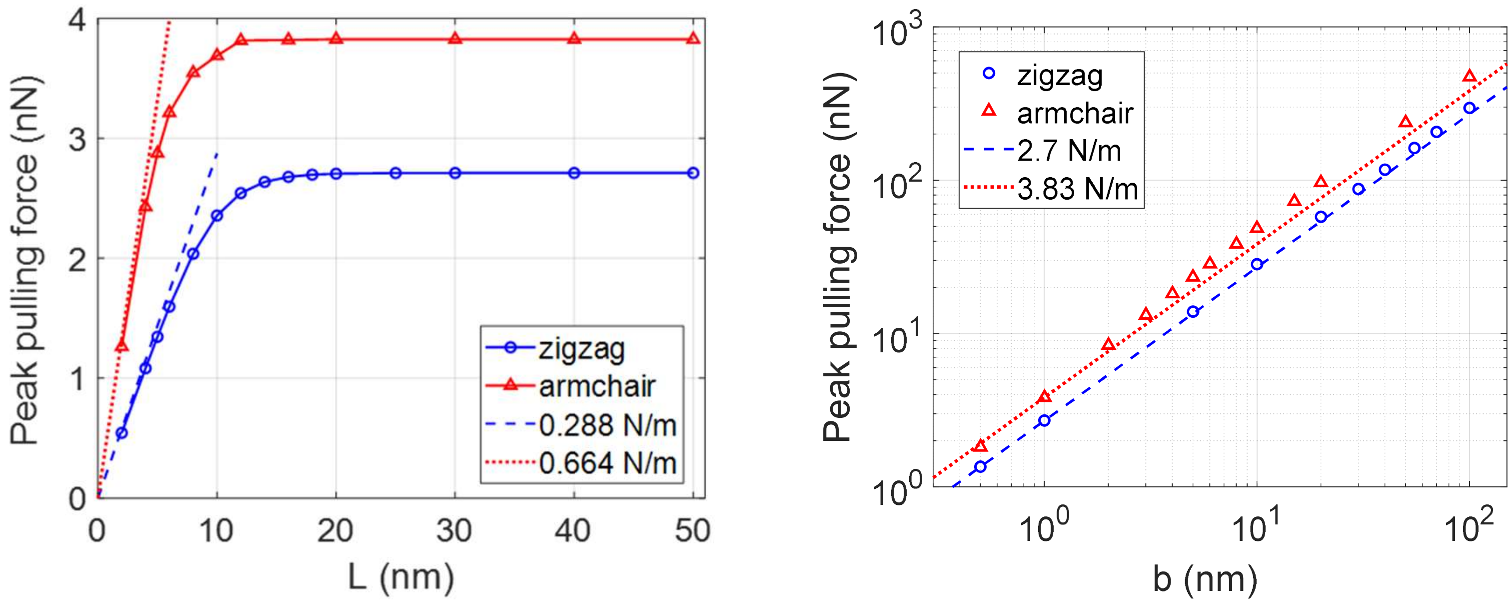

- ❑ The dependence of the peak force on the ribbon length is similar to fully atomistic simulations (Ouyang et al., 2018), with an initial linear rise followed by a plateau beyond a characteristic length of around 10 to 20 nm;
- ❑ The peak pulling force for sliding of relatively long GNRs (L > 20 nm) depends on the ribbon width quasi-linearly;
- ❑ Only for very short GNRs (L < 5 nm), the sliding is approximately uniform like a rigid flake.

Xue et al., J. Mech. Phys. Solids 158, 104698 (2022).

Strain solitons in wide GNRs

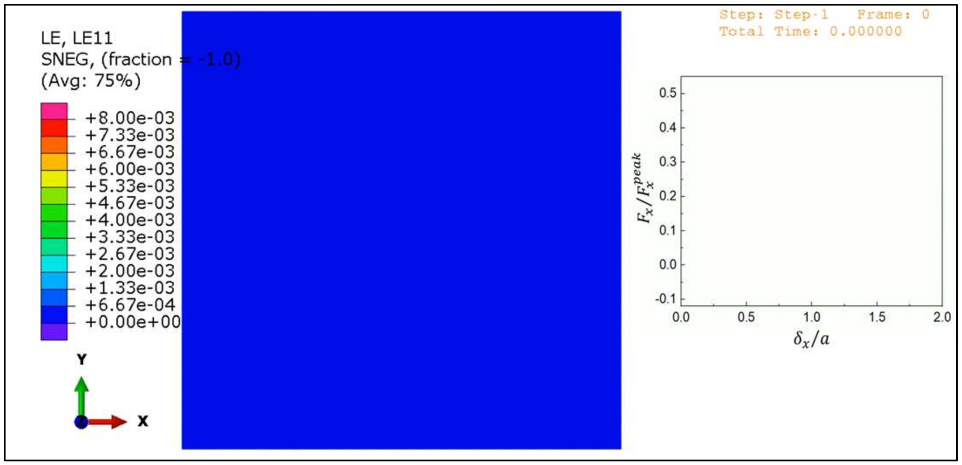

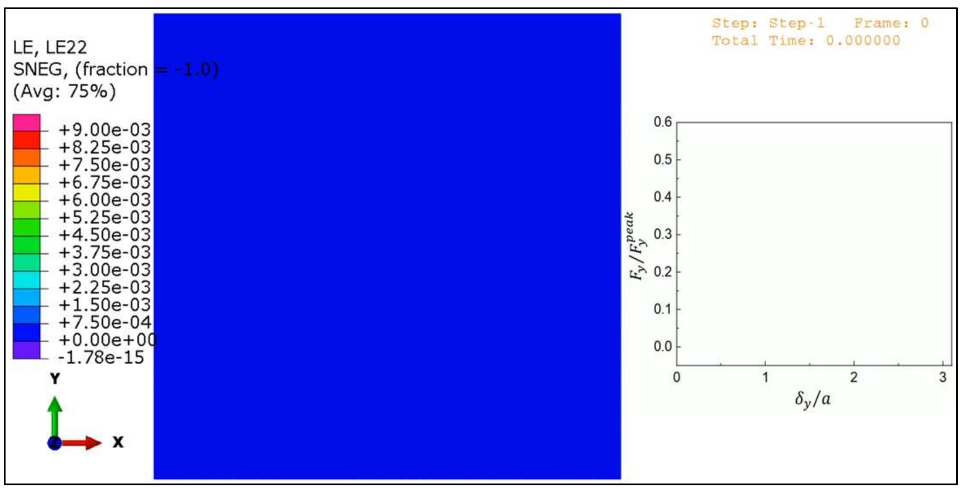

Zigzag direction: mixed type

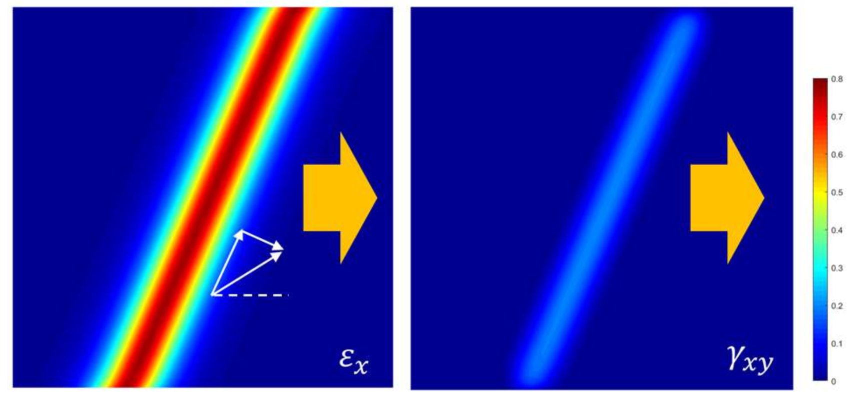

Armchair direction: shear type

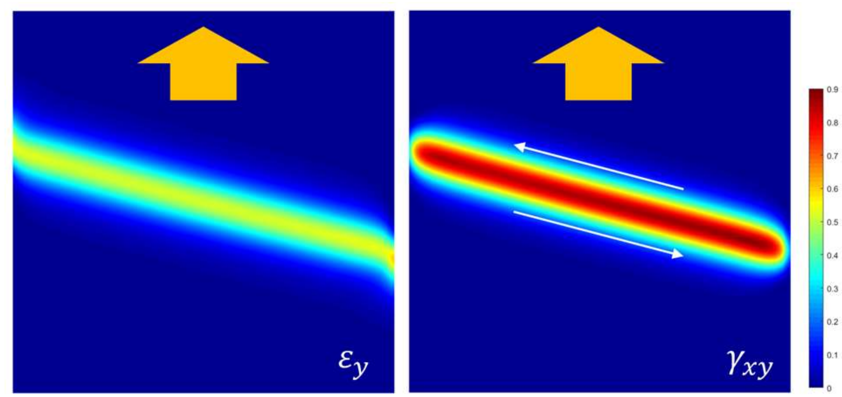

Twisting a graphene sheet atop a rigid graphene substrate

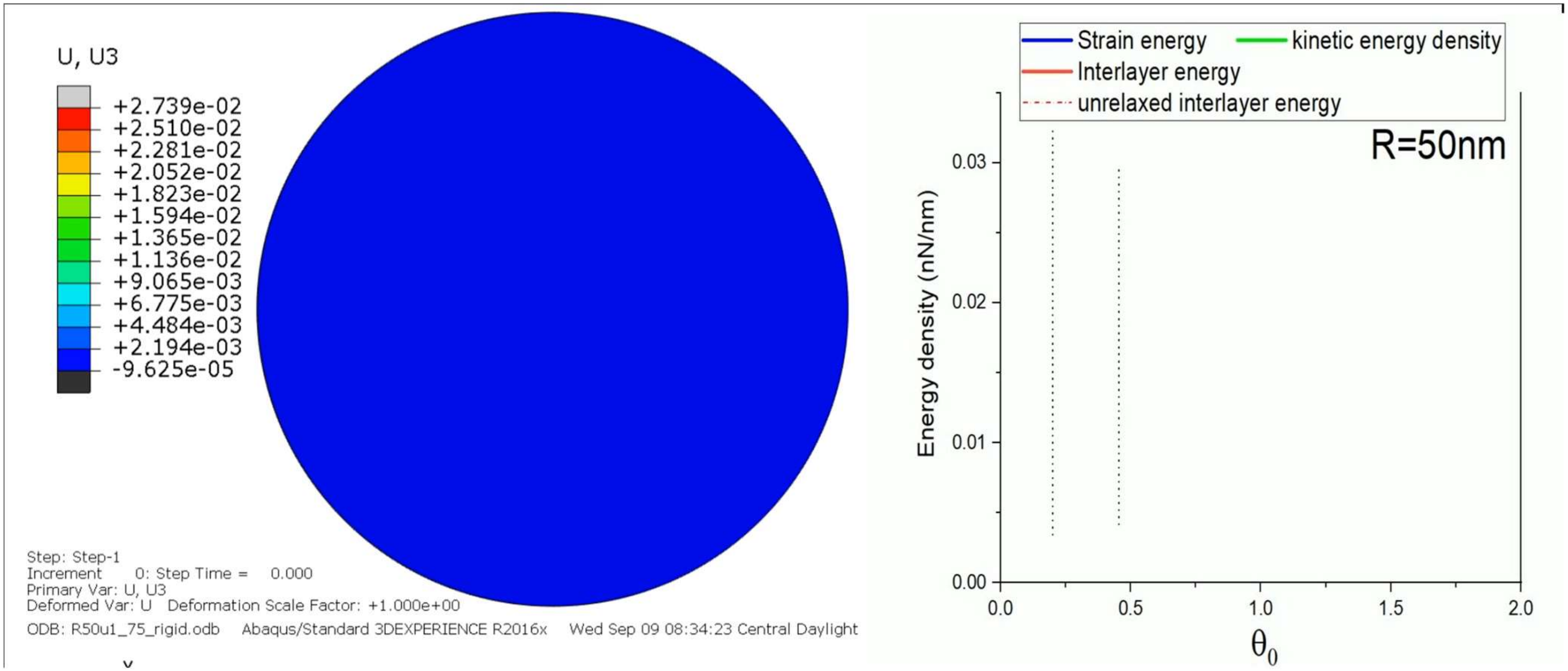

The competition between the interlayer potential energy and the intralayer strain energy leads to structural relaxation and possible phase transition in 2D moiré superlattices.

2D moiré patterns

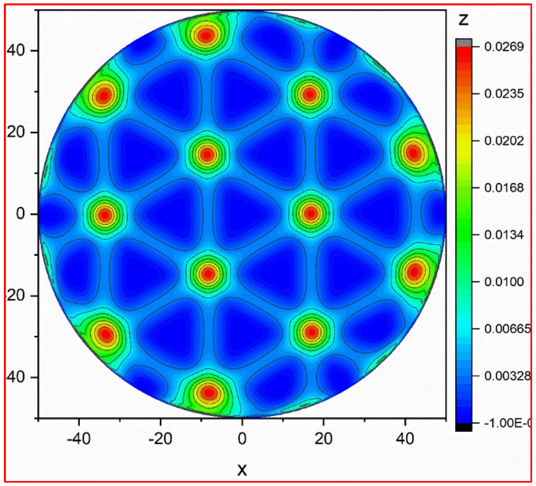

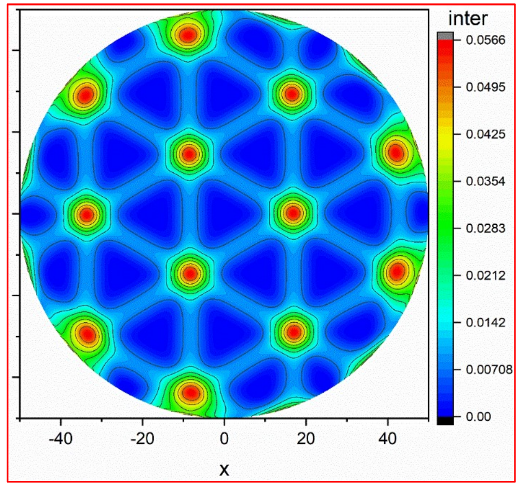

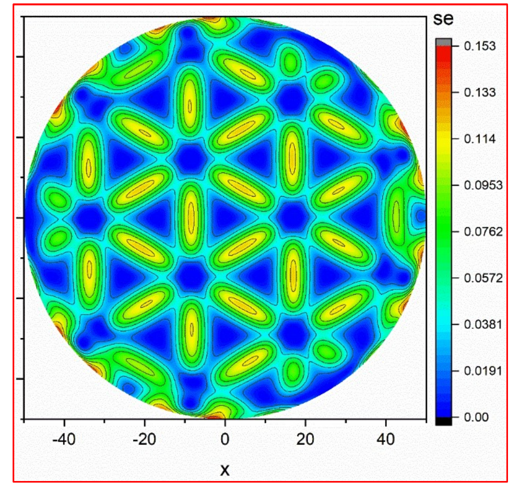

R = 50 nm at $\theta_0 = 0.5°$

Relative rotation:

$$\theta_r = \tan^{-1}\left(\frac{\partial u_y}{\partial x} - \frac{\partial u_x}{\partial y}\right) - \theta_0$$

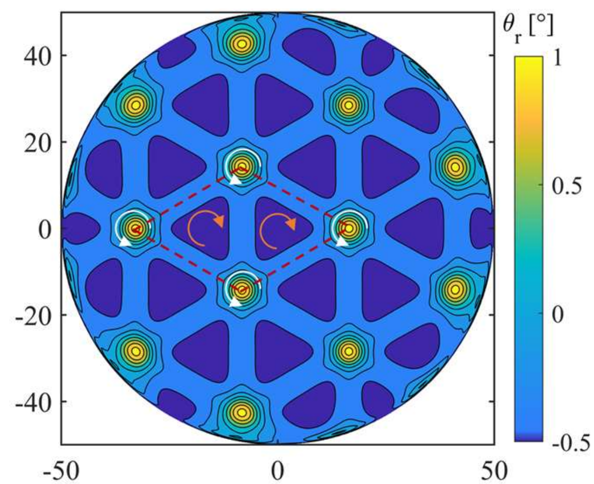

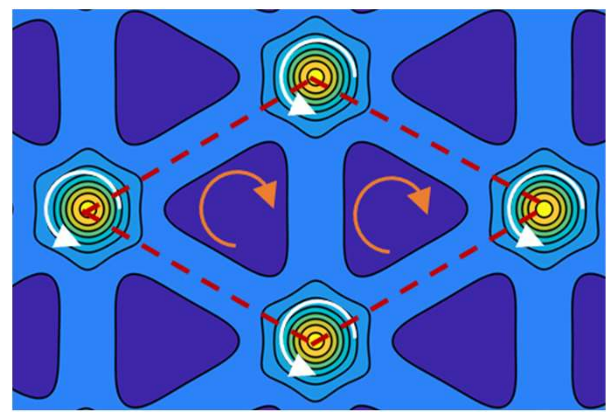

2D moiré: angular dependence and stability

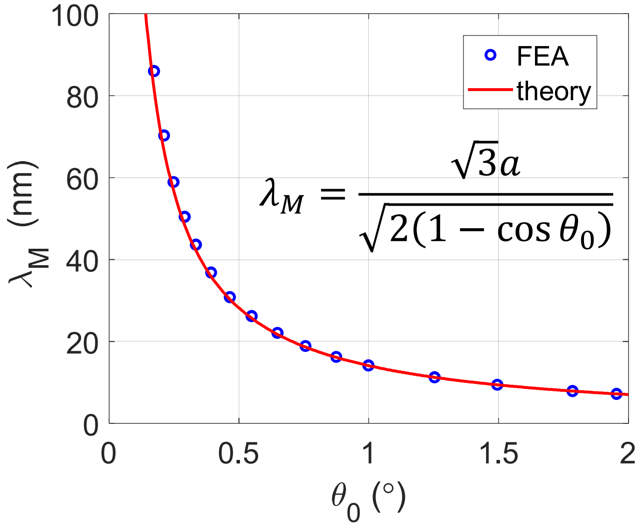

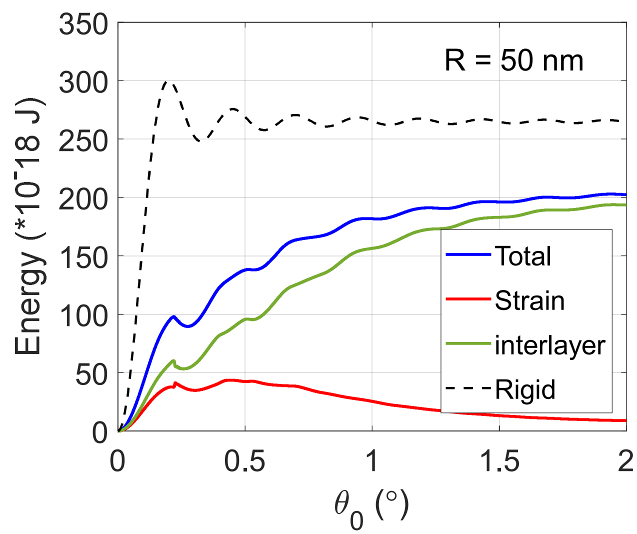

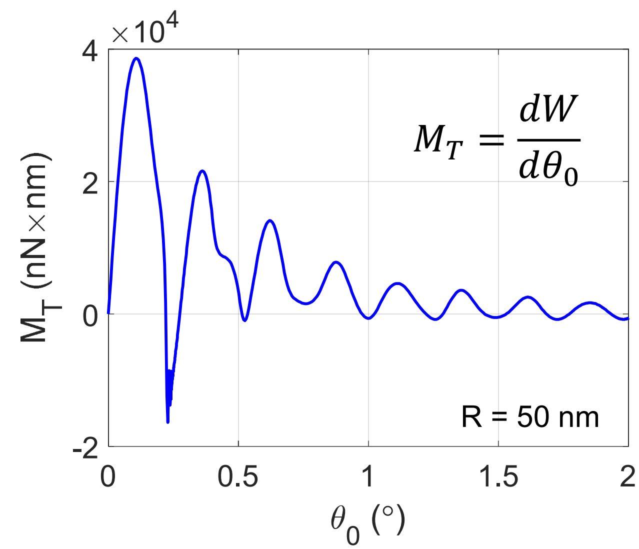

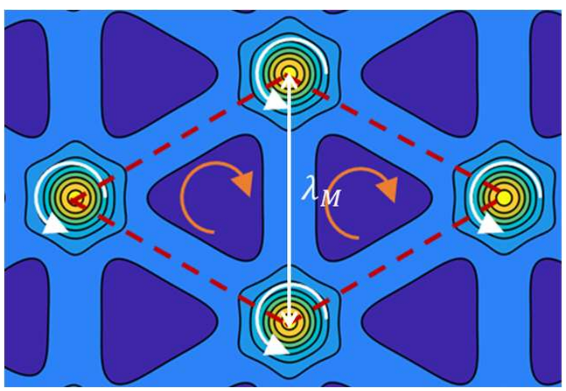

- The relaxed total energy has local extremes at particular angles, where the twisting moment is zero.
- With zero twisting moment, stable moiré patterns are expected at a set of critical angles where the relaxed total energy is a local minimum.

Biaxial strain induced moiré

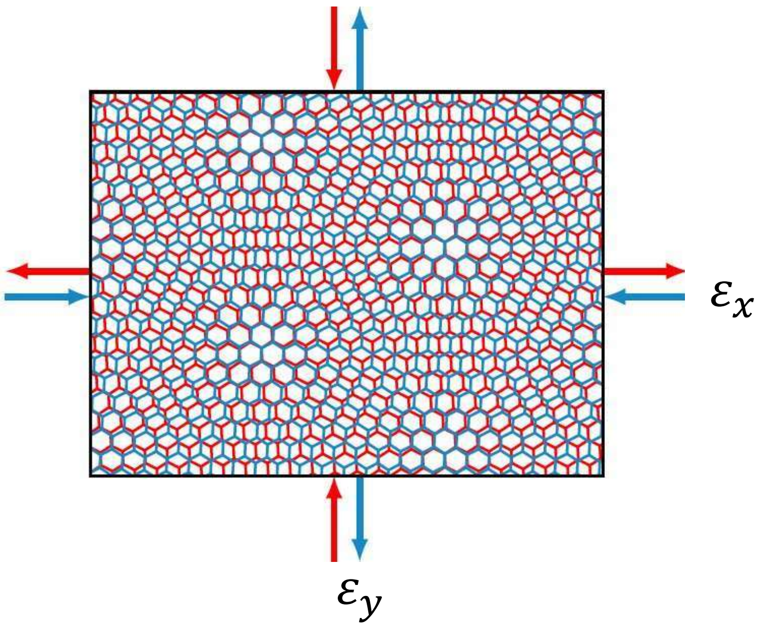

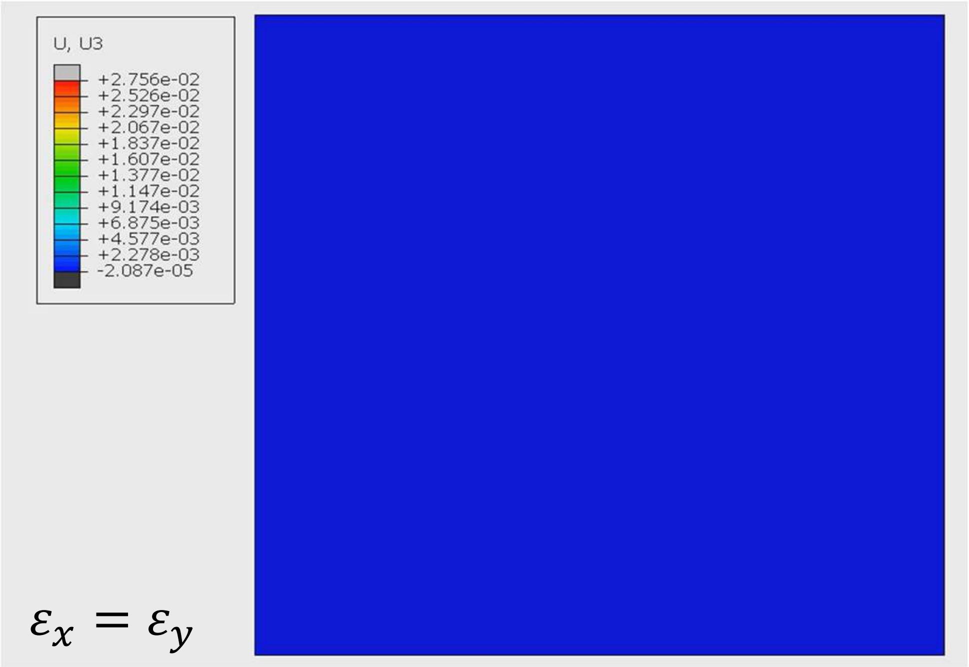

Moiré by equi-biaxial strain

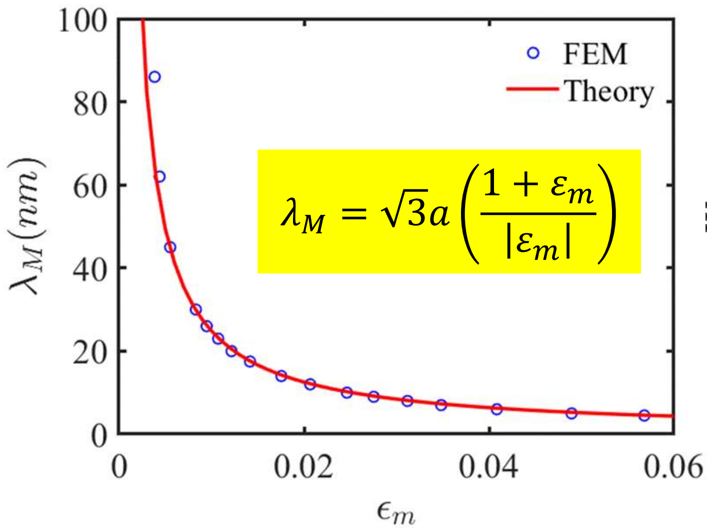

$$\lambda_M = \sqrt{3}a\left(\frac{1+\varepsilon_m}{|\varepsilon_m|}\right)$$

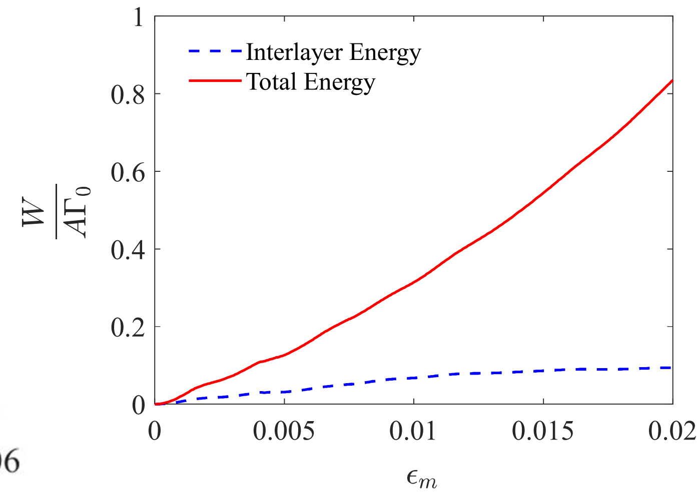

$$dW = (F_x + F_y)du$$

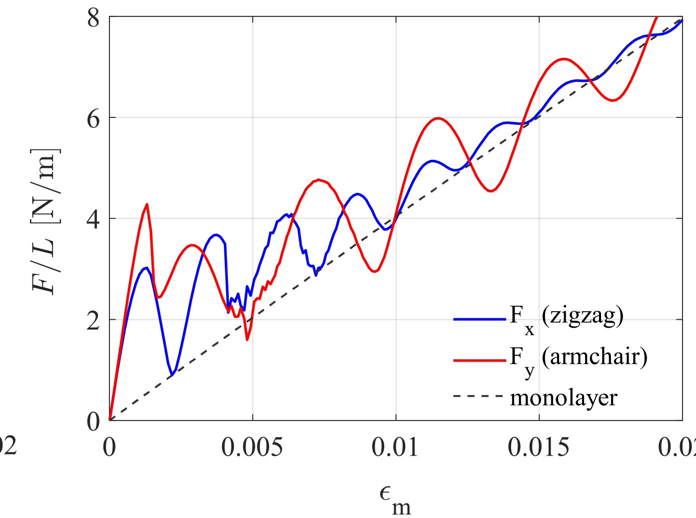

Compare to a monolayer graphene:

$$F_x = F_y = \left(\frac{Et}{1-\nu}\right)u$$

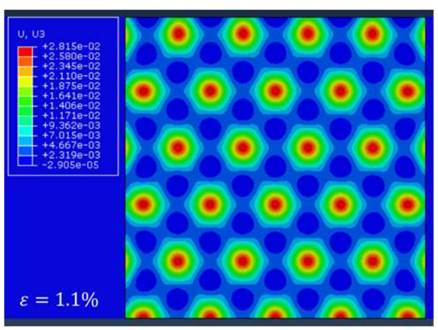

- Interlayer coupling leads to a higher initial stiffness and an anisotropic, serrated stress-strain behavior associated with formation and evolution of 2D moiré patterns.

Moiré by anisotropic strains

The two principal strain components may be controlled independently to obtain different moiré patterns.

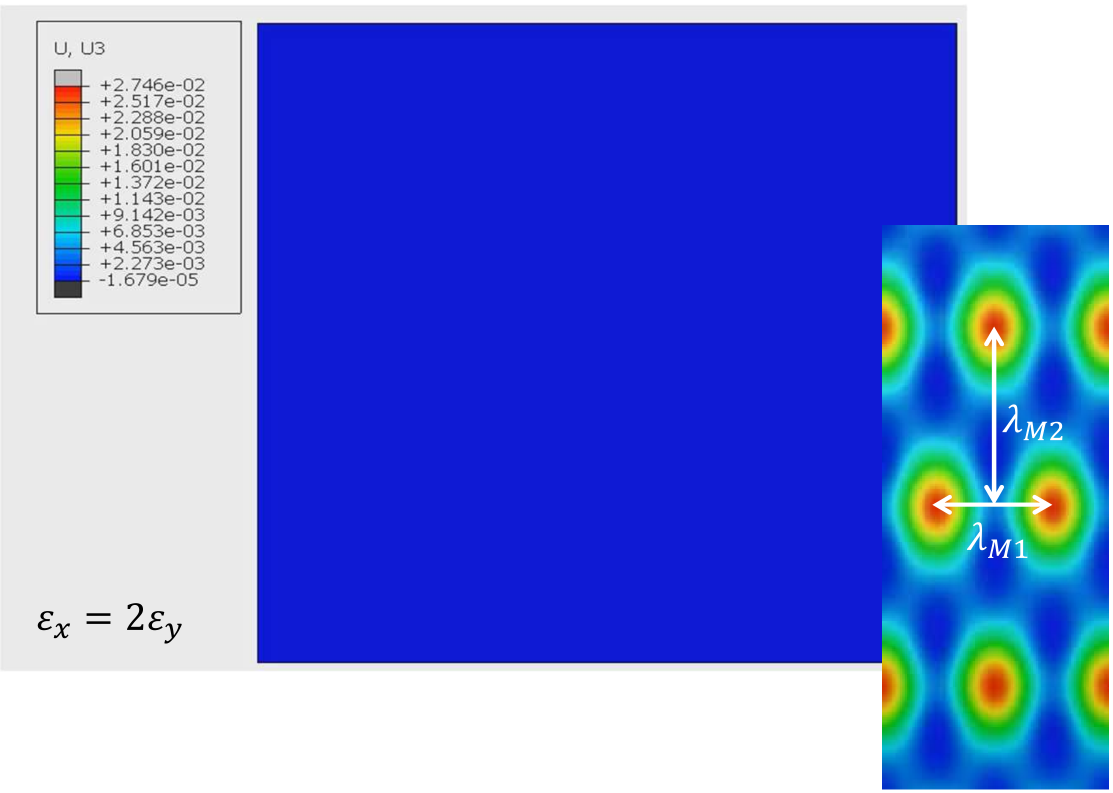

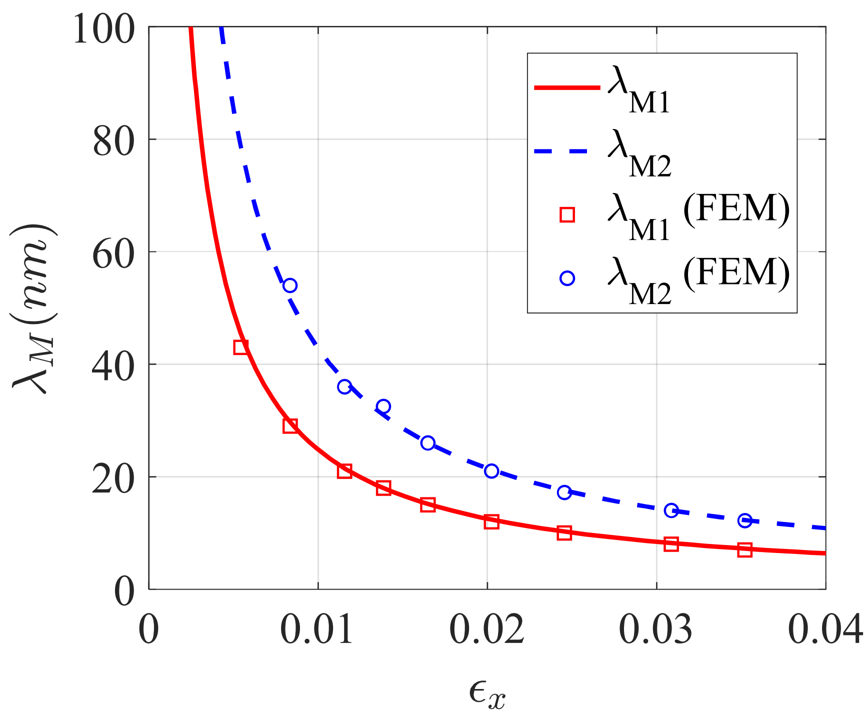

$\lambda_{M1} = \sqrt{3}a\left(\frac{1+\varepsilon_x}{|\varepsilon_x|}\right)$ and $\lambda_{M2} = 1.5a\left(\frac{1+\varepsilon_y}{|\varepsilon_y|}\right)$

Summary

- Part I: Mechanics and mechanical properties of 2D materials
  - Elastic and thermoelastic properties
  - Inelastic properties: strength and toughness
- Part II: Interfacial properties of 2D materials (adhesion and friction)
  - 2D-3D interactions
  - 2D-2D interactions

Thanks to many collaborators including:
Kenneth Liecthi, Nanshu Lu, Pradeep Sharma (UH), Wei Gao (UTSA), Zhaohe Dai, Zhiming Xue, Ganbin Chen, Vahid Morovati

Funding from NSF is acknowledged for part of this work.